Distribution Agreement

In presenting this thesis or dissertation as a partial fulfillment of the requirements for an advanced degree from Emory University, I hereby grant to Emory University and its agents the non-exclusive license to archive, make accessible, and display my thesis or dissertation in whole or in part in all forms of media, now or hereafter known, including display on the world wide web. I understand that I may select some access restrictions as part of the online submission of this thesis or dissertation. I retain all ownership rights to the copyright of the thesis or dissertation. I also retain the right to use in future works (such as articles or books) all or part of this thesis or dissertation.

Signature:

_____   _____
Tyra A. Lamar   Date

Voltage-gated Sodium Channels as Modifiers of *Scn1a*-derived Epilepsy

By

Tyra A. Lamar

Doctor of Philosophy

Graduate Division of Biological and Biomedical Sciences

Neuroscience

_____
Andrew P. Escayg, Ph.D
Advisor

_____   _____
Tamara Caspary, Ph.D   Ellen Hess, Ph.D
Committee Member   Committee Member

_____   _____
Donald Rainnie, Ph.D   David Weinshenker, Ph.D
Committee Member   Committee Member

Accepted:

_____
Lisa A. Tedesco, Ph.D.
Dean of the James T. Laney School of Graduate Studies

_____
Date

Voltage-gated Sodium Channels as Modifiers of *Scn1a*-derived Epilepsy

By

Tyra A. Lamar

B.S., North Carolina Central University, 2010

Advisor: Andrew P. Escayg, Ph.D.

An abstract of
a dissertation submitted to the Faculty of the
James T. Laney School of Graduate Studies of Emory University
in partial fulfillment of the requirement for the degree of
Doctor of Philosophy
in the Graduate Division of Biological and Biomedical Science
Neuroscience
2017

Abstract

Voltage-gated Sodium Channels as Modifiers of *Scn1a*-derived Epilepsy

By Tyra A. Lamar

Mutations in the brain expressed voltage-gated sodium channels (*SCN1A, SCN2A, SCN3A*, and *SCN8A*) are responsible for an increasing number of epilepsy disorders. The most clinically important of these VGSCs is *SCN1A*, which is responsible for a spectrum of disorders ranging from genetic epilepsy with febrile seizures plus (GEFS+) to the severe encephalopathy Dravet syndrome (DS). One hallmark of *SCN1A* disorders is the clinical heterogeneity observed. Within a single GEFS+ pedigree, for example, the phenotype may range from mild febrile seizures to DS. This phenotypic heterogeneity suggests the presence of additional environmental or genetic factors that can influence the phenotype. One such factor is a genetic modifier, an independently segregating gene that can alter the expression of the disease gene. Identifying and investigating candidate modifier genes may improve our understanding of the complex etiology of epilepsy and provide additional gene targets for therapeutic intervention. The goal of this dissertation was to investigate the role of the VGSC genes *SCN3A* and *SCN9A*, as epilepsy genes and as candidate modifiers for *SCN1A*-derived epilepsy. In Chapter 2, we reported a novel, trafficking-deficient *SCN3A* mutation in a patient with partial epilepsy, providing further evidence that *SCN3A* deficiency results in increased seizure risk. We then demonstrated that partial loss of *Scn3a* expression is sufficient to increase seizure susceptibility and produce motor deficits in a hypomorphic mouse line. In Chapter 3, we determined that partial loss of *Scn3a* increases susceptibility to flurothyl-induced seizures but does not alter survival or the behavioral characteristics of a GEFS+ mouse model. Furthermore, in Appendix B, we demonstrated that the presence of a *Scn9a* mutation does not increase the seizure susceptibility observed in the GEFS+ mouse model. In summary, the results of this dissertation provide greater insight into the role of *Scn3a* and *Scn9a* in epilepsy.

Voltage-gated Sodium Channels as Modifiers of *Scn1a*-derived Epilepsy

By

Tyra A. Lamar

B.S., North Carolina Central University, 2010

Advisor: Andrew P. Escayg, Ph.D.

A dissertation submitted to the Faculty of the
James T. Laney School of Graduate Studies of Emory University
in partial fulfillment of the requirement for the degree of
Doctor of Philosophy
in the Graduate Division of Biological and Biomedical Science
Neuroscience
2017

Acknowledgements:

My journey through life has truly been shaped by the maxim "It takes a village…" I could not have completed this dissertation without the prayers, love, and unceasing support of my village of family and friends. I would like to begin by thanking my advisor Dr. Andrew Escayg for guiding and mentoring me throughout these years. Andrew has always challenged me to become a better scientist and given so much of his time and effort to my training. For all the troubleshooting of experiments, the editing of papers and grants, and the continual support, I will forever be extremely grateful to him. Next, I would like to thank my committee for their advice and encouragement through the years: Dr. David Weinshenker for his guidance on behavioral techniques and his thoughtful advice, Dr. Tamara Caspary for her help in exploring the genetic characterization of my mouse line, Dr. Donald Rainnie for his enthusiasm about the mechanisms of my disease model, and Ellen Hess for her thought-provoking questions and challenges for my experimental design.

I am also eternally grateful to my past and present lab mates for making the lab such a wonderful place even in challenging times. Dr. Ligia Papale was my first lab friend and a great mentor. I will never forget how sweetly she would encourage our breeding mice, and I certainly borrowed her technique. Her support and guidance was part of the reason I joined the lab. I am also thankful for Dr. Chris Makinson, who even though years ahead of me in the program, took time from his busy schedule to teach me lab techniques, discuss cool science with me, share his delicious homemade cider, and teach me how to play some of the coolest games in the world. Chris also taught me how to think like a scientist, and I often find myself imagining how he would approach

problems. Words cannot express my gratitude to Dr. Stacey Dutton, who has become a dear friend even beyond the lab. She has stuck with me through crazy late nights troubleshooting Westerns, stressful times, health crises, and a mid-grad school slump. I have always been able to talk to her about anything, and over the course of these six years, she has become like a sister. I am blessed to have her as a friend. I am also incredibly grateful for Dr. Jennifer Wong, my second sister-friend in the lab. We have shared our love for food, our frustrations, and our life events for four years now, and I cannot imagine my life without her. I want to thank her for being a support, a listening ear, and a fun travel buddy. I would also like to thank George Inglis for his fun-loving personality, amazing sense of humor, and delicious baked goods. He has brought such joy to the lab, and has lifted my spirits during stressful moments. A special thanks also goes to Kameryn Butler, who has been a fun, caring, and supportive friend as well. It is always fun to share stories and lunches with her, and I still think she is one of the most creative gift-givers of all time. I am also thankful for Lindsey Shapiro for her cheerful, easygoing personality and for bringing more neuroscience to the lab. She has been such an encouragement to me as a senior student and a fun person to spend time with.

I would also like to thank the Neuroscience Program and Laney Graduate School for the opportunity to study and research a subject that I am passionate about in a collaborative, supportive environment. I especially would like to thank Dr. Shawn Hochman, Dr. Ron Calabrese, and Dr. Yoland Smith for their gracious support of me over the course of my graduate school career. I am also eternally grateful for Dr. Malu Tansey, who served as my advocate in these last couple of years and as an encouraging voice as I made decisions for the next step in my career. I would also like to thank Gary

Longstreet and Sonia Hayden, our program coordinators, for their support, willingness to help whenever needed, and concern for me as an individual.

Next, I would like to thank my amazing family for all of the love and encouragement they have offered, even when my experiences or stress were beyond words. They have cried with me, celebrated with me, and followed my journey to the very end. To my loving, amazing parents, Tyrone and Sylvia Lamar, thank you for all that you have taught me and done to support me. This degree is yours as much as mine. To my sister, Tracye Griswell, and my brother-in-love John Griswell, thanks for the movie and game nights and the unshakeable bond we share. To my amazing grandparents (Nanny, Grandpa Raleigh, Granddaddy, Mamama), my aunts and uncles, my awesome first cousin-siblings, and my family by love if not by blood, thank you for all that you do. Thanks for coming to hear me speak, for cheering me up when I am down, for always providing a hug when I need one. Although there is not room to thank everyone by name, I am so grateful for your presence in my life. Much love to all the members of my village.

Finally, I would like to thank my Lord and Savior, Jesus Christ, for carrying me along this journey and for ordering all my future steps. I can't wait to see what You have in store for the rest of my life.

Blessings to everyone.

CONTENTS

FIGURES AND TABLES

Chapter 1: Sodium Channels as Disease Genes and Genetic Modifiers in Mendelian

Epilepsy: The myth of the monogenic syndrome

1.1 Introduction

Epilepsy is one of the most common neurological diseases, affecting 3% of the worldwide population, and characterized by recurrent, unprovoked seizures. Although the definition of epilepsy suggests a single disorder, it is, in fact, a collection of heterogeneous disorders that vary in etiology, severity, and outcome. Currently, three main classifications have been proposed for epilepsy syndromes based on etiology: structural/metabolic (formerly symptomatic), genetic epilepsy (formerly idiopathic), and epilepsy of unknown cause (formerly cryptogenic) (Berg et al., 2010). While the delineation "epilepsy of unknown cause" is self-explanatory, the remaining two terms require further explanation. Structural/metabolic disorders are those in which epilepsy is secondary to an underlying disease or neurological insult, such as tuberous sclerosis or traumatic brain injury. Genetic epilepsy, which was historically classified as "idiopathic" by the International League Against Epilepsy (ILAE) if the cause was unknown yet presumed to be genetic (1989). Within genetic epilepsy are many complex, polygenic syndromes, in which genetic and environmental factors interact to produce a heterogeneous phenotype (Hempelmann et al., 2006, Helbig, 2015). Much of our progress in gene discovery and insight into the mechanisms of epilepsy, however, have originated from studies of monogenic epilepsy syndromes, in which a single gene is primarily responsible for the disease phenotype. This introduction will be limited to discussion of such epilepsy syndromes.

Although remarkable progress has been made in epilepsy gene discovery, there remains much to understand about the genetic architecture of epilepsy, even within the monogenic syndromes. One complication within families with monogenic epilepsy, such

as disorders caused by mutations in the voltage-gated sodium channel (VGSC) *SCN1A*, is the reduced penetrance of the mutation and variable expressivity of the disease phenotype that is frequently observed (Marini et al., 2003, Gokben et al., 2009, Depienne et al., 2010, Suls et al., 2010, Mhanni et al., 2011). Reduced penetrance indicates that some individuals with the disease-causing mutation are asymptomatic, while variable expressivity means that individuals carrying the same mutation may have different clinical presentations. This phenotypic heterogeneity suggests the presence of additional environmental or genetic factors that can influence the phenotype.

One such factor is a genetic modifier, a gene that usually segregates independently and can alter the expression of the disease gene. Identifying and investigating candidate modifier genes may improve our understanding of the complex etiology of epilepsy and provide additional gene targets for therapeutic intervention. Nevertheless, even when putative modifier genes are identified in patients, validating these discoveries can be challenging, due to the need for large sample sizes and the inability to parse out effects from other genetic or environmental risk factors. Genetic animal models allow us to screen candidate modifier genes, as well as to identify novel modifiers within a controlled biological system.

The goal of this dissertation is to investigate the role of the VGSC genes *SCN3A* and *SCN9A*, as epilepsy genes and as candidate modifiers for *SCN1A*-derived epilepsy. This introduction will first provide a brief history of the genes implicated in epilepsy, then background on the structure, physiology, and distribution of VGSCs, followed by a more extensive discussion of the role of VGSCs in epilepsy. I will then discuss human and animal studies of genetic modifiers in epilepsy syndromes, with particular emphasis

on those derived from mutations in *SCN1A*. Finally, the specific aims of this dissertation will be introduced.

1.2 The History of Gene Discovery in Monogenic Epilepsies

The first evidence that epilepsy had a genetic component originated from studies that showed increased risk in the relatives of patients with epilepsy, and greater risk in monozygotic versus dizygotic twins (Lennox, 1951, Jennings and Bird, 1981, Annegers et al., 1982, Vadlamudi et al., 2004). Decades after these early epidemiological studies, the first identified inherited epilepsy gene, *CHRNA4*, encoding the α4 subunit of the neuronal acetylcholine receptor, was discovered in a family with benign neonatal familial convulsions and a patient with autosomal dominant nocturnal frontal lobe epilepsy (Beck et al., 1994, Steinlein et al., 1995). For the next several years, linkage analysis studies of families with monogenic epilepsy syndromes yielded a number of mutations in ion channel genes, such as potassium channels, calcium channels, GABA receptors, and voltage-gated sodium channels (Singh et al., 1998, Wallace et al., 1998, Escayg et al., 2000, Sugawara et al., 2001, Wallace et al., 2001, Chen et al., 2003). To date, more than 1200 epilepsy mutations have been identified in the VGSCs, integral membrane proteins which initiate and propagate action potentials in excitable cells (Lossin, 2009, Meng et al., 2015). These initial gene discoveries lead to the hypothesis that epilepsy was a channelopathy, a disorder caused by dysfunction of ion channels (Ptacek, 1997, Biervert et al., 1998, Charlier et al., 1998, Wallace et al., 1998, Escayg et al., 2000, Hirose et al., 2000, Claes et al., 2001, Escayg et al., 2001, Cossette et al., 2002, Robinson et al., 2002).

Tremendous progress has since been made in the identification of epilepsy genes due to modern genetic technologies, and the types of genes implicated in epilepsy have

since expanded to include genes involved in cell signaling, migration, transport, and transcription (Myers and Mefford, 2015, Noebels, 2015, McTague et al., 2016). Approximately 40-70% of epilepsy syndromes are now thought to have a genetic basis, and it is now understood that most common genetic epilepsy syndromes are complex, polygenic disorders (Shorvon, 2011, Hildebrand et al., 2013). Mutations in ion channels are still primarily observed in the rare monogenic epilepsy disorders (Subaran and Greenberg, 2014). However, the study of ion channel mutations, particularly mutations in VGSCs, has been vital to our understanding of the etiology, diagnosis, and treatment of epilepsy syndromes.

1.3 Voltage-gated sodium channels: Structure, Physiology, and Distribution

1.3.A. Molecular Structure and Physiology

VGSCs are transmembrane proteins that mediate the influx of sodium ions (Na^+) into cells in response to changes in the cellular membrane potential. These ion channels were first discovered by Hodgkin and Huxley while studying electrical signaling in giant squid axons (Hodgkin and Huxley, 1952c, d, b, a). VGSCs have since been shown to consist of a large (260 kDa) alpha subunit which can associate with one or two smaller (30-40 kDa) beta subunits (Hartshorne and Catterall, 1981). The alpha subunit is composed of four transmembrane domains linked as a single chain by large intracellular loops (Fig. 1.1).

Each transmembrane domain is composed of six helical segments indicated as S1-S6 (Fig. 1.1). The S4 segment corresponds to the positively charged voltage sensor, which changes in conformation in response to depolarization of the membrane, thereby regulating the opening of the channel pore (Yang and Horn, 1995, Chanda and Bezanilla,

2002, Goldschen-Ohm et al., 2013) (Fig. 1.1). The S5 and S6 segments, which are

connected by extracellular linkers called P loops, serve as the pore of the channel (Fig.

1.1). The narrowest region in the channel pore is the selectivity filter, or constriction site,

which exclusively recognizes the size and charge of sodium ions. The selectivity filter is

composed invariably of the residues aspartate (D), glutamate (E), lysine (K), and

asparagine (A) (Heinemann et al., 1992). Studies have demonstrated that the lysine

residue is indispensable for Na^+ selectivity, while either of the carboxyl groups, aspartate

or glutamate, are also necessary to differentiate between Na^+ and K^+ ions (Favre et al.,

1996). There have been a number of hypotheses proposed to explain the Na^+ preference

of the selectivity filter. Favre et al. proposed that the salt bridge between lysine and

aspartate/glutamate constricts the channel pore, conferring Na^+ selectivity (Favre et al.,

1996). Later simulations by Lipkind and Fozzard suggested that the process is more

dynamic, as Na^+ is a stronger alkali metal cation and can therefore successfully repel the

lysine side chain, unblocking the constriction site (Lipkind and Fozzard, 2008).

     There are three functional states of VGSCs: closed (or deactivated), open (or

activated), and inactivated. Sodium channels are closed at rest, activating in response to a

depolarizing shift in the membrane potential of the cell. Once the channels open, the

rapid influx of Na^+ ions causes a sharp increase in depolarization until, within

milliseconds, the channels inactivate. The cell then repolarizes due to the opening of

voltage-gated potassium channels, ultimately returning to the resting membrane potential.

While the opening of the channel is dictated by conformational changes in the voltage

sensors (S4), inactivation is controlled by an inactivation gate, which lies within the

intracellular loop connecting domains DIII and DIV (Eaholtz et al., 1994, Goldin, 2003)

(Fig. 1.1). The prevailing theory for fast inactivation is the "ball and chain" or "hinged lid" model, in which the DIII-DIV intracellular loop swings up to bind to a docking site, thereby occluding the channel pore (Joseph et al., 1990).

As previously mentioned, alpha subunits of VGSCs can be bound by auxillary beta subunits (Fig. 1.1). There are four beta subunits genes (*SCN1B, SCN2B, SCN3B, SCN4B*), encoding the following proteins: β1, β1B (a splice variant of β1), β2, β3, and β4. The subunits β1 and β3 bind non-covalently to alpha subunits, while β2 and β4 bind through disulfide chains (Hartshorne and Catterall, 1984, Morgan et al., 2000, Yu et al., 2003). The beta subunits are transmembrane proteins with the exception of β1B, which is soluble (Patino et al., 2011). While not essential for a functional sodium channel, beta subunits play a critical role in the excitability and trafficking of alpha subunits (Hanlon and Wallace, 2002). Moreover, they are members of a cell adhesion molecule superfamily (CAMs), binding to each other, other adhesion proteins, or directly to the extracellular matrix (Malhotra et al., 2000).
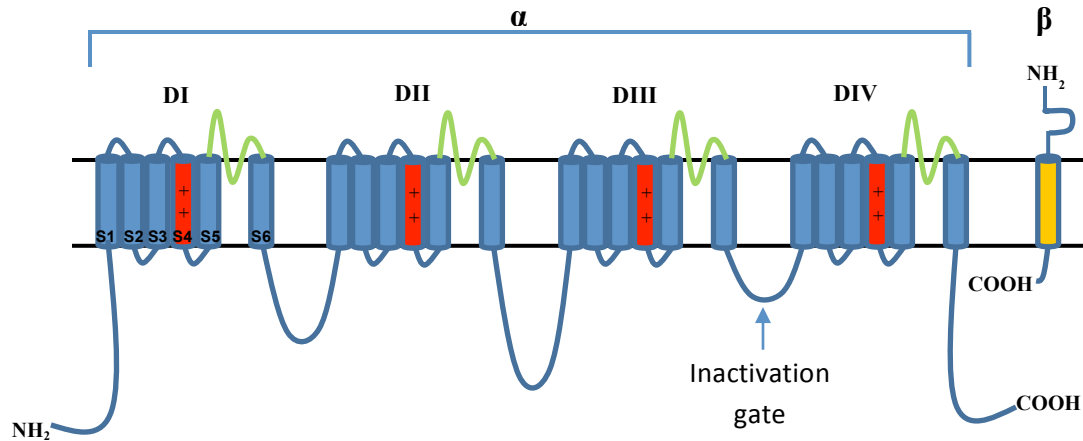
Figure 1.1 Representation of the α and β subunits of the voltage-gated sodium channel.

The VGSC alpha subunit consists of four homologous transmembrane domains (DI-DIV), each with six helical segments (S1-S6). Segment four of each domain (shown in red) is the positively charged voltage sensor, which regulates the channel pore opening. The loop connecting segments 5 and 6 (shown in green) forms the sodium-selective channel pore. The inactivation gate is located within the intracellular loop linking DIII and DIV. The VGSC β subunits (shown in gold), are single transmembrane segments that play a critical role in α subunit excitability and trafficking.

1.3.B. Genomic, Regional and Cellular Distribution of Subunits

There are nine distinct VGSC alpha subunits (*SCN1A, SCN2A, SCN3A, SCN4A, SCN5A, SCN8A, SCN9A, SCN10A,* and *SCN11A*), encoding proteins $Na_v1.1$, $Na_v1.2$, $Na_v1.3$, $Na_v1.4$, $Na_v1.5$, $Na_v1.6$, $Na_v1.7$, $Na_v1.8$, and $Na_v1.9$ respectively (Goldin et al., 2000). Standard gene nomenclature dictates that human gene names be capitalized and italicized, while protein is capitalized without italics. Gene names for other species are italicized, but only the first letter of each gene is capitalized. Similar to human protein names, non-human proteins are written without italics. In this dissertation, the two protein forms (i.e. $Na_v1.1$ and SCN1A) will be used interchangeably.

The VGSCs vary in chromosomal location, sensitivity to the neurotoxin tetrodotoxin (TTX), and expression pattern. Tetrodotoxin-sensitive *SCN1A, SCN2A, SCN3A,* and *SCN9A* are clustered on human chromosome 2q23-24 and mouse chromosome 2, suggesting that these channels arose through evolutionary duplication events. *SCN4A* is localized to human chromosome 17q23-25 and mouse chromosome 11. *SCN5A, SCN10A,* and *SCN11A,* which are the only VGSCs resistant to tetrodotoxin, are grouped within human chromosome 3p21-24 and mouse chromosome 9. *SCN8A* is located on human chromosome 12q13 and mouse chromosome 15. The beta subunit *SCN1B* is located on human chromosome 19q13 and mouse chromosome 7. *SCN2B-SCN4B* are found on human chromosome 11q23 and mouse chromosome 9. Since tetrodotoxin blocks VGSCs by targeting the channel pore, beta subunits, which lack a pore site, are unresponsive to this toxin (Terlau et al., 1991).

All VGSCs are primarily expressed in the nervous system with the exception of *SCN4A* and *SCN5A. SCN4A,* is expressed primarily in skeletal muscle, while *SCN5A* is

found primarily in the heart (George et al., 1991, Gellens et al., 1992). The remaining VGSC alpha subunits can be divided into those primarily found in the central nervous system (*SCN1A, SCN2A, SCN3A, SCN8A*) and those primarily in the peripheral nervous system (*SCN9A, SCN10A, SCN11A*). This chapter will highlight the expression patterns of VGSCs in the central nervous system (CNS), as well as the peripheral nervous system (PNS) VGSC *SCN9A*. The VGSCs are described in order of their significance to the experiments within this dissertation.

Scn1a mRNA and protein levels are barely detectable in rodents during the first postnatal week and increase rapidly to adult levels from the second week to the fourth week (Beckh et al., 1989, Felts et al., 1997b, Gong et al., 1999, Cheah et al., 2013). Similarly, human *SCN1A* expression is low at birth and increases to adult levels during postnatal development (Felts et al., 1997a, Cheah et al., 2013). In adulthood, rodent *Scn1a* is expressed throughout the central nervous system, including interneurons and pyramidal neurons in the cortex, pyramidal neurons of the hippocampal regions CA1-3, the granule layer of the dentate gyrus, the cerebellar Purkinje and granule cells, and spinal motor neurons (Westenbroek et al., 1989, Black et al., 1994, Gong et al., 1999). Although expression is observed in some excitatory neurons, *Scn1a* is preferentially expressed in inhibitory interneurons, particularly parvalbumin-expressing interneurons (Yu et al., 2006, Ogiwara et al., 2007, Dutton et al., 2013, Papale et al., 2013). Additionally, immunohistochemical studies from our lab revealed that *Scn1a* is expressed in a minority of orexinergic, serotonergic, and cholinergic neurons in the hypothalamus and brainstem (Papale et al., 2013). *Scn1a* is localized to the soma and dendrites of inhibitory and excitatory neurons, suggesting that this channel plays a role in

backpropagation of action potentials from the axon into the dendrites, as well as the generation of dendritic spikes (Westenbroek et al., 1989, Lai and Jan, 2006, Araya et al., 2007, Dutton et al., 2013). Scn1a is also abundantly expressed at the nodes of Ranvier and the axon initial segments of inhibitory interneurons, evidence that it is directly responsible for axonal action potential initiation and propagation (Ogiwara et al., 2007, Duflocq et al., 2008, Lorincz and Nusser, 2008).

SCN3A is the only VGSC expressed predominantly in the embryonic and early postnatal brain of both rodents and humans (Beckh et al., 1989, Brysch et al., 1991, Felts et al., 1997b, Gazina et al., 2010, Cheah et al., 2013). In humans, *SCN3A* RNA and protein levels decline during development but it remains widely expressed in the adult brain (Chen et al., 2000, Whitaker et al., 2000, Whitaker et al., 2001b). Rodent *Scn3a* expression, however, declines more dramatically during development (Beckh et al., 1989, Brysch et al., 1991, Felts et al., 1997b, Gazina et al., 2010, Cheah et al., 2013). The consensus of in situ hybridization studies is that *Scn3a* is at low abundance in the adult rodent central nervous system (Brysch et al., 1991, Felts et al., 1997b). However, an immunohistochemical study reported moderate to intense staining in regions such as the cortex, hippocampus, cerebellum, basal ganglia, midbrain, brainstem, olfactory system, and spinal cord (Lindia and Abbadie, 2003). Similar to *Scn1a*, *Scn3a* is localized to the soma and dendrites of most neurons (Whitaker et al., 2001b, Lindia and Abbadie, 2003). *Scn3a* expression is also robust in the axons of neurons in the olfactory system, the striatum, and the cerebellum (Lindia and Abbadie, 2003, Weiss et al., 2011). Little is known about the cell-specific expression of *Scn3a* in the brain. Since studies have identified *Scn3a* expression in granule cells of the dentate gyrus and cerebellum, it can be

assumed that *Scn3a* is expressed in excitatory neuron types (Brysch et al., 1991, Whitaker et al., 2001b, Lindia and Abbadie, 2003). There is also evidence that *Scn3a* is expressed in GABAergic inhibitory interneurons. In *Scn1a* null mice, compensatory upregulation of *Scn3a* is observed in inhibitory interneurons of the dentate gyrus (Yu et al., 2006). Furthermore, a microarray study of genes in parvalbumin-expressing GABAergic interneurons of the mouse cortex revealed high *Scn3a* expression in the first two postnatal weeks, suggesting that *Scn3a* plays a role in inhibition during development (Okaty et al., 2009).

SCN9A has been historically classified as a PNS gene, since it is abundantly expressed throughout the PNS of humans and rodents, particularly in the dorsal root ganglion, sympathetic ganglion, and olfactory sensory neurons (Felts et al., 1997b, Sangameswaran et al., 1997, Toledo-Aral et al., 1997, Weiss et al., 2011). *Scn9a* expression in the brain has not been studied extensively; however, low to moderate RNA and protein levels has been observed in the cortex, hippocampus, spinal cord, and olfactory bulbs (Belcher et al., 1995, Sangameswaran et al., 1997, Raymond et al., 2004, Mechaly et al., 2005, Candenas et al., 2006, Weiss et al., 2011). Abundant expression has also been reported in brainstem nuclei and in the HPA axis, suggesting that *Scn9a* may play a role in the autonomic nervous system (Ahmad et al., 2007, Morinville et al., 2007). In both CNS and PNS neurons, *Scn9a* is localized primarily to axons and soma (Toledo-Aral et al., 1997, Rush et al., 2005, Morinville et al., 2007). Although *Scn9a* is primarily expressed in sensory and motor neurons, this gene was also observed to be highly expressed in adult parvalbumin-expressing inhibitory interneurons of the mouse cortex (Okaty et al., 2009).

In early development, *Scn2a* is expressed in premyelinated axons and is gradually replaced by *Scn8a* at the maturing nodes of Ranvier. In adulthood, *Scn2a* is localized primarily to the axons of unmyelinated excitatory neurons in regions such as the hippocampus, cortex, cerebellum and the globus pallidus (Westenbroek et al., 1989, Gong et al., 1999, Boiko et al., 2003). Generally, *Scn2a* is expressed in more rostral brain regions, such as the cortex, hippocampus, and the striatum, while *Scn1a* has a more caudal distribution (Gordon et al., 1987, Beckh et al., 1989, Furuyama et al., 1993, Black et al., 1994).

Scn8a is not detectable by Western blot analysis until P10, by which time mRNA and protein expression steadily increases, reaching adult levels at the fourth postnatal week (Boiko et al., 2001, Van Wart and Matthews, 2006, Makinson et al., 2014). As the most widely expressed VGSC in the brain, *SCN8A* is distributed throughout the cortex, hippocampus, and cerebellum of humans and rodents (Whitaker et al., 1999a, Whitaker et al., 1999b, Schaller and Caldwell, 2000, Candenas et al., 2006). In adulthood, *Scn8a* is abundantly expressed in the axon initial segment, nodes of Ranvier, and synapses throughout the brain (Caldwell et al., 2000, Boiko et al., 2003, Duflocq et al., 2008). *Scn8a* also has a somatodendritic localization in many neurons, suggesting that this VGSC may also play a role in backpropagation of action potentials (Caldwell et al., 2000, Krzemien et al., 2000). *Scn8a* has been shown to be expressed in both pyramidal and inhibitory interneurons (Lorincz and Nusser, 2008, Royeck et al., 2008).

1.4 Role of Voltage-gated Sodium Channels in Epilepsy

Since VGSCs are the primary mediators of excitability in neurons of the central nervous system, it is unsurprising that the subtypes expressed in the central nervous system have been implicated in epilepsy, a disorder of hyperexcitability in the brain. The following section will discuss the specific role of VGSCs as epilepsy disease genes.

1.4.A. *SCN1A* in Epilepsy

SCN1A mutations have been identified in intractable childhood epilepsy with generalized tonic-clonic seizures and migrating partial seizures of infancy (Fujiwara et al., 2003, Carranza Rojo et al., 2011). However, *SCN1A* mutations are primarily responsible for two syndromes: genetic epilepsy with febrile seizures plus (GEFS+) and Dravet syndrome (DS) (Escayg et al., 2000, Claes et al., 2003, Surovy et al., 2016a, Usluer et al., 2016). GEFS+ is a genetically and clinically heterogeneous disorder characterized by febrile seizures that persist beyond six years of age and the development of afebrile seizure types (Scheffer and Berkovic, 1997, Singh et al., 1999). *SCN1A* missense mutations account for 10% of GEFS+ cases, and within GEFS+ families, individuals with the same *SCN1A* mutation frequently vary in seizure phenotype and severity (Scheffer et al., 2009, Goldberg-Stern et al., 2014, Hoffman-Zacharska et al., 2015, Passamonti et al., 2015).

Dravet syndrome is a catastrophic epileptic encephalopathy in which patients experience febrile seizures followed by severe, typically refractory afebrile seizures within the first year of life (Dravet, 2011). In addition to severe seizures, DS is characterized by hyperactivity, sleep disorders, intellectual disability, ataxia, and increased mortality (Wolff et al., 2006, Dhamija et al., 2014, Berkvens et al., 2015).

Patients with DS may also have a comorbid diagnosis of autism. *SCN1A* mutations, which include missense, nonsense, and truncation mutations, are identified in approximately 70-80% of DS patients, and 80% of these mutations are *de novo* (Marini et al., 2007).

SCN1A epilepsy mutations are overwhelmingly loss of function (Meng et al., 2015). Given the fact that epilepsy is characterized by hyperexcitability, it was not initially understood how decreased VGSC function could produce a seizure phenotype. Mouse models have been used to investigate the consequences of *Scn1a* dysfunction *in vivo*. Global *Scn1a* knockout mice have been shown to recapitulate the Dravet syndrome phenotype, including generalized seizures, increased susceptibility to hyperthermia-induced seizures, ataxia, autistic behaviors, increased mortality, and sleep abnormalities (Mulley et al., 2006, Kalume et al., 2007, Ogiwara et al., 2007, Oakley et al., 2009, Han et al., 2012, Kalume, 2013). Electrophysiological studies in these mice showed that sodium current is significantly reduced in inhibitory interneurons of the cortex, hippocampus, and cerebellum, resulting in loss of sustained, high frequency firing (Yu et al., 2006, Kalume et al., 2007, Ogiwara et al., 2007). These studies provided the foundation for the hypothesis that loss of *Scn1a* causes hyperexcitability by reducing neuronal inhibition. Later studies of conditional knockout mice provided further insight into the mechanisms of *Scn1a* dysfunction. Selective deletion of *Scn1a* in GABAergic interneurons in the forebrain was shown to be sufficient to cause spontaneous seizures and premature lethality (Cheah et al., 2012). Our lab and another group both demonstrated that specific deletion of *Scn1a* from parvalbumin-expressing interneurons also reproduces the seizure phenotype and reduced lifespans observed in global knockout

mice, while deleting *Scn1a* in excitatory neurons does not alter seizure susceptibility (Dutton et al., 2013, Ogiwara et al., 2013). These studies indicate that dysfunction of *Scn1a* in inhibitory interneurons is primarily responsible for the Dravet syndrome phenotype.

The disinhibition model for *SCN1A*-derived disorders is also supported by studies of GEFS+. Our lab has generated two mouse models carrying the human GEFS+ *SCN1A* mutation R1648H: a BAC transgenic mouse and a knock-in mouse line (Escayg et al., 2000, Tang et al., 2009, Martin et al., 2010). In the transgenic mice, the R1648H mutation reduced sodium current, delayed recovery from inactivation and increased use-dependent inactivation exclusively in inhibitory interneurons (Tang et al., 2009). Consistent with the BAC transgenic mouse model, cortical inhibitory interneurons of R1648H knock-in mice (*Scn1a^{RH}*) also exhibited reduced sodium current and increased use-dependent inactivation, along with reduced action potential firing (Martin et al., 2010). A recent study revealed a direct link between reduced firing in inhibitory interneurons from *Scn1a^{RH}* mutant mice and reduced GABAergic inhibition of excitatory neurons (Hedrich et al., 2014). Taken together, these studies demonstrate that loss of function in *Scn1a* results in network disinhibition and, subsequently, hyperexcitability.

1.4.B *SCN3A* in Epilepsy

Upregulation of *SCN3A* has been reported in the hippocampus of epilepsy patients as well as rat epilepsy models, suggesting that *SCN3A* might also play a role in the hyperexcitability observed in epilepsy (Aronica et al., 2001, Whitaker et al., 2001a, Guo et al., 2008, Xu et al., 2013). In 2008, the first epilepsy mutation in *SCN3A*, K354Q, was identified in a patient with childhood partial epilepsy (Holland et al., 2008).

Electrophysiological analysis later revealed that the K354Q mutation increased persistent and ramp currents in HEK293 cells and produced spontaneous firing in hippocampal neurons (Estacion et al., 2010). To date, only five additional *Scn3a* epilepsy mutations have been identified, four of which were found in patients with focal epilepsy and mild to no developmental abnormalities (Vanoye et al., 2014). These mutations resulted in increased persistent sodium current and elevated ramp currents in tsA201 cells, suggesting gain of function (Vanoye et al., 2014). In contrast, the fifth discovered *SCN3A* mutation, N302S, was identified in a GEFS+ patient with severe intellectual disability and resulted in depolarizing shifts in voltage-dependent activation and inactivation, as well as slower recovery from slow inactivation, thus predicting a reduction in channel function (Chen et al., 2015). In Chapter 2 of this dissertation (Lamar et al., 2017), we report another loss of function *SCN3A* mutation, L247P, in a patient with partial epilepsy and autonomic dysfunction. **Table 1.1** summarizes all the *SCN3A* mutations reported to date and their clinical presentation. To date, no other loss of function mutations have been reported. Furthermore, although the human mutations have been functionally characterized, the role of *Scn3a* dysfunction in epilepsy has not been studied in vivo. In Chapter 2 of this dissertation, I report a novel, trafficking-deficient *SCN3A* mutation in a patient with focal epilepsy. In addition, I investigate the role of *Scn3a* deficiency in vivo by characterizing the seizure and behavioral phenotype of an *Scn3a* hypomorphic mouse line.

Table 1.1 Summary of SCN3A epilepsy variants

SCN3A Variant	Location	Age of onset	Behavior	Seizure type	Family Seizures	Refractory	Treatment	References
K354Q	DI S5-S6 linker	2 yrs	Normal	focal	Father (carrier)	YES	Carbamazepine Oxcarbazepine	(Holland et al., 2008)
R357Q	DI S5-S6 linker	4 yrs	ADHD, speech delay	Focal w/ secondary GE	cousin w/ FS	NO	Carbamazepine	(Vanoye et al., 2014)
D766N	DII S2	22 mths	Nonverbal learning disability	Focal	NO	NO	Carbamazepine	
E111K	DII-DIII loop	2 days	Normal	Focal	Paternal aunt	NO	Phenobarbital	
M1323V	DIII S5-S6 linker	16 mths	Normal	Focal + FS	Mother ; paternal grandfather	NO	Oxcarbazepine	
N302S	DI S5-S6 linker	N/A	ID	GEFS+	N/A	N/A	N/A	(Chen et al., 2015)
L247P	DI S5	1 wk	GDD, speech delay	Focal	NO, de novo	YES	N/A	(Lamar et al., 2017)

Abbreviations: yr – years, mths – months, wk – week, ADHD – Attention Deficit Hyperactivity Disorder, ID – intellectual disability, GDD – global developmental delay, GE – generalized epilepsy, FS – febrile seizures, GEFS+ - genetic epilepsy with febrile seizures plus

1.4.C. *SCN9A* in Epilepsy

Singh et al. (2009) identified the *SCN9A* missense mutation N641Y in a large Utah pedigree in which all but one mutation-positive family member exhibited seizure phenotypes ranging from simple febrile seizures to refractory temporal lobe epilepsy (Singh et al., 2009). The N641Y mutation was subsequently knocked into the mouse *Scn9a* gene and the homozygous mutant mice were found to be more susceptible than wild-type (WT) littermates to electrically induced seizures (Singh et al., 2009). Singh et al. (2009) also identified nine inherited *SCN9A* missense mutations in a cohort of 110 unrelated DS patients, five of which were also positive for *SCN1A* mutations. These patients expressed *SCN1A* missense mutations that would be predicted to have modest functional impact, leading to the hypothesis that altered *SCN9A* function might have contributed to the severe epilepsy phenotype observed in these patients. In a more recent study, fifteen additional *SCN9A* variants were identified in a screen of 125 DS patients, nine of which were found in patients also positive for *SCN1A* mutations (Mulley et al., 2013b). Although eight of the identified *SCN9A* mutations were predicted to be potentially pathogenic, it is unclear whether they are disease-causing or risk factors. To determine whether *SCN9A* can influence the phenotype of *SCN1A*-derived epilepsy, I analyzed the seizure susceptibility of mice heterozygous for both the $Scn9a^{NY}$ and $Scn1a^{RH}$ mutations ($Scn9a^{+/NY}/Scn1a^{+/RH}$, Appendix B)

1.4.D. *SCN2A* in Epilepsy

Mutations in *SCN2A* are most commonly identified in patients with benign familial neonatal-infantile seizures, which is characterized by seizures that begin suddenly within the first year of life and remit by thirteen months (Heron et al., 2002,

Schwarz et al., 2016). A growing number of *SCN2A* mutations have also been reported in GEFS+, intractable childhood epilepsy, Dravet syndrome, and epileptic encephalopathy (Haug et al., 2001, Sugawara et al., 2001, Kamiya et al., 2004, Ogiwara et al., 2009, Shi et al., 2009, Howell et al., 2015, Saitoh et al., 2015). The majority of *SCN2A* mutations are missense; however, electrophysiological analyses revealed both gain and loss of function effects (Misra et al., 2008, Liao et al., 2010).

1.4.E. *SCN8A* in Epilepsy

Until recently, the role of *SCN8A* in epilepsy was unknown. In 2012, a gain of function *SCN8A* mutation was identified in a patient with epileptic encephalopathy (Veeramah et al., 2012). Subsequent studies have reported various, usually *de novo*, mutations in patients with epileptic encephalopathy (Carvill et al., 2013, Epi et al., 2013, de Kovel et al., 2014, Estacion et al., 2014, Ohba et al., 2014, Vaher et al., 2014, Blanchard et al., 2015, Boerma et al., 2016, Butler et al., 2016). Recently, *SCN8A* mutations have been identified in patients with benign infantile seizures, thus expanding the phenotype of *SCN8A*-related epilepsy to include milder syndromes (Anand et al., 2016, Gardella et al., 2016). Similar to *SCN3A* and *SCN2A*, most mutations are missense and can exhibit gain of function or loss of function effects (de Kovel et al., 2014, Estacion et al., 2014, Berghuis et al., 2015, Blanchard et al., 2015, Boerma et al., 2016).

1.5 Genetic Modifiers in Epilepsy

As mentioned previously, the variable penetrance and expressivity of monogenic epilepsy syndromes can be explained, in part, by the presence of modifier genes. Modifier genes have been identified in a wide range of monogenic disorders with Mendelian inheritance, such as cystic fibrosis, Huntington's disease, neurofibromatosis

type 1, muscular dystrophy, and sickle cell anemia (Steinberg and Adewoye, 2006, Heydemann et al., 2007, Sabbagh et al., 2009, Becanovic et al., 2015, Corvol et al., 2015). Modifier genes can exacerbate, reduce, alter, or mask disease phenotypes; therefore, the identification of such genes is crucial to both diagnosis and treatment of epilepsy syndromes. Below, I summarize the human and animal studies that have identified or examined the effects of candidate modifier genes in monogenic epilepsy.

1.5.A. Human Studies

To date, a limited number of studies have identified putative modifier genes or modifier loci in families with inherited epilepsy syndromes. In the first of these studies, linkage analysis was performed on a four generation family with a phenotype of febrile seizures, febrile seizures plus (FS+) and childhood absence epilepsy (CAE) (Marini et al., 2003). In most affected family members, a mutation in the GABA receptor gene GABRG2 segregated with febrile seizures and epilepsy (Wallace et al., 2001). Additional loci were identified exclusively in individuals with CAE, including chromosome 10, 13, 14, and 15, raising the possibility that interaction between genes in these loci and GABRG2 is required to produce the CAE phenotype (Marini et al., 2003). A few years later, another four-generation family was identified with febrile seizures, temporal lobe epilepsy, and CAE (Nabbout et al., 2007). The febrile seizure phenotype, which was present in all affected family members, was mapped to chromosome 3, while all individuals with temporal lobe epilepsy or CAE also shared haplotypes on chromosome 18, suggesting a modifier gene at this locus.

Copy number variants have also been proposed as modifiers of epilepsy syndromes. In a family with a 15q13.3 microdeletion disorder, a novel microduplication

in 16q22.1 was hypothesized to cause the intellectual disability and epilepsy phenotype (Banka et al., 2011). Similarly, a 19p13.2 deletion was implicated as a modifier of the clinical presentation in a family with a 16p11.2 deletion disorder (Bassuk et al., 2013) The 16p11.2 deletion is characterized by obesity and intellectual disability, while patients with both deletions also developed generalized epilepsy (Bassuk et al., 2013).

To date, only a few studies have identified putative human epilepsy modifier genes, several of which play a role in *SCN1A*-derived Dravet syndrome. A Dravet patient with a deleterious de novo mutation in *SCN1A* was also found to have a mutation in calcium channel CACNB4, which was inherited from a father with a history of febrile seizures and believed to exacerbate the Dravet phenotype (Ohmori et al., 2008). As mentioned previously, 14 mutations in *SCN9A* were identified in Dravet patients who were also positive for *SCN1A* missense mutations, suggesting that the combination of *SCN9A* and mild *SCN1A* mutations results in a more severe seizure phenotype (Singh et al., 2009, Mulley et al., 2013a).   In addition, a recent study discovered that Dravet patients with mutations in both the calcium channel *CACNA1A* and *SCN1A* experienced more frequent absence seizures than those with only *SCN1A* mutations (Ohmori et al., 2013). In a cohort of unrelated *SCN1A*-positive Dravet patients, two rare variants were identified in the mitochondrial gene *POLG* and proposed to worsen clinical presentation (Gaily et al., 2013). Beyond modifiers of *SCN1A*-derived epilepsy, a mutation in the nicotinic acetylcholine receptor *CHRNB2* was hypothesized to be responsible for the generalized seizure phenotype in a family with primary familial brain calcification (Fjaer et al., 2015).

Although genetic modifiers have been proposed to explain the heterogeneous phenotypes observed in many epilepsy syndromes, linkage analysis studies have yielded a paltry number of modifier genes and loci. As a comparison, studies in the monogenic disorder cystic fibrosis have successfully identified considerably more putative modifiers using linkage analysis, association studies, and candidate gene studies (Egan, 2016). I propose two observations to shed light on these divergent outcomes.

First, unlike disorders like cystic fibrosis, in which mutations in a single gene produce the phenotype, epilepsy is not a monogenic disorder. Although epilepsy syndromes with Mendelian inheritance exist, they are a rarity, while the vast majority of genetic epilepsy disorders are multifactorial and result from individual rare variants (Greenberg and Subaran, 2011). This complicates linkage analysis and association studies, which both require large sample sizes and shared mutations to achieve sufficient statistical power (Heinzen et al., 2012). Secondly, candidate gene studies have not been undertaken for genetic modifiers in epilepsy patients, even though they are more statistically powerful than genome-wide searches and more replicable than linkage analysis. The genes implicated in complex epilepsies have expanded dramatically over the past decade; however, monogenic syndromes are still dominated by ion channel and receptor mutations. It is possible, therefore, to prioritize and sequence genes that are likely to functionally interact with the primary disease gene. This method, once employed, may prove more effective than prior studies.

1.5.B. Animal Studies

One weakness of human studies is the inability to prove that identified mutations are causative. Surprisingly, the normal human genome contains a number of rare, and even potentially deleterious variants in known disease genes, suggesting that analyzing the biophysical effects of a mutation in vitro might not be sufficient to demonstrate pathogenicity (Claes et al., 2001, Pelak et al., 2010, Klassen et al., 2011, Cooper et al., 2013). Studies of genetic animal models allow us to investigate the functional validity of candidate disease and modifier genes in vivo. In this section, I will discuss how interstrain variation in epilepsy mouse models have led to the discovery of novel modifier genes. I will also describe studies that investigated interactions between epilepsy genes by crossing two mutant mouse lines.

For more than a decade, it has been recognized that variation in genetic background can alter susceptibility to seizures in both wild-type and mutant mice (Kosobud and Crabbe, 1990, Ferraro et al., 1995, Oliva et al., 2014, Leclercq and Kaminski, 2015). In particular, strain differences in mutant mouse models suggests the presence of modifier genes that alter the phenotype and severity of the primary mutation. The first modifier locus was identified in the *Scn8a^{med-j}* mouse, a *Scn8a* hypomorphic mouse model (Sprunger et al., 1999). Med-j mice exhibit severe paralysis and early lethality on the C57Bl/6J background, while mice on strain C3H have improved survival and ataxia. The responsible locus was mapped to chromosome 3, and the gene *Scnm1* was later identified as the modifier in this region (Buchner et al., 2003). Background strain variation has also been well-characterized in the transgenic gain of function *Scn2a^{Q54}* mouse. *Scn2a^{Q54}* mice on a SJL/J x C57BL/6J (BL6) mixed background have more

frequent seizures and a reduced lifespan compared to mutants on a congenic BL6 background, suggesting interaction between the primary mutation and a modifier gene within the SJL/J strain (Bergren et al., 2005). Genetic mapping and subsequent behavioral studies have implicated the genes *Hlf* and *Cacna1g* on chromosome 11 and *Kcnv2* on chromosome 19 (Bergren et al., 2009, Jorge et al., 2011, Hawkins and Kearney, 2012, Calhoun et al., 2016, Hawkins and Kearney, 2016). The phenotype of the Scn1a null mouse is also influenced by genetic variation in the background strain. *Scn1a*$^{+/-}$ mice have severe, spontaneous seizures and postnatal lethality on the C57BL/6J background, while heterozygotes on the 129X1/SVJ background have no discernible phenotype (Yu et al., 2006). Modifier loci were later detected on chromosomes 5, 7, 8, and 11 (Miller et al., 2014).

Mouse models have also been used to test possible interactions between two genes, including genes not previously identified in patients (Table 1.2). Connor et al. demonstrated that loss of both *Kvβ1* and *Kvβ2* genes leads to increased lethality compared with loss of either gene alone (Connor et al., 2005). Loss of function of *Kcnq2* has been shown to exacerbate the seizure phenotype and shorten the lifespan of *Scn2a*^{Q54} mice (Kearney et al., 2006). On the other hand, the combination of mutations in *Cacna1a* and *Kcna1*, which individually produce absence seizures and severe partial seizures respectively, results in the rescue of these phenotypes (Glasscock et al., 2007).

Studies of gene interactions in *Scn1a* mutant mice have yielded a number of candidate modifier genes (Table 1.2). Our own laboratory discovered that *Scn2a* and *Kcnq2* each interact with *Scn1a* to exacerbate the phenotype of mice expressing the human GEFS+ *SCN1A* R1648H mutation (Hawkins et al., 2011). We have also shown

that the $Scn8a^{med-jo}$ mutation can restore normal seizure thresholds and lifespans to heterozygous $Scn1a^{RH}$ mice (Hawkins et al., 2011) and to heterozygous $Scn1a$ knockout mice, a DS model (Martin et al., 2007). Taken together, these studies suggest that genetic modifiers may play an important role in altering the phenotypic consequences of $SCN1A$ dysfunction, either to increase severity or ameliorate the phenotype.

Table 1.2 Genetic interactions between mutations in epilepsy mouse models

Mutant mice	Phenotype of combined mutations	References
$Kv\beta2^{-/-}$ ↓ lifespan (20% lethality) sp. Seizures $Kv\beta1^{-/-}$ sp. seizures	↓ lifespan (50% lethality)	(Smart et al., 1998, Connor et al., 2005)
$Kcnq2^{SZT1/+}$ ↑ seizure susceptibility $Kcnq2^{V182M/+}$ ↑ seizure susceptibility $Scn2a^{Q54}$: ↓ lifespan (25% lethality) sp. Seizures	$Scn2a^{Q54}/Kcnq2^{SZT1/+}$ ↓ age of onset for sp. seizures ↓ lifespan (90% lethality) $Scn2a^{Q54}/Kcnq2^{V182M/+}$ ↓ age of onset for sp. seizures ↓ lifespan (90% lethality)	(Kearney et al., 2006)
$Cacna1a^{tg/tg}$ sp. seizures $Kcna1^{-/-}$ ↓ lifespan (74% lethality) sp. seizures ↑ hippocampal bursting	↑ lifespan (13% lethality) ↓ seizure susceptibility ↓ hippocampal bursting	(Glasscock et al., 2007)
$Scn1a^{+/RH, RH/RH}$ sp. seizures ↓ lifespan (RH/RH: 100%) ↑ seizure susceptibility $Kcnq2^{V182M/+}$ $Scn2a^{Q54}$ $Scn8a^{med-jo/+}$ ↓ seizure susceptibility sp. seizures	$Scn1a^{+/RH}/Kcnq2^{V182M/+}$ ↑ sp. seizures ↓ lifespan (53% lethality) $Scn1a^{+/RH}/Scn2a^{Q54}$ ↑ sp. seizures ↓ lifespan (100% lethality) $Scn1a^{+/RH}/Scn8a^{med-jo/+}$ ↓seizure susceptibility $Scn1a^{RH/RH}/Scn8a^{med-jo/+}$ ↑ lifespan (53% lethality)	(Hawkins et al., 2011)
$Scn1a^{+/-, -/-}$ Sp. Seizures ↓ lifespan (+/-: 100% , -/-: 100%) ↑ seizure susceptibility (+/-)	$Scn1a^{+/-}/ Scn8a^{med-jo/+}$ ↑ lifespan ↓ seizure susceptibility	(Martin et al., 2007)

1.6 Specific Aims

In Chapter 3 and Appendix B, I use mouse models expressing mutations in *Scn3a* and *Scn9a*, respectively, to evaluate the potential role of these two VGSCs as modifiers of the phenotype of the *Scn1a* R1648H knock-in mouse (*Scn1a^{RH}*, see Section 1.3.A), a model of GEFS+. The *Scn3a* mouse model used in these experiments (*Scn3a^{Hyp}*) is a hypomorphic gene trap mouse line. Although a small number of *SCN3A* mutations have been identified in epilepsy patients, all but one are gain of function mutations (Chen et al., 2014a, Vanoye et al., 2014). In Chapter 2, I characterized for the first time the effects of *Scn3a* deficiency *in vivo* on seizure susceptibility and behavior.

In addition to the role as a disease-causing gene, recent findings support the role of *SCN3A* as a candidate modifier of *SCN1A*-related disorders. Firstly, *SCN3A* and *SCN1A* are both found in the soma and dendrites of neurons in the central nervous system (Westenbroek et al., 1989, Westenbroek et al., 1992, Whitaker et al., 2001b). Secondly, the age at which *SCN3A* expression declines and *SCN1A* expression increases in humans and mice correlates with the age of onset of disease in DS patients with *SCN1A* mutations (Cheah et al., 2013). This correlation suggests that *SCN3A* might confer protection against loss of *SCN1A* in early development, thereby delaying disease progression. Thirdly, *Scn3a* was shown to be upregulated in hippocampal inhibitory interneurons of homozygous *Scn1a* null mice, providing support for *Scn3a* compensation in the presence of *Scn1a* dysfunction (Yu et al., 2006). In Chapter 3, I investigated whether *Scn3a* and *Scn1a* interact by crossing the *Scn3a^{Hyp}* mouse line with the *Scn1a^{RH}* line. The double heterozygous offspring (*Scn3a^{+/Hyp}/Scn1a^{+/RH}*) were evaluated for alterations in survival, seizure susceptibility, and behavioral deficits.

The second mouse model studied is the $Scn9a^{NY}$ mutant mouse, which carries the human epilepsy mutation N641Y as described in Section 1.3.C. As mentioned previously, a number of Dravet syndrome patients are positive for both *SCN9A* and missense *SCN1A* mutations, suggesting that *SCN9A* may modify the severity of the Dravet phenotype (Singh et al., 2009, Mulley et al., 2013a). To determine whether *Scn9a* interacts with *Scn1a,* the $Scn9a^{NY}$ mutant line was crossed with the $Scn1a^{RH}$ line to produce compound heterozygotes ($Scn9a^{+/NY}/Scn1a^{+/RH}$), which were evaluated for increased susceptibility to hyperthermia-induced and flurothyl-induced seizures (Appendix B). The results of this dissertation provide greater insight into the role of *Scn3a* and *Scn9a* in epilepsy.

1.7 Conclusions

Although epilepsy is a complex, genetically heterogeneous disorder, monogenic epilepsy syndromes have facilitated a better understanding of disease mechanisms and lead to the identification of potential genetic targets for treatments. Even within inherited, monogenic syndromes, however, variable penetrance and expressivity is observed, suggesting the presence of genetic modifiers. Identifying genetic modifiers in epilepsy patients has been challenging; nevertheless, epilepsy mouse models can be exploited in order to discover new modifier genes and to validate those identified in patient studies or proposed from *a priori* assumptions. This dissertation seeks to investigate two VGSCs, Scn3a and Scn9a, as disease genes and as modifiers of *Scn1a* dysfunction in a GEFS+ mouse model.

Chapter 2: *SCN3A* deficiency associated with increased seizure susceptibility

Adapted from:

2.1 Abstract

Mutations in voltage-gated sodium channels expressed highly in the brain
(*SCN1A*, *SCN2A*, *SCN3A*, and *SCN8A*) are responsible for an increasing number of
epilepsy syndromes. In particular, mutations in the *SCN3A* gene, encoding the pore-
forming $Na_v1.3$ α subunit, have been identified in patients with focal epilepsy.
Biophysical characterization of epilepsy-associated *SCN3A* variants suggests that both
gain- and loss-of-function *SCN3A* mutations may lead to increased seizure susceptibility.
In this report, we identified a novel *SCN3A* variant (L247P) by whole exome sequencing
of a child with focal epilepsy, developmental delay, and autonomic nervous system
dysfunction. Voltage clamp analysis showed no detectable sodium current in a
heterologous expression system expressing the SCN3A-L247P variant. Furthermore, cell
surface biotinylation demonstrated a reduction in the amount of SCN3A-L247P at the cell
surface, suggesting the SCN3A-L247P variant is a trafficking-deficient mutant. To
further explore the possible clinical consequences of reduced *SCN3A* activity, we
investigated the effect of a hypomorphic *Scn3a* allele (*Scn3a^{Hyp}*) on seizure susceptibility
and behavior using a gene trap mouse line. Heterozygous *Scn3a* mutant mice (*Scn3a$^{+/Hyp}$*)
did not exhibit spontaneous seizures nor were they susceptible to hyperthermia-induced
seizures. However, they displayed increased susceptibility to electroconvulsive (6 Hz)
and chemiconvulsive (flurothyl and kainic acid) induced seizures. *Scn3a$^{+/Hyp}$* mice also
exhibited deficits in locomotor activity and motor learning. Taken together, these results
provide evidence that loss-of-function of *SCN3A* caused by reduced protein expression or
deficient trafficking to the plasma membrane may contribute to increased seizure
susceptibility.

2.2 Introduction

Voltage-gated sodium channels (VGSCs) are responsible for the initiation and propagation of action potentials in excitable cells such as neurons. In the mammalian brain, the most highly expressed VGSC α subunits are *SCN1A, SCN2A, SCN3A*, and *SCN8A,* which encode $Na_v1.1$, $Na_v1.2$, $Na_v1.3$, and $Na_v1.6$ respectively. Mutations in these VGSCs are responsible for an increasing number of epilepsy syndromes (Escayg et al., 2000, Sugawara et al., 2001, Estacion et al., 2014, Fung et al., 2015, Howell et al., 2015, Schwarz et al., 2016, Surovy et al., 2016b). Mutations in *SCN1A* have been established as the main cause of Dravet syndrome and have also been identified in some families with generalized epilepsy with febrile seizures plus (GEFS+) (Scheffer et al., 2009, Escayg and Goldin, 2010, Volkers et al., 2011). *SCN2A* mutations have been identified in patients with benign familial neonatal-infantile seizures, and both *SCN2A* and *SCN8A* mutations have been identified in some cases of severe epileptic encephalopathies (Sugawara et al., 2001, Heron et al., 2002, Veeramah et al., 2012, de Kovel et al., 2014, Estacion et al., 2014, Hackenberg et al., 2014, Vaher et al., 2014).

To date, only a few *SCN3A* mutations have been identified in patients with focal epilepsy. Electrophysiological analysis of these mutations in either transfected rat hippocampal pyramidal neurons (Holland et al., 2008, Estacion et al., 2010) or tsA201 cells (Vanoye et al., 2014, Chen et al., 2015) revealed increased persistent sodium current or elevated ramp currents. In contrast, there is one report of an *SCN3A* mutation, N302S, identified through a genetic screen of GEFS+ patients, that resulted in depolarizing shifts in voltage-dependent activation and inactivation, as well as slower recovery from slow inactivation, thereby predicting a reduction in channel activity (Chen et al., 2015). These

results suggest that both gain- and loss-of-function *SCN3A* mutations may lead to epilepsy.

Epilepsy syndromes, including those caused by sodium channel mutations, are often accompanied by neuropsychiatric comorbidities, such as anxiety, autism spectrum disorders, and intellectual disability (Han et al., 2012, Baasch et al., 2014, de Kovel et al., 2014). Consistent with this, developmental delay or behavioral abnormalities have been reported in patients with *SCN3A* mutations. For example, one patient presented with speech delay and attention-deficit/hyperactivity disorder (Vanoye et al., 2014). Another patient was diagnosed with nonverbal learning disability, and the patient carrying the N302S mutation was diagnosed with intellectual disability (Chen et al., 2014b, Vanoye et al., 2014).

In this study, we report a novel *SCN3A* mutation (L247P) associated with childhood focal epilepsy and global developmental delay. Using a combination of electrophysiology and cell surface biotinylation experiments, we demonstrate that *SCN3A*-L247P encodes a trafficking deficient channel. To more broadly investigate the possible clinical consequences of reduced *SCN3A* activity, we characterized the seizure and behavioral phenotypes of the available *Scn3a*$^{Gt(OST52130)Lex}$ mouse line, which expresses a hypomorphic *Scn3a* allele (*Scn3a*^{Hyp}). Heterozygous mutants (*Scn3a*$^{+/Hyp}$) displayed increased susceptibility to induced seizures, but did not exhibit spontaneous seizures. Additionally, *Scn3a*$^{+/Hyp}$ mice showed deficits in locomotor activity and motor learning. These observations demonstrate that reduced *SCN3A* function via reduced trafficking or expression can result in increased seizure susceptibility.

2.3 Material and Methods

Clinical presentation

Parental consent for release of de-identified medical information was obtained. An 18 month-old female patient was evaluated due to concerns for global developmental delay, central hypotonia, right-sided renal pelviectasis, and microcephaly. She was the second child of a 39-year-old mother and 50-year-old father, both of whom denied consanguinity. The pregnancy was uncomplicated, amniocentesis was declined, and the child was born at full term. At birth, her weight was 2950 g (10%), her length was 50 cm (20%), and her head circumference was 33 cm (10%). Her Apgar scores were 9 and 9. At two days of age she had an episode of cyanosis, apnea, tonic posturing and bradycardia. EEG recording at that time was normal.

Beginning during the first week of life, two distinct types of episodes were observed, and occasionally coincided. The first type consists of a "scared look" followed by paroxysmal events, which include apnea, eyes rolling back, and limbs stiffening. These episodes occur approximately once a month and were subsequently identified as focal seizures. The second type of episode includes skin flushing and sweating and occurs several times a day for 30-second intervals. This clinical presentation is consistent with Harlequin syndrome, which is characterized by unilateral facial erythema with contralateral pallor that is strikingly demarcated at the midline. Although the color change is limited to the head, it can initiate on one side and shift to the other side within the same episode. This coincides with contralateral pupil dilation and ipsilateral ptosis. Video EEG at 14 months of age revealed right frontal-temporal electrographic seizures compatible with focal epilepsy. Various anticonvulsant medications were tried with

limited success. The EEG abnormalities were not associated with the autonomic changes; therefore, it was concluded that the episodes of autonomic dysregulation are not epileptic by nature. The patient also developed progressive microcephaly, although her brain and cervical spine MRIs were normal. A routine cardiology examination, which included EKG, echocardiogram, and Holter monitor, showed no abnormalities. On telemetry, however, several episodes of sinus and junctional bradycardia were noted and thought to correspond with vagal activity and the Harlequin flushing. The child was also diagnosed with global developmental delay. She did not sit without support until 16 months after birth and was still unable to walk on her last evaluation at two years of age. Her speech development was also delayed. Additionally, her height, weight and head circumference were below the third percentile for two year olds. She also had trunkal hypotonia and mid-face hypoplasia.

Metabolic screening was negative. Familial Dysautonomia was ruled out by observation of normal fungiform tongue papillae and normal axon flare on intradermal histamine testing. Chromosomal microarray analysis was normal. Clinical whole-exome sequencing revealed a single, novel, *de novo* heterozygous sequence change in the gene *SCN3A*, L247P. *In silico* analysis concluded that this change was "likely pathogenic". Other changes reported were deemed as "benign" or were rare population variants inherited from an unaffected parent, suggesting they were not pathogenic (Table A.1). Results were confirmed by Sanger sequencing.

Plasmids and Cell Transfection

Electrophysiology and biochemistry experiments were conducted using tsA201 cells (HEK-293 stably transfected with SV40 large T antigen) grown at 37°C with 5% CO_2 in Dulbecco's modified Eagle's medium (DMEM) supplemented with 10% fetal bovine serum, 2 mM L-glutamine, and penicillin (50 U/ml)-streptomycin (50 μg/ml). These cells are commonly used for functional analysis studies of voltage-gated sodium channel (Rhodes et al., 2004, Rusconi et al., 2009, Liu and Zheng, 2013). Only cells from passage number < 13 were used. A plasmid encoding the major splice isoform of the human *SCN3A* with exon 5 adult (5A) and exon 12v1 (646 bp) splice variants was used (Wang et al., 2010). Full-length $Na_v1.3$ was propagated in STBL2 cells at 30°C (Invitrogen), and the open reading frame of all plasmid preparations was fully sequenced prior to transfection. The L247P variant was introduced by site-directed mutagenesis. Plasmids encoding the human Na_v channel accessory subunits β1 or β2 in vectors containing the marker genes CD8 (pCD8-IRES-β1) or GFP (pGFP-IRES-β2) were also used.

For electrophysiology experiments, expression of $Na_v1.3$, β1, and β2 subunits was achieved by transient transfection (2 μg of total cDNA: *SCN3A*, β1, β2 mass ratio was 10:1:1) using Superfect Transfection Reagent (QIAGEN, Valencia, CA, USA). Cells were incubated as described above for 48 hours after transfection before use in electrophysiology experiments. For low temperature rescue experiments, cells were incubated for 24 hours at 37°C followed by 24 hours at 28°C prior to electrophysiology. Transfected cells were dissociated by brief exposure to trypsin/EDTA, resuspended in supplemented DMEM medium, plated on glass coverslips, and allowed to recover for ~2

hrs at 37°C or 28°C in 5% CO_2. Polystyrene microbeads pre-coated with anti-CD8 antibody (Dynabeads M-450 CD 8, Dynal, Great Neck, NY, USA) were added and only cells positive for both CD8 antigen (i.e., β1 expression) and GFP fluorescence (i.e., β2 expression) were studied.

For cell surface biotinylation experiments, expression of $Na_v1.3$, β1 and β2 subunits was achieved by transient transfection (2 μg of total cDNA: *SCN3A*, β1, β2 mass ratio was 10:1:1) using Lipofectamine 2000 (Life Technologies, Grand Island, NY, USA). Before use in these experiments, cells were incubated as described above for 48 hours after transfection.

Electrophysiology

Coverslips were placed into a recording chamber on the stage of an inverted epifluorescence microscope (IX 50, Olympus, Center Valley, PA, USA) and allowed to equilibrate for 10 min in bath solution prior to starting experiments. Bath solution contained (in mM): 145 NaCl, 4 KCl, 1.8 $CaCl_2$, 1 $MgCl_2$, 10 HEPES (N-(2-hydroxyethyl) piperazine-N′-2-ethanosulphonic acid), pH 7.35, 310 mOsm/kg. The composition of the pipette solution was (in mM): 10 NaF, 110 CsF, 20 CsCl, 2 EGTA (ethyleneglycol-bis-(β-aminoethylether), 10 HEPES, pH 7.35, 310 mOsm/kg. Osmolarity and pH values were adjusted with sucrose and NaOH, respectively. A 2% agar-bridge with composition similar to the bath solution was utilized as a reference electrode. Junction potentials were zeroed with the filled pipette in the bath solution. Unless otherwise stated, chemicals were obtained from Sigma-Aldrich (St. Louis, MO, USA).

Patch pipettes were pulled from thin-wall borosilicate glass (World Precision Instruments, Inc., Sarasota, FL, USA) using a multistage P-97 Flaming-Brown

micropipette puller (Sutter Instruments Co., San Rafael, CA, USA) and fire-polished with

a Micro Forge MF 830 (Narashige, Japan). After heat polishing, the resistance of the

patch pipettes was 1–3 MΩ in standard bath and pipette solutions. Once whole-cell

recording mode was achieved, the access resistance averaged 2.5 ± 0.1 MΩ. Whole-cell

sodium currents were recorded as previously described (Lossin et al., 2002, Vanoye et al.,

2006) at room temperature (20–23°C) in the whole-cell configuration of the patch-clamp

technique (Hamill et al., 1981) using an Axopatch 200B series amplifier (Molecular

Devices Corp, Sunnyvale, CA, USA). Cells were allowed to equilibrate for 10 min after

establishment of the whole-cell configuration before currents were recorded. Pulse

generation was performed with Clampex 8.1 (Molecular Devices Corp.) and whole-cell

currents were acquired at 20 kHz and filtered at 5 kHz. Linear leak and residual

capacitance artifacts were subtracted out using the P/4 method. To reduce voltage errors,

80–90% series resistance and prediction compensation were applied. Cells were excluded

from analysis if the predicted voltage error exceeded 3 mV or the current at the holding

potential (-120 mV) was >5% of the peak current.

Peak currents were measured using 20 ms pulses between -80 and +50 mV every

5 s from a holding potential of -120 mV. The peak current was normalized for cell

capacitance and plotted against voltage to generate peak current density–voltage

relationships.

Data were collected from at least 2 transient transfections per experimental

condition. Results are reported as means ± SEM, and number of cells used for each

experimental condition are listed on the legends or figures. Current values were

normalized to membrane capacitance.

Cell Surface Biotinylation

Forty-eight hours post-transfection, cell surface proteins of transfected tsA201 cells were labeled with cell membrane impermeable Sulfo-NHS-Biotin (Thermo Scientific, Waltham, MA, USA). The biotinylation reaction was quenched with 100mM glycine, and the cells were subsequently lysed with RIPA lysis buffer (Thermo Scientific) containing Complete protease inhibitors (Roche Applied Science, Indianapolis, IN, USA) and clarified by centrifugation. An aliquot of the supernatant was retained as the total protein fraction. Biotinylated surface proteins (300 to 600 μg per sample) were recovered from the remaining supernatant by incubation with streptavidin-agarose beads (Thermo Scientific) and elution in Laemmli sample buffer. Total (5 to 10 μg per lane) and surface fractions were analyzed by Western blotting using rabbit anti-pan VGSC α subunit (1:250; Alomone, Jerusalem, Israel), mouse anti-transferrin receptor (1:500; Life Technologies), and rabbit anti-calnexin (H70) (1:250; Santa Cruz Biotechnology, Dallas, TX, USA) primary antibodies. Peroxidase-conjugated mouse anti-rabbit immunoglobulin G (IgG; 1:20,000; Jackson ImmunoResearch, West Grove, PA, USA) and goat anti-mouse IgG (1:40,000, Jackson ImmunoResearch) secondary antibodies were utilized. Blots were probed for each protein in succession, stripping in between with Restore Western Blot Stripping Buffer (Pierce Biotechnology, Rockford, IL, USA). Calnexin immunoreactivity was present in total protein lysates and absent from cell surface fraction, confirming the selectivity of biotin labeling for cell surface proteins. Densitometry was performed using NIH ImageJ software. Transferrin receptor was

utilized as a loading control for $Na_v1.3$ immunoreactive bands. Surface fractions were analyzed from two independent transfections, while total fractions were analyzed from three independent transfections.

Mouse Model

The $Scn3a^{Gt(OST52130)Lex}$ mouse line (Lexicon Pharmaceuticals Inc.), containing a gene trap vector upstream of the first coding exon, was purchased from the Mutant Mouse Regional Resource Center (University of North Carolina at Chapel Hill, NC, USA). The line was maintained by backcrossing to C57BL/6J mice (Jackson Laboratories, Bar Harbor, ME, US). RNA and protein analysis in adult mice as well as all seizure and behavioral experiments were performed on heterozygous mutants and WT littermates generated by crossing N6-N7 $Scn3a^{+/Hyp}$ males to C57BL/6J females. WT, heterozygous, and homozygous littermates (P1) that were used for RNA and protein analysis were generated by mating heterozygous siblings from the N8-N9 generations. Mice were housed in an animal facility with a 12-hour light/dark cycle (lights on 7:00am – lights off 7:00pm) with food and water available *ad libitum*. All experiments were performed in accordance with the guidelines of the Emory University Institutional Animal Care and Use Committees. Unless stated otherwise, adult (4-6 month old) mice were used for the following experiments.

Genotyping

Genotyping was performed on DNA extracted from tail biopsies. To detect the wild-type allele, forward and reverse PCR primers were designed in the intronic sequences flanking the vector insertion site (3AF: GAGGATCAGGCTTAGCGGTG; 3AR: TCTGGTCTGTTATGTCAGAAGGC) to produce a 337 bp PCR product. To

detect the mutant allele, a forward primer was designed in the vector sequence (VECTF: TATGTATTTTTCCATGCCTTGC) and paired with the 3AR reverse primer to produce a 233 bp PCR product.

Quantitative real-time PCR (qRT-PCR)

Total RNA was extracted from whole brain samples of 1-day old (P1) homozygous ($Scn3a^{Hyp/Hyp}$; n = 3) and heterozygous ($Scn3a^{+/Hyp}$; n = 5) mutants and wild-type (WT; n = 4) littermates. RNA extraction and cDNA synthesis were performed as previously described (Makinson et al., 2014). PCR amplification of *Scn1a*, *Scn2a*, *Scn3a* and *Scn8a* was performed using primers designed to span two exons. The following primer pairs were used: *Scn1a* (F: CAGGAGGAAGGGGTTTCGCTTC, R: CCCCACATCCTTGGCTCGCCCTC), *Scn2a* (F: CTGCAACGGTGTGGTCTCCCTAG, R: ATGTAGGGTCTTCCAACAAGTCC), *Scn3a* (F: CCTGGACCCCTACTACGTCA, R: TGTGTACTCTACATTCTTCGTCCA), and *Scn8a* (F: AGATTTAGCGCCACTCCTGC, R: GGACCATTCGGGAGGGTTAC). Each primer pair produced standard curves with 90-100% efficiency. Real-time analysis was performed in technical triplicate using the BioRad CFX96 Real-Time PCR Detection System and SYBR Green fluorescent dye (BioRad, Hercules, CA, USA). Expression levels were normalized to beta-actin (F: CAGCTTCTTTGCAGCTCCTT, R: ACGATGGAGGGGAATACAGC). Expression relative to WT was determined using the Pfaffl calculation (Pfaffl, 2001).

Western Blot Analysis

Whole brains were extracted from P1 WT (n = 5), *Scn3a*$^{+/Hyp}$ (n = 6)*, and *Scn3a*$^{Hyp/Hyp}$ littermates (n = 4). Tissue was homogenized with a Dounce homogenizer in cold protease inhibitor buffer (50mM Tris, pH 7.5; 10mM EGTA; 1 protease inhibitor cocktail tablet (Roche) per 50mL of buffer). The homogenate solution was centrifuged at 3500 RPM for 10 minutes at 4°C. The resulting supernatant was centrifuged at 38,000 RPM for 30 minutes at 4°C. The membrane-enriched pellet was resuspended in protease inhibitor buffer and then stored at -80°C. Protein was quantified using the BCA protein assay (Pierce, Rockford, Il, USA). The protein (50 μg) was then denatured, separated by SDS-PAGE, and transferred to PVDF membrane. The membranes were blocked with 5% milk, then incubated at 4°C overnight with either polyclonal rabbit anti-Na$_v$1.1 (1:200; Millipore, Billerica, MA), Na$_v$1.2 (1:200; Millipore), Nav1.3 (1:200; Alomone), or Na$_v$1.6 (1:200; Millipore), followed by HRP-conjugated donkey anti-rabbit secondary antibody (1:3000; GE Healthcare Life Sciences, Little Chalfont, UK) for 1 hour. To normalize for variation in protein loading, membrane blots were also incubated for 1 hour with monoclonal mouse anti-tubulin (1:5000; Sigma-Aldrich) followed by HRP-conjugated goat anti-mouse secondary antibody (1:3000; Jackson ImmunoResearch). Following each secondary antibody, all blots were incubated in HyGlo Quick Spray (Denville Scientific, Holliston, MA, USA) and imaged. Protein expression was quantified using Image J software (NIH).

Hyperthermia-induced Seizures

Susceptibility to hyperthermia-induced seizures in P21-22 $Scn3a^{+/Hyp}$ mutants (n =

12) and WT littermates (n = 13) was determined as previously described (Dutton et al.,

2013). Since mice are not sexually mature at this age, results from male and female mice

were combined. Briefly, the body temperature of each mouse was monitored and

controlled via a rectal temperature probe that was connected to a heating lamp and

temperature controller (TCAT 2DF, Physitemp, Clifton, NJ, USA). Each mouse was

placed in a clear cylinder and held at 37.5°C for 10 minutes. The core body temperature

of each mouse was then increased by 0.5°C every two minutes until either a seizure

occurred or a temperature of 42.5°C was reached. The temperature at which each mouse

exhibited a GTCS was compared between genotypes. Behavioral seizures were also

scored using a modified Racine scale (Racine, 1972): 1 – staring, 2 – head nodding, 3 –

unilateral forelimb clonus, 4 – bilateral forelimb clonus, 5 – rearing and falling, 6 –

generalized tonic-clonic seizure (GTCS).

6 Hz Seizure Induction

The topical anesthetic tetracaine (0.5%, Bausch and Lomb, Rochester, NY, USA)

was applied to each eye 30 minutes prior to seizure induction. Adult male $Scn3a^{+/Hyp}$

mutants and WT littermates (n = 10/genotype) were subjected to 6 Hz corneal stimulation

(0.2 ms pulse width, 3 s duration) using an ECT unit (Ugo Basile; Comerio, Italy). Each

mouse was tested once per week, over a 3-week period, using a current of 16, 24, or 30

mA. Behavioral seizures were scored using a modified Racine scale: 0 – no seizure, 1 –

staring, 2 – forelimb clonus, and 3 – rearing and falling. For each genotype, the CC_{50} (the

convulsive current at which 50% of mice seize) was established as well as the average

Racine scores at each current.

Flurothyl Seizure Induction

Seizure induction using flurothyl (2,2,2-trifluroethyl ether, Sigma-Aldrich) was

performed as previously described (Martin et al., 2007, Makinson et al., 2014, Sawyer et

al., 2014). Briefly, 5-8 week old $Scn3a^{+/Hyp}$ male and female mutants (n = 29/sex) and

WT littermates (male n = 33; female n = 32) were placed in a clear chamber and flurothyl

was introduced at a constant rate of 20 µl/min. Latencies to the first myoclonic jerk, first

generalized tonic-clonic seizure (GTCS) with loss of posture, and hind limb extension

were recorded.

EEG cortical/depth electrode surgery

Electroencephalogram (EEG) electrodes were surgically implanted in adult male

$Scn3a^{+/Hyp}$ mice (n = 6) and WT littermates (n = 4) as previously described (Martin et al.,

2007, Dutton et al., 2013, Papale et al., 2013, Makinson et al., 2014). Briefly, two pairs of

bipolar stainless steel screw electrodes (Vintage Machine Supplies, OH, USA) were

implanted in the skull at the following coordinates (relative to bregma): anterior-poster

(AP) +0.5 mm and medial-lateral (ML) -2.2 mm; AP +2.0 mm and ML +1.2 mm; AP -

3.5 mm and ML −2.2 mm; AP -1.5 mm and ML +1.2 mm. Two fine-wire electrodes were

implanted in the dorsal neck muscles to record electromyography (EMG) activity.

Depth EEG recordings were obtained in adult male $Scn3a^{+/Hyp}$ mice (n = 3) and

WT littermates (n = 2). Two depth electrodes were implanted into the hippocampus

(relative to bregma): AP -1.8 mm, ML ±1.6 mm, dorsal-ventral (DV) -1.7 mm. Two

cortical electrodes were also implanted (relative to bregma): AP +2.0 mm and ML+1.2

mm; AP +0.5 mm and ML -2.2 mm. EMG electrodes were not implanted for depth EEG recordings.

For all surgeries, mice were administered Meloxicam (2 mg/kg; Norbrook Laboratories, Lenexa, KS, USA) preoperatively and postoperatively for two days following surgery (1 mg/kg). Each mouse was allowed to recover from surgery for at least 7 days before the onset of EEG recording. Twelve days of continuous video/EEG recording were collected from each mouse, and EEG signals were analyzed with Stellate Harmonie EEG software (Natus Medical Inc., San Carlos, CA, USA) using a high-pass filter of 0.5 Hz and a low-pass filter of 35 Hz. For the cortical-only recordings, EMG signals were analyzed using a high-pass filter of 10 Hz and a low-pass filter of 70 Hz. Two montages were used to manually score the cortical-only and depth EEG recordings. In the first montage, one muscle electrode was used as the reference. Since muscle electrodes were not implanted during the depth electrode surgery, the second montage used a cortical electrode as a reference. Seizure activity was defined as synchronous discharges of increasing frequency with amplitudes at least twice the background.

Kainic Acid Seizure Induction

Male $Scn3a^{+/Hyp}$ mutants (n = 8) and WT littermates (n = 5) were administered kainic acid (i.p., 20 mg/kg, Sigma-Aldrich) and observed for two hours. Seizures were confirmed by EEG analysis using cortical electrode and hippocampal depth electrodes as described above. Behavioral seizures were scored using a modified Racine scale: 0 – no behavior, 1 – freezing/staring, 2- head nodding, 3 – tail clonus, 4 – forelimb clonus, 5 – rearing and falling, and 6 – death (Martin et al., 2007, Tang et al., 2009, Makinson et al.,

2014). The latency to the first electrographic seizure in each mouse as well as the average seizure severity during the observation period were compared.

Locomotor Activity

Adult male $Scn3a^{+/Hyp}$ mice and WT littermates (n= 8/genotype) were placed in novel transparent cages (40 × 20 × 20 cm) equipped with 7 infrared photobeams, each beam spaced 5 cm apart and 5 cm from the cage wall (San Diego Instruments Inc., San Diego, CA, USA). Activity was monitored for 48 hours, and ambulation was recorded as the number of consecutive beam breaks during the time period.

Rotarod

Adult male $Scn3a^{+/Hyp}$ mice (n =11) and WT littermates (n= 9) were trained on a fixed speed (5 RPM) rotating rod (AccuScan Instruments, Columbus, OH, USA) daily for five minutes across two days. Experimental trials were performed on an accelerating (acceleration: 4-40 RPM) rotarod (Columbus Instruments, Columbus, OH, USA) for three days following training. Animals were subjected to three 5-minute trials each day, with a rest period of 30 minutes between each trial. The latency to fall was recorded for each trial.

Statistical Analysis

Data was analyzed using the following software: Clampfit 8.1 (Molecular Devices Corp.), Excel 2002 (Microsoft, Seattle, WA, USA), SigmaPlot 10 (Systat Software, Inc., San Jose, CA, USA), Prism 5-6 (GraphPad Software, Inc., La Jolla, CA, USA), and SPSS Statistical Software (IBM, Armonk, NY, USA). mRNA expression (normalized to β-actin), protein expression (normalized to α-tubulin and reported in optical density units), latencies to flurothyl-induced seizures, and latencies to the first KA-induced

electrographic seizure were analyzed with a two-tailed Student's t-test when comparing two genotypes or one-way Analysis of Variance (ANOVA) followed by the Tukey pairwise *post hoc* comparison when comparing three genotypes. The log-rank (Mantel-Cox) test was used to analyze the number of animals that seized in the hyperthermia-induced seizure paradigm and the temperature at which each mouse seized per genotype. The 6 Hz CC_{50} and respective confidence intervals were determined for each genotype using log-probit analysis. Racine scores at each current in the 6 Hz paradigm were analyzed using the nonparametric Mann-Whitney Rank Sum test. A two-way repeated measures ANOVA followed by Bonferroni's multiple comparisons *post hoc* analyses was used to analyze the time course of KA-induced seizure severity, the number of ambulations during locomotor activity, and latency to fall during the rotarod task. All bar graphs indicate the means, and all error bars represent ± standard error of the mean (SEM).

2.4. Results

2.4.A. The SCN3A-L247P variant is associated with childhood epilepsy and encodes a trafficking deficient channel

Clinical whole-exome sequencing identified a single de novo variant, SCN3A-L247P, in an 18 month-old female patient exhibiting focal seizures, global developmental delay, and autonomic dysfunction. This non-synonymous variant was not present in either parent, or in publically available exome databases (Exome Aggregation Consortium (ExAC), 2016; Exome Variant Server, 2016). *SCN3A* is highly intolerant of variation with genic intolerance score of -2.48 for missense variants, putting it amongst the top 1% most intolerant of genes (Petrovski et al., 2013). The SCN3A-L247P variant

resulted in a non-conservative amino acid substitution at the cytoplasmic face of the S5

transmembrane segment in domain 1 (Fig. 2.1A and 2.1B). We attempted to functionally

characterize this variant using recombinant human $Na_v1.3$ co-expressed with human β1

and β2 subunits in a heterologous expression system (tsA201 cells). However, SCN3A-

L247P mutant channels failed to exhibit significant sodium current (Fig. 2.1C-D).

Incubation at low temperature (28°C) for 24 hours did not rescue any significant sodium

current (Fig. 2.1D). Two independent recombinant $Na_v1.3$ clones expressing the L247P

mutation were tested. The open reading frame of both clones was fully sequenced to rule

out cloning artifacts.

The absence of detectable sodium current in cells transfected with SCN3A-L247P

suggests that either the mutation affected the level of channel protein at the cell surface,

or the mutant channel is expressed at the cell surface but does not conduct sodium. To

determine the level of cell surface expression of SCN3A-L247P, we performed cell

surface biotinylation (Fig. 2.1E). There was a significant reduction in the amount of

SCN3A-L247P at the level of the cell surface relative to SCN3A-WT (normalized surface

VGSC expression = 1.0 for SCN3A-WT and 0.18 for SCN3A-L247P; n = 2). There was

also a trend toward a decrease in total cellular SCN3A expression between SCN3A-WT

and SCN3A-L247P (normalized total VGSC expression = 1.0 for SCN3A-WT and 0.66

for SCN3A-L247P; p = 0.11, Student's t-test; n = 3). Fewer $Na_v1.3$ channels at the cell

surface would be predicted to reduce the magnitude of the inward current, which may

contribute to disease pathogenesis.
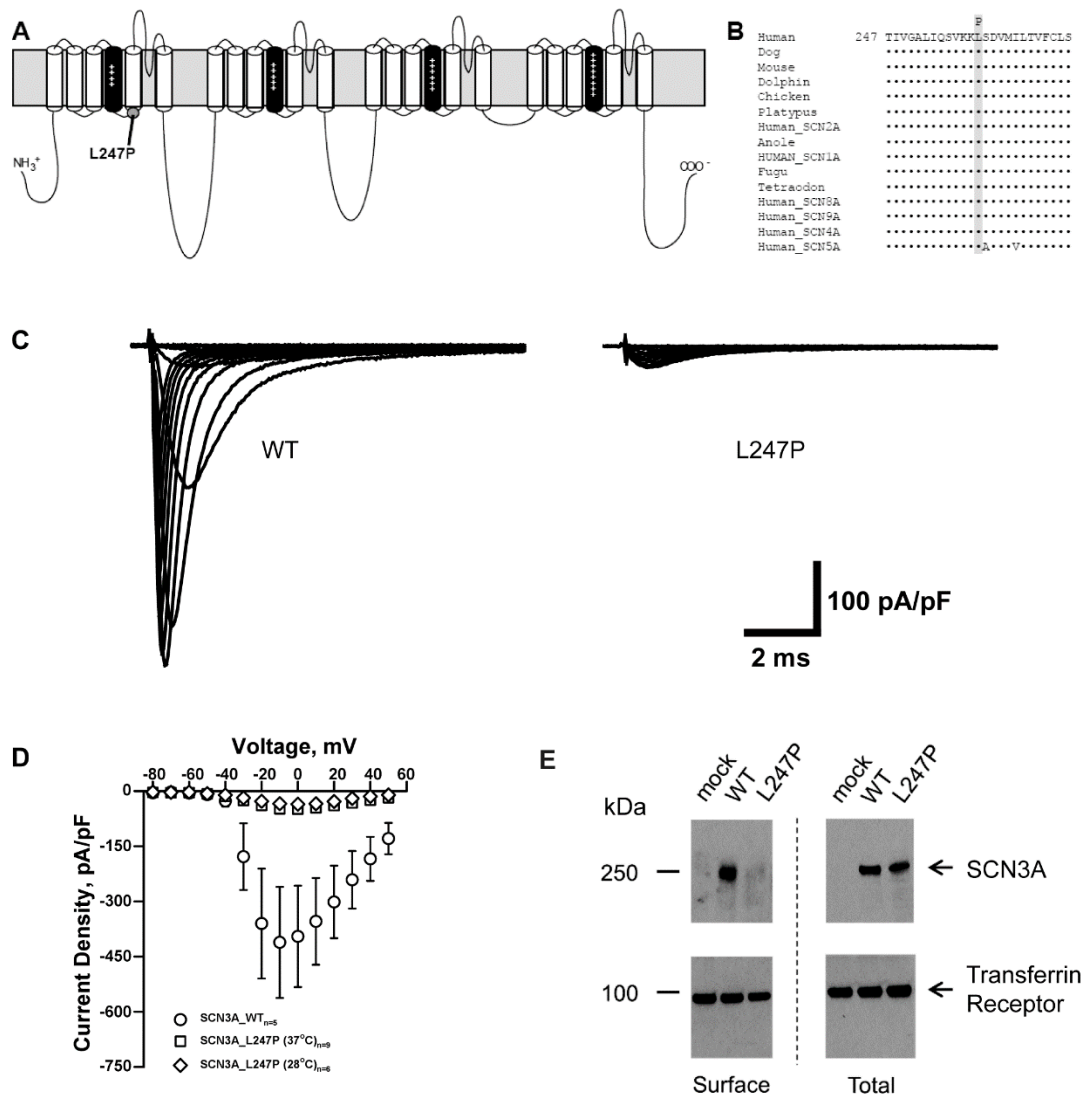
Figure 2.1 SCN3A-L247P is a trafficking deficient mutant.

(A) Predicted transmembrane topology of Na$_v$1.3 showing the location of the L247P

variant characterized in this study. The S4 segments are shown in black with plus (+)

signs and the grey rectangle behind the depiction represents the plasma membrane. (B)

Multiple alignment of human homologs and species orthologs of Na$_v$1.3 (Clustal Omega;

(Sievers et al., 2011)). The variant amino acid L247P (shaded) is contained within a

region of strong evolutionary conservation. (C) Average sodium current traces for

SCN3A-WT and SCN3A-L247P co-expressed with β1 and β2 in a heterologous

expression system (tsA201 cells). (D) Average current density-voltage relationships are

shown for whole-cell currents tsA201 cells transiently co-expressing β1 and β2 with

SCN3A-WT or SCN3A-L247P incubated at 37°C or 28°C for 24 hours prior to

recording. (E) Total and surface protein were detected with anti-pan VGSC α subunit

antibody or anti-transferrin receptor antibody as indicated. The WT SCN3A protein

traffics normally to the cell surface, whereas trafficking of SCN3A L247P to the cell

surface is significantly impaired.

2.4.B. Scn3a mRNA and protein expression is reduced in *Scn3a*$^{+/Hyp}$ and *Scn3a*$^{Hyp/Hyp}$ mice

To better understand the contribution of *SCN3A* to disease, we evaluated the *Scn3a* gene trap mouse line, *Scn3a*$^{Gt(OST52130)Lex}$, developed by Lexicon Pharmaceuticals. The original description of this mouse line reported the observation of only two homozygotes from 63 pups at the F2 generation (WT: 20, heterozygous: 41, homozygous: 2; Chi-squared: 16.016, df = 2, p < 0.001), neither of which survived beyond four weeks of age (http://www.informatics.jax.org/external/ko/lexicon/1392.html; Lexicon personal communication). We generated WT, heterozygous, and homozygous pups for our study by mating heterozygous siblings that had been backcrossed 8-9 generations onto the C57BL/6J strain. Although fewer homozygotes were born than WT pups, we did not observe statistically significant deviations from Mendelian ratios in animals born (WT: 21, heterozygous: 36, homozygous: 10; Chi-squared: 3.985, df = 2, p = 0.14). However, in order to appropriately model the heterozygous *SCN3A* mutation observed in the patient, we used heterozygous mutants and WT littermates, generated from crossing male heterozygous mutants to female C57BL/6J mice, for all behavioral experiments. Gross brain morphology of adult heterozygous mutants was normal except for focal cortical anomalies, including disruptions in cortical lamination and invaginations (Fig. A.1). These were observed in the majority of *Scn3a*$^{+/Hyp}$ mice examined, but not in WT littermates. However, cortical malformations have been reported to occur in WT C57BL/6J mice at a low level (Ramos et al., 2008). To confirm disruption of *Scn3a* in mutant mice, quantitative real-time PCR analysis was performed on whole brain samples from one-day old (P1) WT, heterozygous and homozygous

littermates. We observed approximately 70% and nearly 100% reduction of *Scn3a*

mRNA expression (relative to WT) in the brains of heterozygous and homozygous

mutants, respectively (p < 0.0001, Fig. 2.2A). Western blotting indicated that $Na_v1.3$

protein expression in the brains of P1 heterozygous and homozygous mutants, compared

to WT, was reduced by approximately 35% (p < 0.05) and 60% (p < 0.001), respectively

(Fig. 2.2B). These observations indicate that the *Scn3a* gene trap allele is hypomorphic

(defined henceforth as *Scn3a^{Hyp}*). In adult heterozygous *Scn3a$^{+/Hyp}$* mice, *Scn3a* mRNA

expression was reduced by approximately 60% compared to WT in both the hippocampus

and cerebellum (p < 0.05; Fig. A.2). $Na_v1.3$ protein expression was undetectable in the

brains of adult WT and *Scn3a$^{+/Hyp}$* mice.

    To determine whether *Scn3a* deficiency could alter the expression levels of other

CNS VGSCs, we compared *Scn1a*, *Scn2a*, and *Scn8a* mRNA and protein levels from the

brains of *Scn3a^{Hyp}* mutant mice and WT littermates. Although *Scn1a* (Fig. 2.3A), *Scn2a*

(Fig. 2.3B), and *Scn8a* (Fig. 2.3C) mRNA levels were comparable between P1 *Scn3a$^{+/Hyp}$*

pups and WT littermates, they were significantly reduced in *Scn3a$^{Hyp/Hyp}$* pups (p < 0.05).

No significant differences in mRNA expression of *Scn1a*, *Scn2a*, and *Scn8a* were

observed between adult *Scn3a$^{+/Hyp}$* mice and WT littermates (Fig. A.2 B-D). $Na_v1.1$,

$Na_v1.2$, and $Na_v1.6$ protein expression was undetectable by Western blotting for all

genotypes of P1 mice (data not shown). No significant differences in protein levels of

$Na_v1.1$, $Na_v 1.2$ and $Na_v 1.6$ were observed in adult *Scn3a$^{+/Hyp}$* mutant mice compared

with WT littermates (Fig. A.2 B-D).
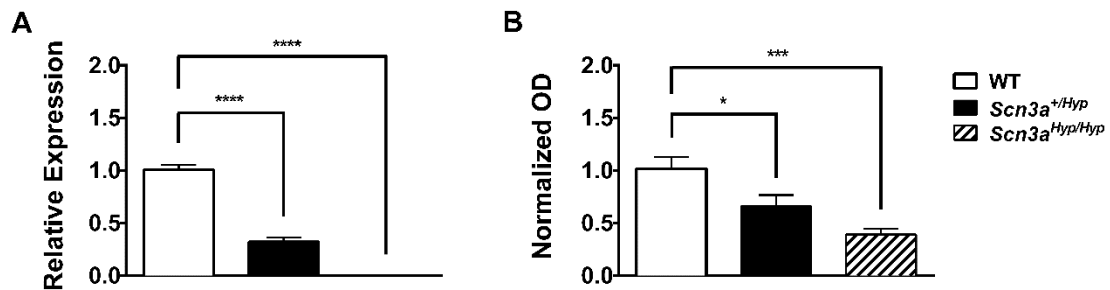
Figure 2.2 Scn3a expression is reduced in Scn3a$^{+/Hyp}$ mice.

(A) *Scn3a* mRNA expression is reduced by approximately 70% (p < 0.0001) and nearly

100% (p < 0.0001) in *Scn3a$^{+/Hyp}$* and *Scn3a$^{Hyp/Hyp}$* mice respectively. mRNA expression,

quantified from real-time PCR analysis, was normalized to β-actin. Expression values for

each genotype are relative to WT levels. n = 4 (WT), 5 (*Scn3a$^{+/Hyp}$*), 3 (*Scn3a$^{Hyp/Hyp}$*). (B)

Scn3a protein expression, quantified from Western blot analysis, is reduced by

approximately 35% (p < 0.05) and 60% (p < 0.001) in membrane-enriched whole brain

homogenate from *Scn3a$^{+/Hyp}$* and *Scn3a$^{Hyp/Hyp}$* mice, respectively. Optical density (OD)

expression values are relative to WT and normalized to α-tubulin; n = 5 (WT), 6

(*Scn3a$^{+/Hyp}$*), 4 (*Scn3a$^{Hyp/Hyp}$*). Protein results represent the means of triplicate values for

each genotype. *p < 0.05, *** < 0.001, ****p < 0.0001; One-way ANOVA. Error bars

indicate SEM.
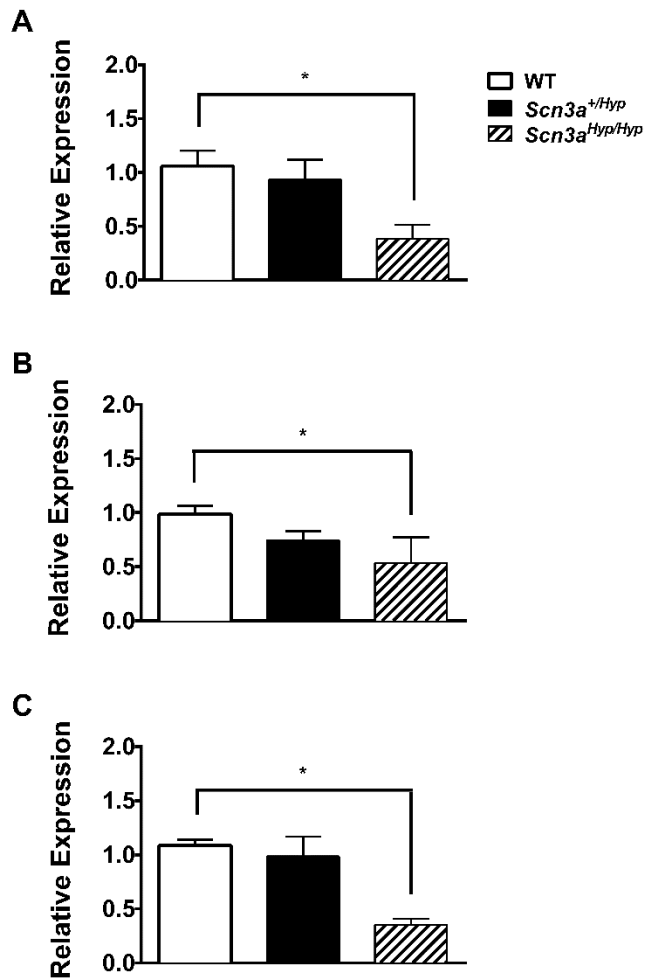
Figure 2.3 Expression of Scn1a, Scn2a, and Scn8a in *Scn3a*$^{+/Hyp}$ mice.

(A) *Scn1a*, (B) *Scn2a*), and (C) *Scn8a* mRNA expression, quantified from real-time PCR analysis, is significantly reduced in whole brain samples from P1 *Scn3a*$^{Hyp/Hyp}$ mice. n = 4 (WT), 5 (*Scn3a*$^{+/Hyp}$), 3 (*Scn3a*$^{Hyp/Hyp}$). Expression values are relative to WT and normalized to β-actin. *p < 0.05, One-way ANOVA. Error bars indicate SEM.

2.4.C. Scn3a$^{+/Hyp}$ mice exhibit increased seizure susceptibility

We first determined whether reduced *Scn3a* expression increases susceptibility to hyperthermia-induced seizures. Core body temperature of P21-P22 *Scn3a*$^{+/Hyp}$ mutants and WT littermates was increased by 0.5°C every two minutes until either a generalized tonic-clonic seizure (GTCS) was observed or 42.5°C is reached. No statistically significant differences were observed in the number of mice exhibiting seizures, the temperature at which the seizure occurred, nor the seizure severity between *Scn3a*$^{+/Hyp}$ mice and WT littermates (Fig. 2.4).

Next, we assessed the susceptibility of male *Scn3a*$^{+/Hyp}$ mutants to focal seizures using the 6 Hz "psychomotor" seizure induction paradigm (Toman, 1951, Brown et al., 1953). Male *Scn3a*$^{+/Hyp}$ mutants and WT littermates were tested at current intensities of 16 mA, 24 mA, and 30 mA. Seizure incidence and severity (based on a modified Racine score, denoted RS) was compared between *Scn3a*$^{+/Hyp}$ mutants and WT littermates at each current (Fig. 2.5). Both genotypes displayed minimal seizure response at 16 mA. However, at 24 mA, 50% (5/10) of *Scn3a*$^{+/Hyp}$ mutants seized (3RS1, 2RS2), compared with 10% (1/10) of WT (1RS3). At 30 mA, 90% (9/10) *Scn3a*$^{+/Hyp}$ mutants seized (4RS1, 3RS2, 2RS3) compared with 56% (5/9) of WT littermates (1RS1, 1RS2, 3RS3). Based on these results, the CC_{50} was found to be significantly lower in the *Scn3a*$^{+/Hyp}$ mutants [CC_{50} = 24 mA; 95% CI: 19.8 to 25.4] when compared with WT littermates [CC50 = 29 mA; 95% CI: 26.7 to 38.4] (Fig. 2.5A). No statistically significant differences were observed in seizure severity between mutant and WT littermates at the currents tested (Fig. 2.5B).
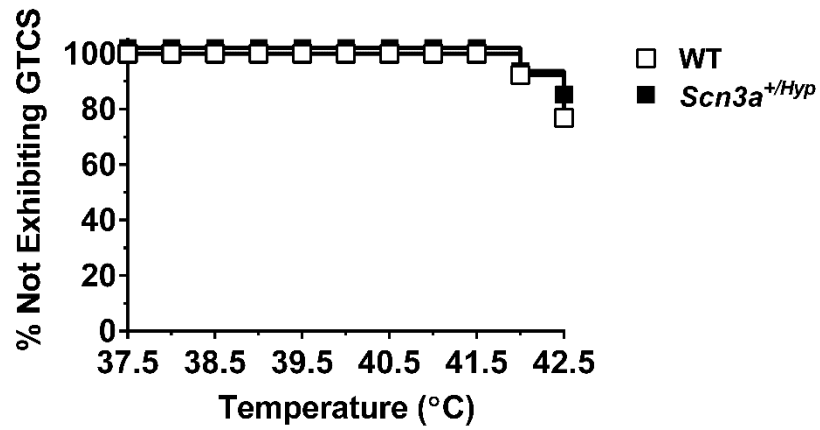
Figure 2.4 *Scn3a^{+/Hyp}* mice do not exhibit increased susceptibility to hyperthermia-induced seizures.

Seizure generation in response to increasing body temperature was comparable between *Scn3a^{+/Hyp}* mutants (n = 12) and WT littermates (n = 13). Log-Rank Survival Test.
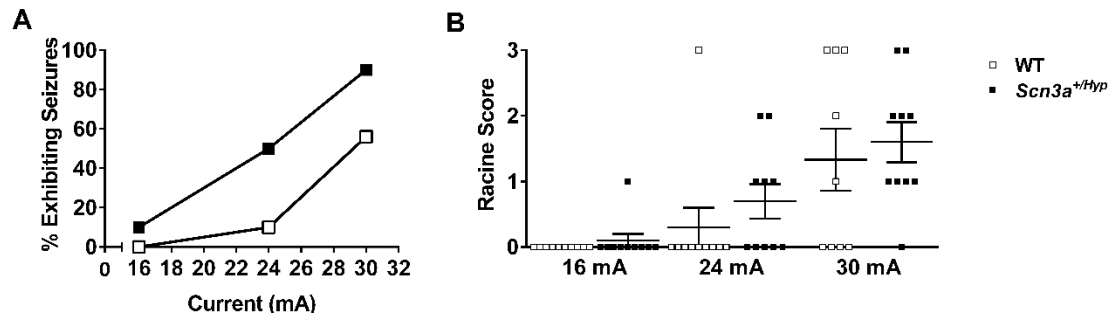
Figure 2.5 *Scn3a^{+/Hyp}* mice exhibit increased susceptibility to 6 Hz psychomotor seizures.

(A) The CC_{50} is significantly lower for *Scn3a^{+/Hyp}* mice compared with WT littermates; n = 10/genotype. (B) The difference in the average Racine score between *Scn3a^{+/Hyp}* mutants and WT littermates was not statistically significant for any current. Mann-Whitney Rank Sum test. Error bars indicate SEM.

Latencies to flurothyl-induced seizures were examined in both sexes of $Scn3a^{+/Hyp}$ mutants and WT littermates (Fig. 2.6). The average latency to the first myoclonic jerk was reduced in $Scn3a^{+/Hyp}$ mutants compared to WT littermates in both sexes. Average latencies to the first GTCS were comparable between male $Scn3a^{+/Hyp}$ mutant and male WT littermates (Fig. 2.6A); however, female $Scn3a^{+/Hyp}$ mutants exhibited significantly reduced latencies to the GTCS when compared to female WT littermates ($p < 0.01$, Fig. 2.6B). In both sexes, $Scn3a^{+/Hyp}$ mice progressed to hindlimb extension significantly faster than WT littermates (male: $p < 0.001$; female: $p < 0.001$).

The response of male $Scn3a^{+/Hyp}$ mutants and WT littermates to kainic acid (KA)-induced seizures was also compared (Fig. 2.7). $Scn3a^{+/Hyp}$ mutants exhibited significantly higher average Racine scores compared to WT littermates from 20 minutes to 2 hours following KA administration ($p < 0.05$, Fig. 2.7A). The latency to the first observed electrographic seizure was also significantly reduced in $Scn3a^{+/Hyp}$ mice ($p < 0.05$, Fig. 2.7B). An example of an EEG-confirmed KA-induced seizure in a $Scn3a^{+/Hyp}$ mutant is shown in Fig. 2.7C.

2.4.D. $Scn3a^{+/Hyp}$ mutants do not exhibit spontaneous seizures

Male $Scn3a^{+/Hyp}$ mutants (n= 6) and WT littermates (n= 4) were implanted with cortical electrodes and continuous video/EEG analysis was performed for 12 days (288 hours each mouse). No spontaneous seizures were detected during the recording period. Since patients with $SCN3A$ mutations exhibit focal seizures, we also performed EEG analysis on $Scn3a^{+/Hyp}$ mice (n= 3) and WT littermates (n = 2) using depth electrodes positioned bilaterally in the dorsal hippocampus. Each mouse was continuously

monitored by video/EEG analysis for 12 days; however, no spontaneous seizures were detected.

2.4.E. *Scn3a*$^{+/Hyp}$ mutants are hypoactive and display deficits in motor learning

The locomotor activity of male *Scn3a*$^{+/Hyp}$ mice and WT littermates was continuously monitored for 48 hours and the number of ambulations were recorded (Fig. 2.8A). *Scn3a*$^{+/Hyp}$ mutants traveled significantly less than WT littermates during the first dark cycle (8:00-11:00 pm; hours 6.5 to 9.5) and during the second dark cycle (9:00 – 9:30 pm; hours 31.5-32.0) ($p < 0.05$, Fig. 2.8A). We also compared motor learning between *Scn3a*$^{+/Hyp}$ mice and WT littermates using an accelerating rotarod. All mice underwent three trials per day for three days. There were no differences in average latencies to fall between the genotypes during the first five trials. During the remaining trials, however, *Scn3a*$^{+/Hyp}$ mutants fell from the accelerating rotarod significantly faster than WT littermates (Fig. 2.8B). A battery of behavioral tests was also conducted on the *Scn3a*$^{+/Hyp}$ mutants and WT littermates to evaluate exploratory activity, anxiety, memory, social behavior, depressive-like behavior, vision, and sensorimotor gating (Table 2). No statistically significant differences were observed between mutants and WT littermates in any of these behavioral tasks, with the exception of the open field in which *Scn3a*$^{+/Hyp}$ mice entered the center zone significantly fewer times when compared to WT littermates ($p < 0.05$).
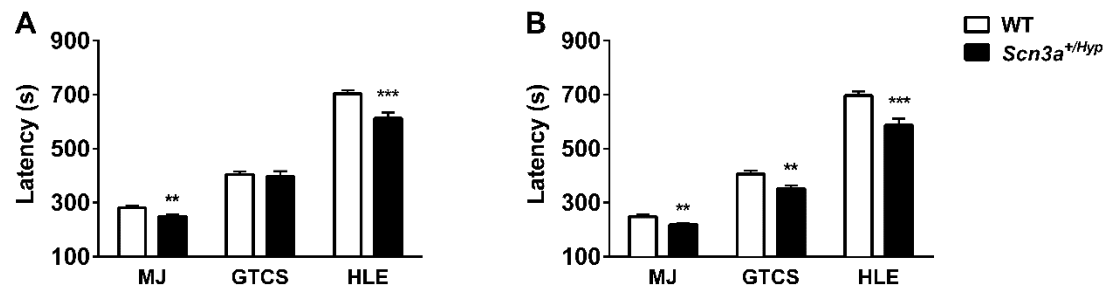
Figure 2.6 *Scn3a$^{+/Hyp}$* mice exhibit increased susceptibility to flurothyl-induced seizures.

(A) Male *Scn3a$^{+/Hyp}$* mutants exhibit significantly shorter latencies to the first MJ and HLE when compared to WT littermates. (B) Female *Scn3a$^{+/Hyp}$* female mice have significantly shorter latencies to all three seizure components when compared to WT; male n = 33 (WT), 29 (*Scn3a$^{+/Hyp}$*); female n = 32 (WT), 29 (*Scn3a$^{+/Hyp}$*). **p < 0.01, ***p < 0.001, Two-tailed Student's t-test. Error bars indicate SEM.
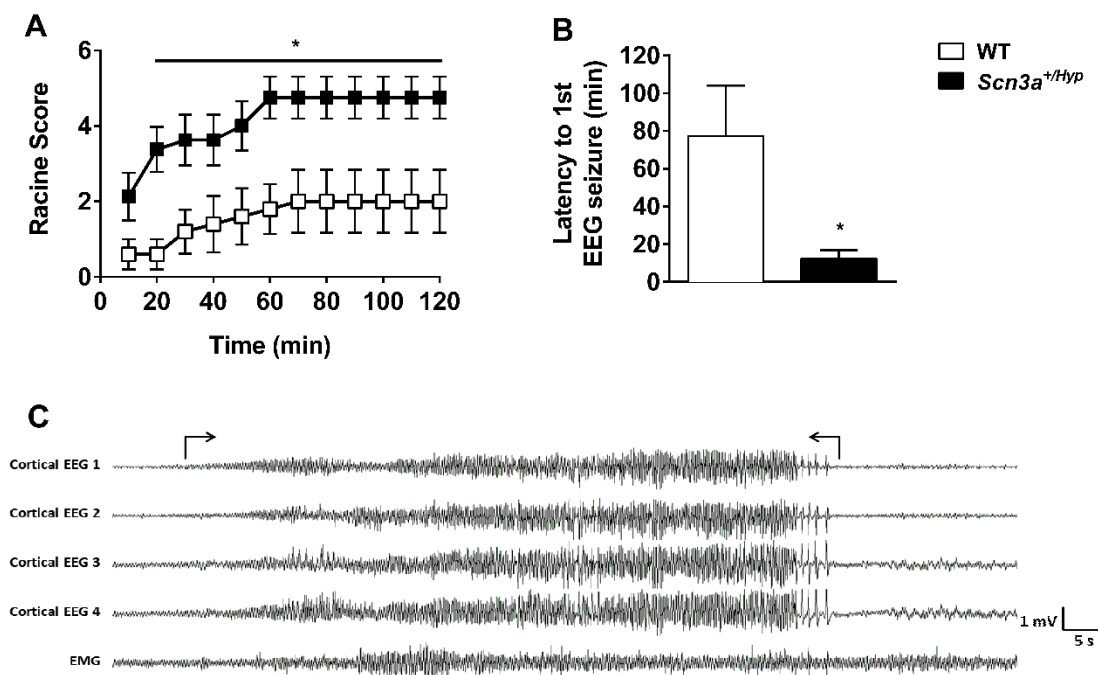
Figure 2.7 *Scn3a^{+/Hyp}* mice exhibit increased susceptibility to KA-induced seizures.
(A) Following the administration of KA, *Scn3a^{+/Hyp}* mutants (n = 8) exhibited
significantly more severe seizure phenotypes when compared to WT littermates (n = 5).
$*p < 0.05$; Two-way repeated measures ANOVA. (B) Average latency to the first
electrographic seizure was shorter in *Scn3a^{+/Hyp}* mutants. $*p < 0.05$, Two-tailed Student's
t-test. (C) A representative EEG recording during a KA-induced seizure in a mutant
mouse. Seizure onset and termination are indicated within brackets. EEG montage:
Cortical EEG 1, Cortical EEG 2, Cortical EEG 3, and Cortical EEG 4 – cortical
electrodes. EMG – muscle electrodes. All cortical electrodes and EMG referenced to a
second EMG electrode. Error bars indicate SEM.

A

B

□ WT
■ *Scn3a*$^{+/Hyp}$

Figure 8   Day 1   Day 2   Day 3
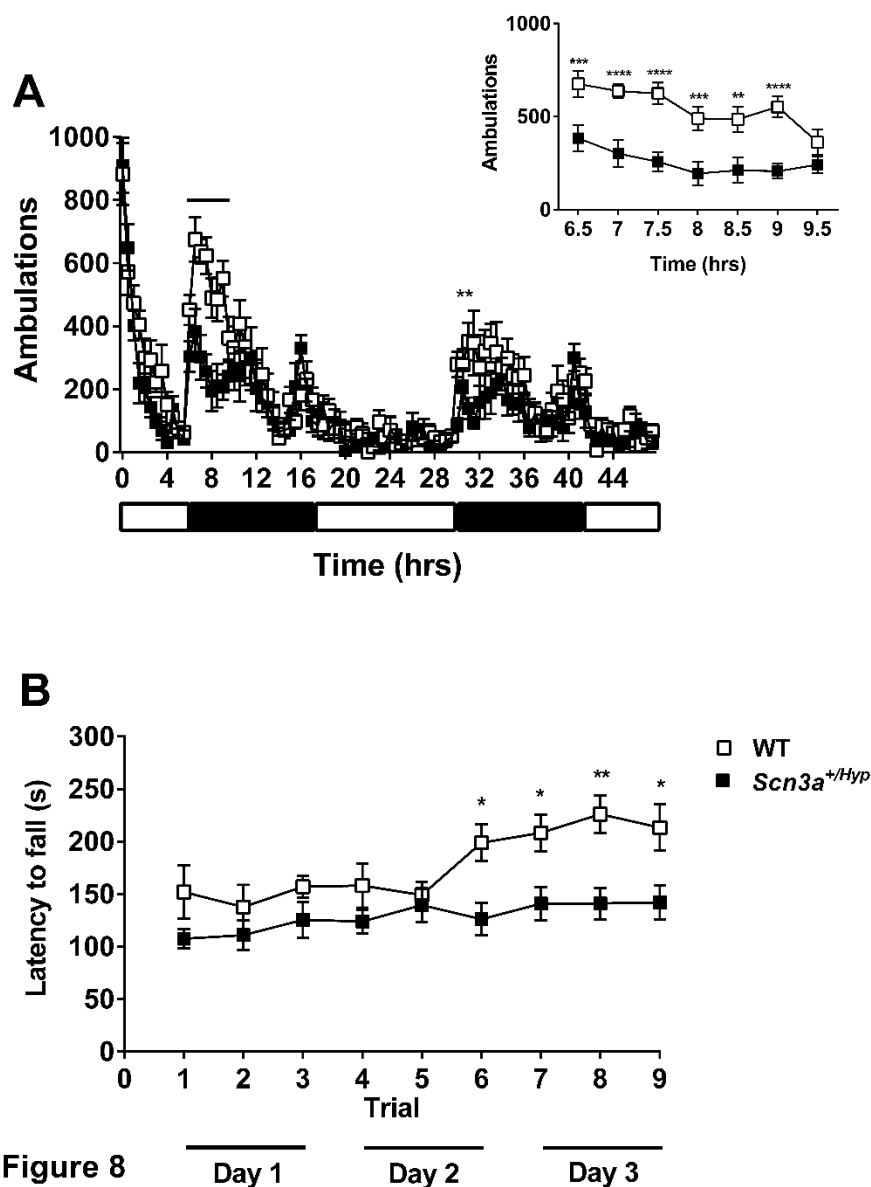
Figure 2.8 *Scn3a*$^{+/Hyp}$ mice exhibit deficits in motor behavior.

(A) *Scn3a*$^{+/Hyp}$ mice (n = 8) traveled significantly less than WT (n = 8) during the first

dark phase (hours 6.5-9.5) and the second dark phase (hour 31.5-32.0). Inset shows

locomotor activity during hours 6.5-9.5. **$p < 0.01$, ***$p < 0.001$, ****$p < 0.0001$;

Two-way repeated measures ANOVA (Genotype x Time). White and black bars below the

X-axis represent the light and dark periods, respectively. (B) Latency to fall from the

rotarod was significantly shorter for $Scn3a^{+/Hyp}$ mutants (n = 11) when compared to WT littermates (n = 9) from trial 6 (Day 2) to the last trial (trial 9) on Day 3. *$p < 0.05$, **$p < 0.01$, Two-way repeated measures ANOVA (Genotype x Time). Error bars indicate SEM.

2.5. Discussion

2.5.A. A novel *SCN3A* variant (L247P) is associated with childhood epilepsy and displays reduced trafficking to the cell surface

Clinical whole-exome sequencing identified a novel, non-synonymous missense variant in the *SCN3A* gene, encoding the $Na_v1.3$ VGSC α subunit, in a female patient with childhood epilepsy, global developmental delay, and autonomic nervous system dysfunction. The L247P substitution replaces a highly conserved leucine residue with proline at the cytoplasmic face of the DIS5 transmembrane domain (Fig. 2.1B). This substitution is predicted to affect the secondary structure of *SCN3A*, which could alter the function or trafficking of the channel (Table A.1). We demonstrate herein that SCN3A-L247P is a trafficking deficient mutant. This finding provides further support for loss-of-function of *SCN3A* as a pathogenic mechanism.

There is a precedent for the rescue of trafficking-deficient sodium channel mutants by co-expression of VGSC β subunits, other interacting proteins, or pharmacologic agents (Rusconi et al., 2007, Rusconi et al., 2009, Thompson et al., 2012, Cestele et al., 2013, Bechi et al., 2015). The biochemical and functional assays of SCN3A-L247P were performed in cells co-transfected with β1 and β2 subunits, suggesting that β1 and β2 are not sufficient to rescue the trafficking of SCN3A-L247P. Further experimentation will be necessary to ascertain whether the trafficking of SCN3A-L247P can be rescued by other interacting proteins or pharmacologic agents.

2.5.B. In vivo characterization of *Scn3a* haploinsufficiency

In order to further explore the potential of reduced *SCN3A* activity to confer elevated seizure risk *in vivo*, we studied the gene trapped *Scn3a*[Gt(OST52130)Lex] line. *Scn3a* mRNA expression in P1 mice was found to be significantly reduced in heterozygous mutants, and Na$_v$1.3 protein levels were approximately 35% lower than in WT littermates. Interestingly, although *Scn3a* mRNA in homozygous mutants was almost undetectable, Na$_v$1.3 protein was still detected, indicating that this mouse line is hypomorphic. It is well recognized that mRNA and protein expression levels do not always correlate due to experimental noise, the stability of the RNA or protein, or modifications at the transcriptional or translational level (Nie et al., 2006, Raj et al., 2006, Maier et al., 2009). We were unable to detect Na$_v$1.3 protein in the adult WT mouse brain by Western blot, which is consistent with observations from a previous study (Cheah et al., 2013). The lack of detectable Na$_v$1.3 protein in adult brain also confirmed the specificity of the Scn3a antibody, since we showed that all other CNS VGSCs are detectable in the adult brain.

Previous observations by Lexicon indicated reduced viability of homozygous *Scn3a*[Hyp/Hyp] mutants, suggesting that *Scn3a* is critical during early development. In the current study, we did not observe significant skewing of Mendelian ratios when the three genotypes (WT, *Scn3a*[+/Hyp], *Scn3a*[Hyp/Hyp]) were examined at P1. However, Lexicon observations were based on numbers at the time of genotyping (P10 at earliest); therefore, homozygous mutants likely exhibit postnatal lethality. We also investigated whether the expression of the other brain VGSCs would be altered due to the reduced expression of *Scn3a*. Previous studies have demonstrated that sodium channel deficiency can result in

changes in expression of other VGSCs. For example, *Scn1b*-null mice exhibit reduced

$Na_v1.1$ and increased $Na_v1.3$ protein levels (Chen et al., 2004). Analysis of *Scn1a*

knockout mice also showed compensatory upregulation of $Na_v1.3$ in hippocampal

interneurons, although this increase was insufficient to restore normal levels of sodium

current (Yu et al., 2006). In the current study, *Scn1a*, *Scn2a*, and *Scn8a* mRNA levels

were unchanged in P1 *Scn3a*[+/Hyp] mice, while mRNA expression was significantly

reduced in homozygous mutants. However, since $Na_v1.1$, $Na_v1.2$, and $Na_v1.6$ proteins

are undetectable by Western blot in P1 mice, further investigation will be required to

determine whether these observed reductions in mRNA levels are functionally important.

To date, only two reported patients with *SCN3A* mutations (M1323V, N302S)

have presented with febrile seizures, suggesting that this is not a common seizure type for

SCN3A mutations (Vanoye et al., 2014, Chen et al., 2015). Consistent with clinical

observations, *Scn3a*[+/Hyp] mice did not show increased susceptibility to hyperthermia-

induced seizures. However, *Scn3a*[+/Hyp] mice did exhibit increased susceptibility to

flurothyl, KA, and 6 Hz-induced seizures. The results from the KA and the 6 Hz

paradigms are particularly relevant since these approaches model limbic seizures, which

are the most commonly observed seizure type in patients with *SCN3A* mutations,

including the patient with the L247P mutation (Barton et al., 2001, Holland et al., 2008,

Vanoye et al., 2014). Taken together, these clinical and experimental findings suggest a

role for *SCN3A* in the development of generalized and partial epilepsy.

While the *Scn3a*[+/Hyp] mutant did not express the L247P mutation identified in the

patient, the observation of increased seizure susceptibility in the mutants provides support

for the association between reduced *SCN3A* activity and increased seizure susceptibility.

Although we did not observe spontaneous seizures in the *Scn3a* mice, we cannot exclude the possibility of infrequent seizures that were not captured during the periods of EEG analysis. It is noteworthy that two of the six *Scn3a*$^{+/Hyp}$ mice fitted with cortical electrodes were observed exhibiting brief, seizure-like behaviors, including rearing and falling. However, these behaviors did not correspond with electrographic seizure activity. Furthermore, we cannot exclude the possibility that the spontaneous seizures in the patient are the result of the toxic accumulation of mutant Na$_v$1.3 protein in the cells due to defective trafficking.

One general caveat of mouse models is that gene expression patterns can differ from humans. *SCN3A* is highly expressed during early development in humans and rodents, with expression declining into adulthood (Black et al., 1994, Felts et al., 1997b, Chen et al., 2000, Whitaker et al., 2001b). However, the relative reduction in adult *Scn3a* levels appears to be greater in the mouse. Nevertheless, a number of studies have revealed that *Scn3a* expression is still detectable in certain brain regions, including the hippocampus and cortex, during adulthood (Beckh et al., 1989, Furuyama et al., 1993, Lindia and Abbadie, 2003). The observation of increased seizure susceptibility in *Scn3a*$^{+/Hyp}$ mutants suggest that *Scn3a* is still functionally important in the adult mouse. However, it is also possible that reduced *Scn3a* during early development results in long-term alterations in neuronal excitability or cortical organization. Future studies will investigate these possibilities.

2.5.C. A putative role for Scn3a in motor function and coordination

$Scn3a^{+/Hyp}$ mice exhibited reduced locomotor activity, suggesting hypoactivity, and decreased latency to fall from a rotarod. Interestingly, average latencies to fall from the rotarod were not significantly different between the genotypes during the initial trials; however, the performance of the mutants did not improve over time, indicating a deficit in motor learning. Poor rotarod performance suggests dysfunction of the cerebellum, since this brain region plays a crucial role in movement, motor coordination, and motor learning (Reeber et al., 2013). Studies in both rat and human have identified *SCN3A* expression in the granule, molecular, and deep cerebellar layers of the cerebellum, suggesting that *SCN3A* is expressed in excitatory granule cells as well as inhibitory cell types in the molecular layer. (Furuyama et al., 1993, Whitaker et al., 2000, Whitaker et al., 2001b, Lindia and Abbadie, 2003). The patient with mutation L247P was unable to sit without support or walk at two years of age, suggesting a deficit in motor function. Additionally, the patient exhibits hypotonia, or low muscle tone, which can be partially attributed to cerebellar dysfunction (Koziol and Barker, 2013). Taken together, these results suggest a role for *Scn3a* in cerebellum-regulated motor function.

2.6. Conclusions

We report the identification of the novel *de novo* variant *SCN3A*-L247P in a patient with childhood epilepsy. SCN3A-L247P was demonstrated to cause a defect in trafficking, which would be predicted to functionally reduce *SCN3A* activity. Consistent with the clinical observations, $Scn3a^{+/Hyp}$ mice display increased seizure susceptibility, hypoactivity, and impaired motor learning. These observations support a role for *SCN3A*

loss of function mutations, whether by reduced protein expression or defective trafficking, in epileptogenesis.

Chapter 3: Exploring the possibility that *Scn3a* can function as a genetic modifier in *Scn1a* mutant mice

3.1 Abstract

More than 1200 mutations in *SCN1A* have been identified in epilepsy syndromes, including GEFS+ and Dravet syndrome. Clinical heterogeneity is frequently observed in *SCN1A*-derived epilepsies, suggesting that additional genetic and/or environmental factors contribute to the clinical presentation. Previous studies in mouse models identified *Scn2a* and *Scn8a* as modifiers of *Scn1a* dysfunction. To determine whether *Scn3a* also acts as a genetic modifier, we crossed the *Scn1a* R1648H GEFS+ mouse model with the *Scn3a* hypomorphic line ($Scn3a^{+/Hyp}$). Mice with both *Scn3a* and *Scn1a* dysfunction ($Scn3a^{+/Hyp}/Scn1a^{+/RH}$ mice) did not exhibit altered survival or growth rates compared to *Scn3a* and *Scn1a* mutant mice. $Scn3a^{+/Hyp}/Scn1a^{+/RH}$ mice did exhibit increased susceptibility to flurothyl-induced seizures but not hyperthermia-induced or 6 Hz-induced seizures. Finally, $Scn3a^{+/Hyp}/Scn1a^{+/RH}$ mice did not exhibit alterations in anxiety, exploration, or motor leaning compared to both *Scn3a* and *Scn1a* mutant mice. Taken together, these results suggest that *Scn3a* is unlikely to be a major modifier of *Scn1a*.

3.2 Introduction

Epilepsy is a disorder of hyperexcitability and hypersynchrony; therefore, it is unsurprising that many of the genes implicated in this disorder encode voltage-gated sodium channels (Escayg et al., 2000, Singh et al., 2009, Saitoh et al., 2015, Boerma et al., 2016). In particular, more than 1200 mutations in the voltage-gated sodium channel *SCN1A* have been identified in epilepsy syndromes ranging from genetic epilepsy with febrile seizures plus (GEFS+) to Dravet syndrome (Meng et al., 2015). Studies in mouse models of *Scn1a* dysfunction have revealed that *Scn1a* mutations lead to epilepsy by

reducing the excitability of inhibitory interneurons, resulting in an overall increase in network excitability (Yu et al., 2006, Ogiwara et al., 2007, Cheah et al., 2013, Dutton et al., 2013, Ito et al., 2013).

We previously generated a mouse model of GEFS+ ($Scn1a^{RH}$ line) by introducing the human *SCN1A* mutation R1648H, which was identified in a large GEFS+ family, into the orthologous mouse *Scn1a* gene (Escayg et al., 2000; Martin et al., 2010). Homozygous $Scn1a^{RH/RH}$ mice exhibit frequent spontaneous generalized seizures and premature lethality, while $Scn1a^{+/RH}$ heterozygous mice exhibit infrequent spontaneous generalized seizures, as well as increased susceptibility to hyperthermia-induced seizures and to chemically- and electrically-induced seizures (Martin et al., 2010). After backcrossing for 12 generations on the C57BL/6J background, $Scn1a^{+/RH}$ mice were found to have reduced lifespan compared to wildtype (WT) littermates, and to exhibit hyperactivity and deficits in spatial memory, cued fear conditioning, pre-pulse inhibition, social behavior, and risk assessment (Sawyer et al., 2016).

As mentioned in Chapter 1, few epilepsy mutations have been identified in the VGSC *SCN3A* in comparison to *SCN1A*. The first mutation, K345Q, was discovered through genetic screening of a cohort of refractory partial epilepsy patients (Holland et al., 2008). This mutation was shown to result in increased persistent and ramp currents when measured in rat hippocampal pyramidal neurons. Four additional mutations were subsequently identified in patients with partial epilepsy, all of which were demonstrated to increase ramp currents when tested in tsA201 cells, suggesting gain of function (Vanoye et al., 2014). However, functional analysis demonstrated that the *SCN3A* N302S mutation, identified in a patient with GEFS+ and severe intellectual disability, increased

recovery time from slow inactivation, suggesting that mutations that reduce channel activity may also result in epilepsy (Chen et al., 2015). We have also recently reported the identification of a trafficking deficient mutation in SCN3A, L247P, in a patient with partial epilepsy and developmental delay (Chapter 2). To investigate the effects of reduced *SCN3A* activity in vivo, an *Scn3a* hypomorphic mouse model (*Scn3a*$^{+/Hyp}$) was characterized and shown to exhibit increased seizure susceptibility, providing further support that reduced *SCN3A* activity can increase seizure risk (Chapter 2). These mice also displayed reduced locomotor activity and deficits in motor learning during the accelerating rotarod task (Lamar et al., 2017).

Within GEFS+ pedigrees, affected individuals co-segregating the same *SCN1A* mutation often exhibit different types of epilepsy and variable severity, including cases of Dravet syndrome, supporting the notion that additional genetic and/or environmental factors contribute to the clinical presentation (Marini et al., 2007, Suls et al., 2010, Mhanni et al., 2011). Although a few studies have identified modifier genes in patients with Dravet syndrome, variation in genetic background in mouse lines has provided a greater number of putative modifier loci and genes (Sprunger et al., 1999, Bergren et al., 2005, Papale et al., 2009, Calhoun et al., 2016, Hawkins and Kearney, 2016). Furthermore, studies with *Scn1a*$^{+/RH}$ and *Scn1a* null mice have demonstrated that *Scn1a* functionally interacts with other ion channels such as Kcnq2, Scn2a, and Scn8a (Martin et al., 2007, Hawkins et al., 2011). Co-expression of mutations in either Kcnq2 or Scn2a significantly reduces the lifespan of RH mutants, while some Scn8a mutations have been shown to ameliorate the seizure phenotype of RH mice. In both mice and humans, a limited number of modifier genes have been investigated. More comprehensive

knowledge of epilepsy modifier genes would contribute towards understanding disease mechanisms and the development of improved treatments.

Although no studies to date have investigated potential interactions between *Scn1a* and *Scn3a*, a number of observations raise the possibility that *Scn3a* might function as a modifier of *Scn1a* function. First, *Scn3a* and *Scn1a* are both localized in the soma and dendrites of neurons in the central nervous system (Westenbroek et al., 1989, Westenbroek et al., 1992, Whitaker et al., 2001b). Second, the decline of *SCN3A* expression in humans and mice coincides with the increase in expression of *SCN1A* and with the onset of disease in DS patients with *SCN1A* mutations (Cheah et al., 2013). These complementary expression patterns suggest that *SCN3A* might play an important role in the regulation of neuronal excitability during early development prior to the robust expression of *SCN1A*. Finally, *Scn3a* was shown to be upregulated in the hippocampus of homozygous *Scn1a* null mice, providing support for *Scn3a* compensation in the presence of *Scn1a* dysfunction (Yu et al., 2006). Based on these observations, we hypothesized that *Scn3a* can function as a genetic modifier of *Scn1a*.

In the present study, we sought to obtain evidence for a functional interaction between *Scn1a* and *Scn3a* by crossing the *Scn1a* R1648H GEFS+ model with the *Scn3a* hypomorphic line (*Scn3a$^{+/Hyp}$*). We examined the progeny of this cross for alterations in life span, weight, seizure susceptibility, and behavior. Co-expression of *Scn3a* and *Scn1a* mutations exacerbated susceptibility to flurothyl-induced seizures but not hyperthermia-induced or 6 Hz-induced seizures. Furthermore, the presence of both mutations did not alter survival, weight, or behavior when compared to littermates expressing each

individual mutation, suggesting that *Scn3a* is unlikely to be a major modifier of *Scn1a* in vivo.

3.3 Materials and Methods

Animals

Scn3a^{Hyp} mice were generated as previously described (Chapter 2). The line was maintained by backcrossing to C57BL/6J mice (Jackson Laboratories, Bar Harbor, ME) for nine generations. *Scn1a*^{RH} mice were generated as previously described (Martin et al., 2010) and backcrossed to C57BL/6J mice for 14 generations. *Scn3a*$^{+/Hyp}$ males were crossed to *Scn1a*$^{+/RH}$ females to obtain double heterozygotes (designated *Scn3a*$^{+/Hyp}$/*Scn1a*$^{+/RH}$). Littermates were used in all experiments to avoid confounds due to differences in genetic background and rearing conditions. To assess survival, a cohort of the *Scn3a*$^{+/Hyp}$/*Scn1a*$^{+/RH}$ mice and littermates were monitored weekly from postnatal day 6 (P6) to P58 (8 weeks old). The mice were also weighed every three days from P6 to P21. Unless stated otherwise, 6-9 week old mice were used for all experiments. Mice were housed in an animal facility with a 12-hour light/dark cycle (lights on 7:00am – lights off 7:00pm). Food and water were available *ad libitum*. All experiments were performed in accordance with the guidelines of the Emory University Institutional Animal Care and Use Committees.

Genotyping

To detect the *Scn3a*^{Hyp} allele, genotyping was performed as described in Chapter 2. Genotyping of the *Scn1a*$^{+/RH}$ allele was performed separately as previously described (Sawyer et al., 2016). *Scn3a*$^{+/Hyp}$/*Scn1a*$^{+/RH}$ mice were identified by the presence of WT and mutant bands for both *Scn3a* and *Scn1a*.

Flurothyl Seizure Induction

Flurothyl seizure induction was performed as described in Chapter 2. Male and female 5-9 week old $Scn3a^{+/Hyp}/Scn1a^{+/RH}$ mice and littermates were used.

Hyperthermia-induced Seizures

$Scn3a^{+/Hyp}/Scn1a^{+/RH}$ mice and littermates, aged P14-P15, were examined for susceptibility to hyperthermia-induced seizures as described in Chapter 2.

6 Hz psychomotor Seizures

Hz corneal stimulation was performed as described in Chapter 2. The topical anesthetic 0.5% proparacaine hydrochloride (Akorn, Lake Forrest, Il, USA) was applied to each eye 15 minutes prior to seizure induction. Two to four month old $Scn3a^{+/Hyp}/Scn1a^{+/RH}$ mice and littermates were tested at five different currents in increasing intensity (5 mA, 8 mA, 10 mA, 14 mA, and 18 mA), with 1-week recovery between each current. Immediately following electrical stimulation, each mouse was released into an empty cage, and behavior was scored using a modified Racine scale: 0 – no seizure, 1 – staring, 2 – forelimb clonus, 3 – rearing and falling.

Open field

The open field test was performed as described in Chapter 2.

Novel cage

The novel cage task was performed as described in Chapter 2.

Rotarod

The rotarod performance task was performed as described in Chapter 2.

Statistical Analysis

All bar graphs indicate the means, and all error bars represent ± standard error of the mean (SEM). All data was analyzed using Prism 6 (GraphPad Software, Inc., La Jolla, CA, USA). Unrelated parametric data (latencies to flurothyl-induced seizures, open field measures, novel cage measures) were analyzed with one-way Analysis of Variance (ANOVA) followed by the Bonferroni *post hoc* comparison if a significant difference was detected. The % survival, number of animals that seized in the hyperthermia-induced seizure paradigm, and the temperature at which each mouse seized were analyzed using the log-rank (Mantel-Cox) test. The average Racine score for each genotype was compared at each 6 Hz current using the nonparametric Kruskal-Wallis test. Weights and the latency to fall from the rotarod was analyzed using a two way repeated measures ANOVA followed by Bonferroni's multiple comparisons *post hoc* analysis.

3.4 Results

3.4.A. Differences in lifespan and pre-weaning weight among $Scn3a^{+/Hyp}/Scn1a^{+/RH}$ mice and littermates are sex-dependent.

To investigate potential interactions between *Scn3a* and *Scn1a*, we crossed $Scn3a^{+/Hyp}$ mice with $Scn1a^{+/RH}$ mice to produce double heterozygotes ($Scn3a^{+/Hyp}/Scn1a^{+/RH}$), as well as WT, $Scn3a^{+/Hyp}$, and $Scn1a^{+/RH}$ littermates. First, we characterized the effect of genotype on survival and pre-weaning weight (Fig. 3.1). Due to the possibility of sex differences on survival and weight, male and female data were analyzed separately. This study also allowed provided the opportunity to further examine the phenotype of $Scn3a^{+/Hyp}$ and $Scn1a^{+/RH}$ mice. Consistent with the results of Chapter 2 (Lamar et al., 2017), the mortality rate of $Scn3a^{+/Hyp}$ mice was not significantly different

than WT for either sex. However, the survival of $Scn1a^{+/RH}$ mice varied by sex, with female mutants exhibiting a significantly higher mortality rate (36% higher; p < 0.0001) when compared to WT (Fig. 3.1B). Both male and female $Scn3a^{+/Hyp}/Scn1a^{+/RH}$ mice exhibited significantly higher mortality rates than WT (22% higher, p < 0.02 and 29%, higher p < 0.0003 respectively), but the mortality rate of the double heterozygotes was similar to $Scn1a^{+/RH}$ littermates (p = 0.21, 0.50 respectively; Fig. 3.1A-B). These results suggest that the effects on survival and weight gain are driven by the $Scn1a$ mutation and not altered by reduced function in $Scn3a$.

We also compared weights among male and female littermates. Male $Scn3a^{+/Hyp}$ mice gained significantly less weight than WT and $Scn1a^{+/RH}$ littermates from P9 to P21 (p < 0.05; Fig. 3.1C). No differences were observed between male $Scn1a^{+/RH}$ and WT mice at any age (p > 0.70 for P6-P21; Fig. 3.1C). However, female $Scn3a^{+/Hyp}$ and $Scn1a^{+/RH}$ mice both exhibited slower growth rates than WT from P9-P21 (Fig. 3.1D). $Scn3a^{+/Hyp}/Scn1a^{+/RH}$ mice also displayed a sex-dependent slower growth rate. The average weight of male $Scn3a^{+/Hyp}/Scn1a^{+/RH}$ mice was similar to that of $Scn3a^{+/Hyp}$ mice, and was significantly lower than that of WT and $Scn1a^{+/RH}$ mice (Fig. 3.1C). On the other hand, the weights of female double heterozygotes were not significantly different than either single heterozygote at any age.
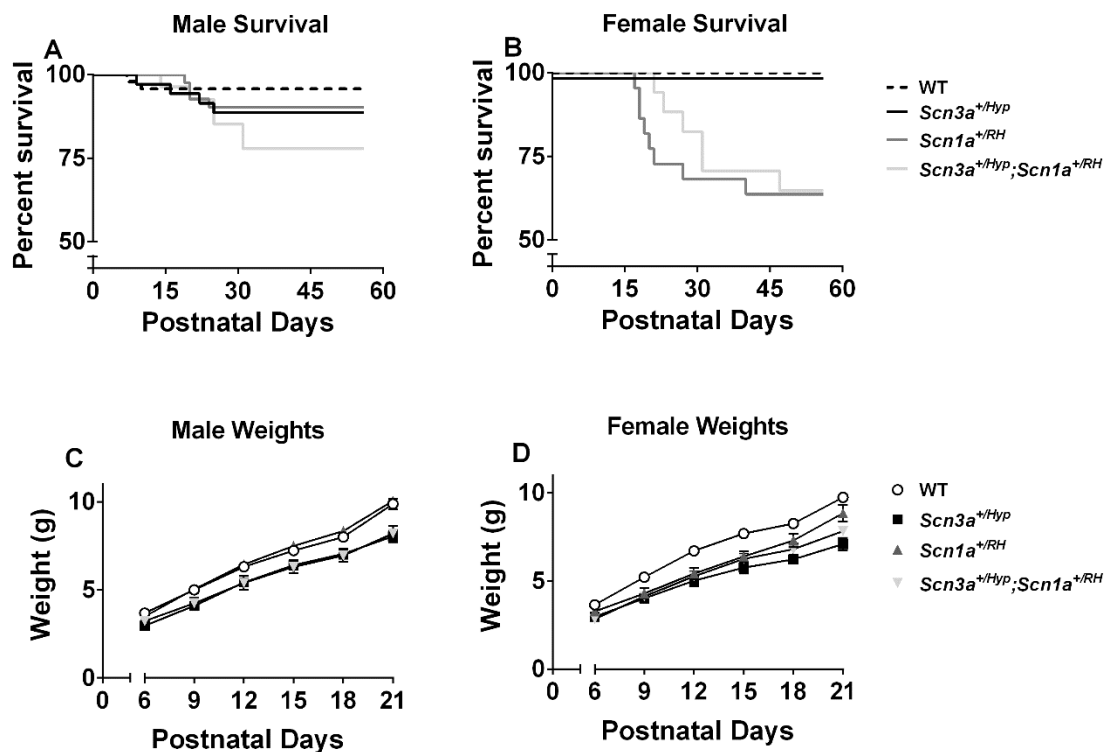
Figure 3.1 Characterization of survival and body weight

Both male and female $Scn3a^{+/Hyp}/Scn1a^{+/RH}$ mice and littermates were monitored for survival from P6-P56 and weighed every three days from P6-P21. **(A)** Male $Scn3a^{+/Hyp}/Scn1a^{+/RH}$ mice exhibited significantly higher mortality when compared to WT (22%, p < 0.02) but not $Scn1a^{+/RH}$ littermates (p > 0.05). n=27-47. **(B)** Both $Scn3a^{+/Hyp}/Scn1a^{+/RH}$ and $Scn1a^{+/RH}$ females exhibited significantly higher mortality than WT (29%, p < 0.0001; 36%, p < 0.0001 respectively). There is no difference in lifespan between $Scn3a^{+/Hyp}/Scn1a^{+/RH}$ and $Scn1a^{+/RH}$ mice (p = 0.50). n = 14-44. **(C)** Male $Scn3a^{+/Hyp}/Scn1a^{+/RH}$ and $Scn3a^{+/Hyp}$ mice had significantly lower weights compared to WT and $Scn1a^{+/RH}$ littermates from P9 to P21 (p < 0.05, n = 11-33). **(D)** Female mutants exhibit lower average weights compare to WT from P9-P21 (p < 0.05, n = 10-33). Error bars represent SEM.

3.4.B. *Scn3a^{+/Hyp}/Scn1a^{+/RH}* mice are more susceptible to flurothyl-induced seizures than either single heterozygote.

To examine seizure susceptibility, we compared latencies to flurothyl-induced seizures in the *Scn3a^{+/Hyp}/Scn1a^{+/RH}* mice to littermates. Due to sex differences, male and female data was analyzed separately. No differences were observed between any of the female genotypes at any seizure endpoint (data not shown). In males, the average latency to the myoclonic jerk (the first behavioral seizure response) was lower for both *Scn3a^{+/Hyp}* and *Scn3a^{+/Hyp}/Scn1a^{+/RH}* mice compared to WT, although these trends did not reach statistical significance (p = 0.13, 0.05 respectively; Fig. 3.2A). In contrast, the latency to the first generalized tonic-clonic seizure (GTCS) was not significantly reduced in *Scn3a^{+/Hyp}* or *Scn1a^{+/RH}* mice compared to WT (p = 0.65, 0.14 respectively) (Fig. 3.2B). Male *Scn3a^{+/Hyp}/Scn1a^{+/RH}* mice, however, exhibited significantly reduced latencies to the first GTCS compared with all other genotypes (Fig. 3.2B). There were no differences between the genotypes in latency to the hindlimb extension (data not shown).
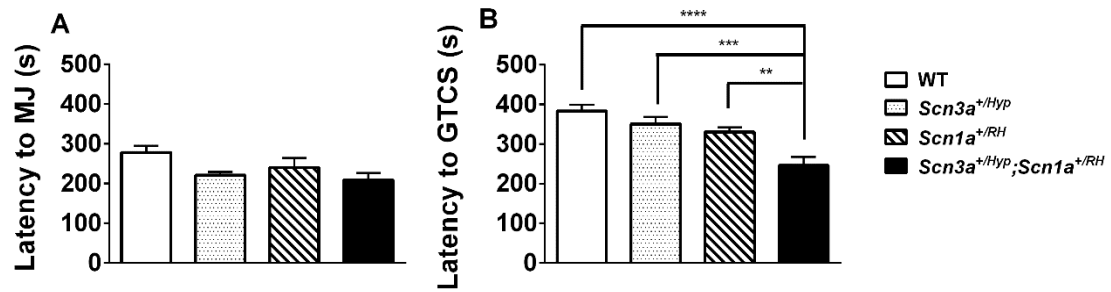
Figure 3.2 Male *Scn3a^{+/Hyp}/Scn1a^{+/RH}* mice are more susceptible to flurothyl-induced seizures.

(A) The latency to the myoclonic jerk (MJ) is comparable among all genotypes for male mice. **(B)** Male *Scn3a^{+/Hyp}/Scn1a^{+/RH}* mice exhibit significantly reduced latencies to the generalized tonic-clonic seizure (GTCS) compared to the other genotypes. $**p < 0.01$, $***p < 0.001$, $****p < 0.0001$. Error bars represent SEM, n = 8-10.

3.4.C. *Scn3a$^{+/Hyp}$/Scn1a$^{+/RH}$* and *Scn1a$^{+/RH}$* mice exhibit similar thresholds to hyperthermia-induced seizures and 6 Hz-induced seizures.

We also examined susceptibility to hyperthermia-induced seizures, a model of febrile seizures, in male and female *Scn3a$^{+/Hyp}$/Scn1a$^{+/RH}$* mice and littermates (Fig. 3.3). Since the mice were not sexually mature at the age at which they were tested (P14-15), both sexes were combined for analysis. As was previously reported in Chapter 2, there were no significant differences in the percentage of *Scn3a$^{+/Hyp}$* mice exhibiting seizures or the average temperature at which the seizures occurred compared to WT littermates. Also consistent with previous reports, *Scn1a$^{+/RH}$* mice were more susceptible to hyperthermia-induced seizures when compared to WT littermates (p < 0.05, leftward shift in curve, Fig. 3.3). There were no significant differences between *Scn1a$^{+/RH}$* and *Scn3a$^{+/Hyp}$/Scn1a$^{+/RH}$* mice in their response to the increasing temperature (p = 0.83).

We also investigated the susceptibility of each genotype to 6 Hz-induced electroconvulsive seizures. Only male mice were studied using this seizure paradigm. Seizure incidence and severity were determined at five currents: 5 mA, 8 mA, 10 mA, 14 mA, and 18 mA (Fig. 3.4A-E). At all currents, a greater number of *Scn1a$^{+/RH}$* and *Scn3a$^{+/Hyp}$/Scn1a$^{+/RH}$* mice exhibited a seizure response, and were more severely affected when compared to WT littermates but not compared to each other. At 5 mA, 82% (9/11) of *Scn1a$^{+/RH}$* mice (1RS1, 7RS2, 1RS3) and 73% (8/11) of *Scn3a$^{+/Hyp}$/Scn1a$^{+/RH}$* mice (1RS1, 5RS2, 2RS3) seized. At 8 mA, 91% (10/11) of *Scn1a$^{+/RH}$* mice (1RS1, 4RS2, 5RS3) and 82% (9/11) of *Scn3a$^{+/Hyp}$/Scn1a$^{+/RH}$* mice (6RS2, 3RS3) seized. At 10 mA, 82% (9/11) of *Scn1a$^{+/RH}$* mice (1RS1, 3RS2, 5RS3) and 55% (6/11) of *Scn3a$^{+/Hyp}$/Scn1a$^{+/RH}$* mice (3RS2, 3RS3) seized. At 14 mA, 82% (9/11) of *Scn1a$^{+/RH}$*

mice (9RS3) and 73% (8/11) of $Scn3a^{+/Hyp}/Scn1a^{+/RH}$ mice (1RS1, 7RS3) seized. At 18 mA, 90% (9/10) of $Scn1a^{+/RH}$ mice (9RS3) and 100% (11/11) of $Scn3a^{+/Hyp}/Scn1a^{+/RH}$ mice (2RS1, 1RS2, 8RS3) seized.

A greater number of $Scn3a^{+/Hyp}$ mice also exhibited a seizure response and were more severely affected than WT at all currents, although this difference was not statistically significant. WT mice were resistant to 6 Hz-induced seizures until 18 mA.
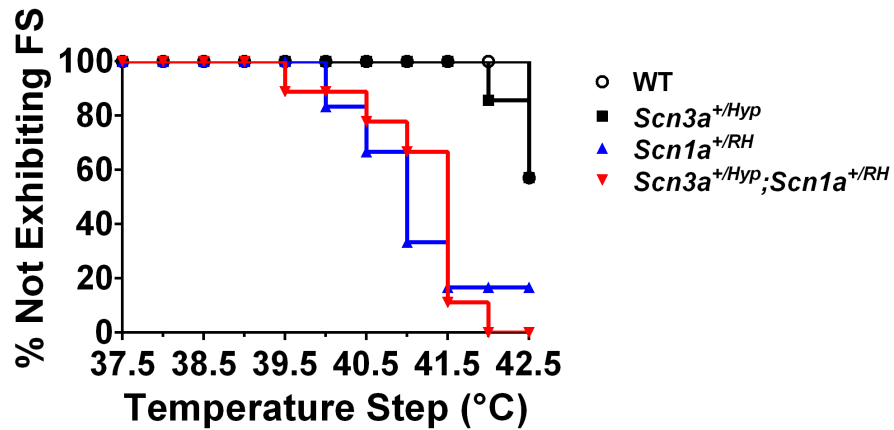
Figure 3.3 *Scn3a*^{+/Hyp}*/Scn1a*^{+/RH} **mice exhibit increased susceptibility to hyperthermia-induced seizures**

Both *Scn3a*^{+/Hyp}*/Scn1a*^{+/RH} and *Scn1a*^{+/RH} mice exhibit greater susceptibility to hyperthermia-induced seizures when compared to WT ($p < 0.05$), but are not significantly different from each other ($p = 0.83$). n = 6-9.
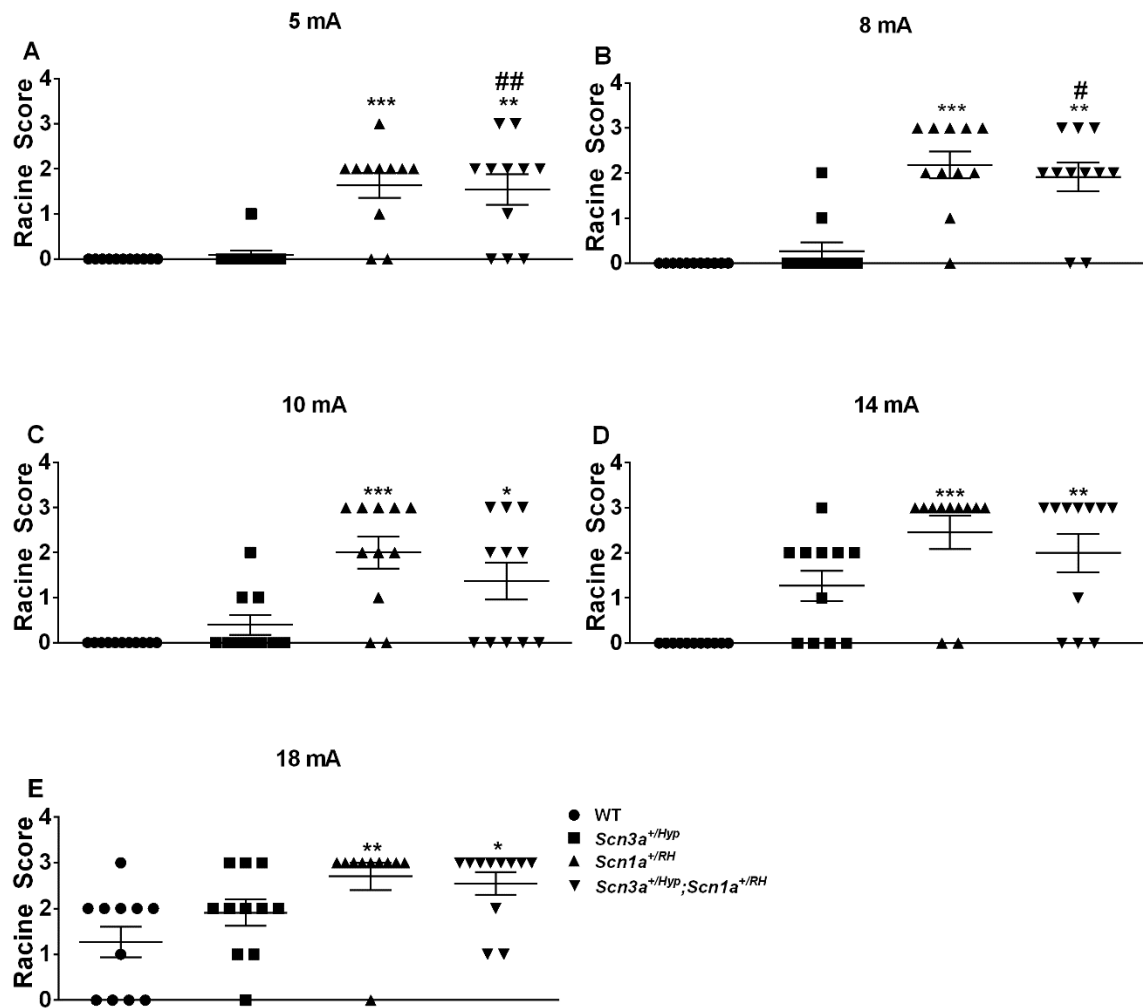
Figure 3.4 *Scn3a^{+/Hyp}/Scn1a^{+/RH}* and *Scn1a^{+/RH}* mice exhibit similar susceptibility to 6 Hz-induced seizures

Scn3a^{+/Hyp}/Scn1a^{+/RH} and *Scn1a^{+/RH}* mice exhibit significantly higher average Racine scores than WT littermates at **(A)** 5 mA, **(B)** 8 mA, **(C)** 10 mA, **(D)** 14 mA, and **(E)** 18 mA. The average Racine score of *Scn3a^{+/Hyp}/Scn1a^{+/RH}* mice was significantly higher than *Scn3a^{+/Hyp}* mice at currents of 5 mA and 8 mA. The seizure severity of *Scn3a^{+/Hyp}/Scn1a^{+/RH}* and *Scn1a^{+/RH}* mice was comparable at each current. $*p < 0.05$ vs.

WT, **p < 0.01 vs. WT, ***p < 0.001 vs. WT, #p < 0.05 vs. $Scn3a^{+/Hyp}$, ##p < 0.01 vs.

$Scn3a^{+/Hyp}$. Error bars represent SEM, n = 11 for each group.

3.4.D Behavioral responses of the *Scn3a*^{+/Hyp}/*Scn1a*^{+/RH} mice were similar to *Scn3a*^{+/Hyp} mutants.

We also compared the behavioral characteristics of the $Scn3a^{+/Hyp}$/$Scn1a^{+/RH}$ mice to littermates of each genotype. Tests were conducted to measure anxiety (open field), response to novelty (novel cage exploration) and motor coordination and motor learning (rotarod). In the open field test, there were no differences in time spent in the center of the field (Fig. 3.5A). There were also no differences in distance traveled and speed during the open field test (data no shown). In the novel cage exploration task, the time spent digging, rearing, and grooming while in the novel environment was measured. $Scn3a^{+/Hyp}$/$Scn1a^{+/RH}$ mice spent significantly more time rearing than WT and $Scn1a^{+/RH}$ mice, but not more than $Scn3a^{+/Hyp}$ mice (Fig. 3.5B). There were no differences in the time spent digging among any of the genotypes (Fig. 3.5C). $Scn3a^{+/Hyp}$/$Scn1a^{+/RH}$ mice also spent significantly more time grooming than WT littermates ($p < 0.01$; Fig. 3.5D). Although $Scn3a^{+/Hyp}$/$Scn1a^{+/RH}$ mice also groomed more than $Scn3a^{+/Hyp}$ and $Scn1a^{+/RH}$ mice, these differences did not reach statistical significance (0.14 and 0.06 respectively).

We compared the motor behavior of the double heterozygotes to their littermates by measuring performance on an accelerating rotarod (Fig. 3.6). Consistent with the data in Chapter 2 (Lamar et al., 2017), $Scn3a^{+/Hyp}$ mice failed to improve on the rotarod and fell more quickly than WT littermates. $Scn3a^{+/Hyp}$/$Scn1a^{+/RH}$ mice also exhibited significantly reduced latencies to fall when compared with WT and $Scn1a^{+/RH}$ mice; however, the difference between $Scn3a^{+/Hyp}$/$Scn1a^{+/RH}$ and $Scn3a^{+/Hyp}$ mice was not statistically significant.
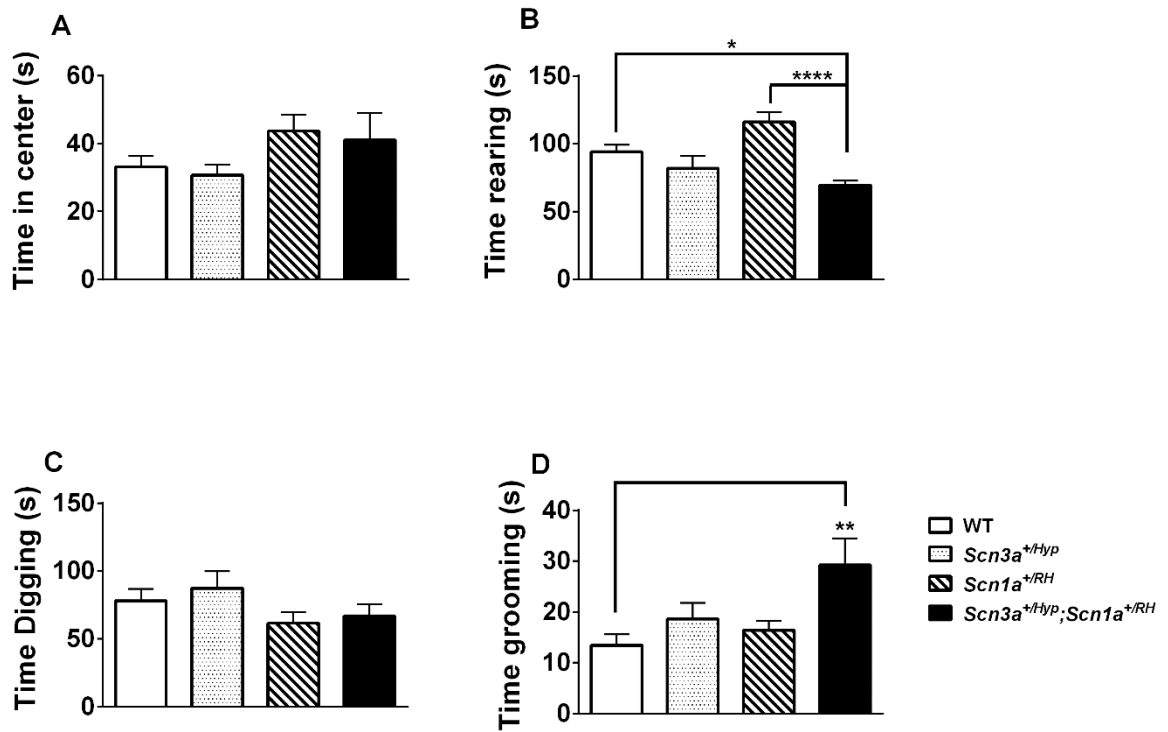
Figure 3.5 *Scn3a^{+/Hyp}/Scn1a^{+/RH}* mice do not exhibit increased anxiety or exploratory behaviors.

(A) No differences were observed between the genotypes in time spent in the center of the open field. n = 11-14. **(B)** *Scn3a^{+/Hyp}/Scn1a^{+/RH}* mice spent significantly more time rearing during novel cage exploration than WT and *Scn1a^{+/RH}* littermates, but time rearing was similar to *Scn3a^{+/Hyp}* mice. **(C)** No differences were observed in time spent digging during the novel cage test. **(D)** *Scn3a^{+/Hyp}/Scn1a^{+/RH}* mice groomed significantly more than WT during novel cage, but not more than *Scn3a^{+/Hyp}* and *Scn1a^{+/RH}* mice (p = 0.14, 0.06 respectively). *p < 0.05, **p < 0.01, ****p < 0.0001. Error bars represent SEM, n = 14-16.
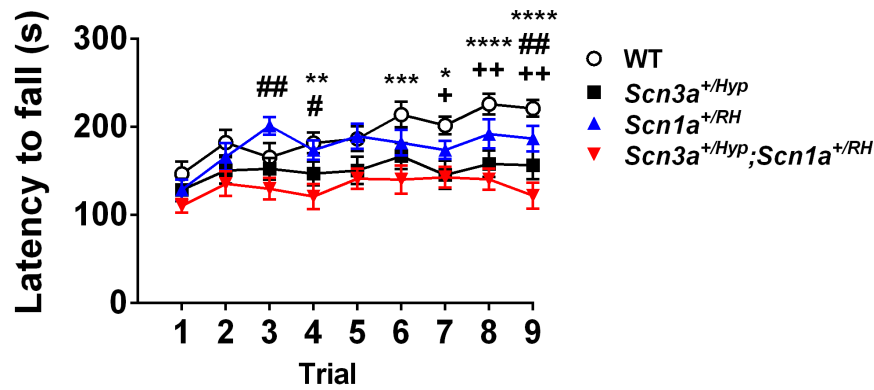
Figure 3.6 *Scn3a^{+/Hyp}/Scn1a^{+/RH}* and *Scn3a^{+/Hyp}* littermates had impaired rotarod performance.

Scn3a^{+/Hyp}/Scn1a^{+/RH} (*p < 0.05, **p < 0.01, ***p < 0.001, ****p < 0.0001) and *Scn3a^{+/Hyp}* mice (^+p < 0.05, ^{++}p < 0.01) exhibited significantly reduced latencies to fall compared with WT littermates. *Scn3a^{+/Hyp}/Scn1a^{+/RH}* mice also had significantly reduced latencies compared to *Scn1a^{+/RH}* mice (^#p < 0.05, ^{##}p < 0.01). Error bars represent SEM, n = 14-16.

3.5 Discussion

We have previously shown that the VGSCs *Scn2a* and *Scn8a* can interact with *Scn1a* to worsen or ameliorate the GEFS+ phenotype (Martin et al., 2007, Hawkins et al., 2011). Recent evidence suggests that *Scn3a* may partially compensate for *Scn1a* dysfunction, supporting the hypothesis that both genes may serve a similar role in the brain. Therefore, dysfunction in both genes could potentially exacerbate seizure and behavior phenotypes. In order to investigate this hypothesis, we generated mice heterozygous for both a hypomorphic *Scn3a* allele and the GEFS+ *Scn1a* mutation R1648H. We compared the responses of *Scn3a$^{+/Hyp}$/Scn1a$^{+/RH}$* mice, littermates with each mutation, and WT littermates using a number of seizure induction paradigms, and we also compared anxiety, exploration, and motor behavior.

Scn3a$^{+/Hyp}$/Scn1a$^{+/RH}$ mice were more susceptible to flurothyl-induced seizures than any other genotype, which seems to support genetic interaction between the two genes. Flurothyl is believed to act as a GABA receptor antagonist, so it is possible that, similar to *Scn1a*, *Scn3a* functions within GABAergic neurons to regulate inhibition (Hashimoto et al., 2006). Interestingly, we were unable to replicate previous findings that both single mutants were also significantly more susceptible to flurothyl-induced seizures than WT. This is possibly due to the smaller sample size compared with previous studies and the variability typically observed with flurothyl. Notably, in light of our sample size, the findings for the double heterozygotes were particularly robust ($p < 0.01 - 0.0001$), bolstering our confidence in the result.

In all other seizure paradigms and behavioral tests, *Scn3a$^{+/Hyp}$/Scn1a$^{+/RH}$* mice exhibited the same phenotype as the more severe phenotype of the two single mutants. As

an example, $Scn3a^{+/Hyp}/Scn1a^{+/RH}$ mice were more susceptible to hyperthermia-induced

seizures than WT, a phenotype observed in the $Scn1a^{+/RH}$ mice but not $Scn3a^{+/Hyp}$

mutants. This observation and the remaining results presented in this Chapter suggest that

Scn3a is largely independent of *Scn1a* in function. One explanation for this result could

be that both genes are often expressed in different cell types and therefore might perform

distinct functions. One example of a task where this may be the case is the accelerating

rotarod test, in which *Scn3a* and $Scn3a^{+/Hyp}/Scn1a^{+/RH}$ mice exhibit a motor learning

impairment. Motor learning is regulated by the cerebellum, a region in which *Scn3a* and

Scn1a are expressed in different neuron types: the granule cells and Purkinje cells,

respectively (Black et al., 1994, Lindia and Abbadie, 2003). Another potential

explanation for the lack of interaction between these two genes is the complementary

timing of their expression. Although *Scn3a* is still expressed in select regions during

adulthood, it declines dramatically after birth, the period during which *Scn1a* expression

increases (Beckh et al., 1989, Cheah et al., 2013). These inversely correlated expression

patterns may naturally limit interactions between the two VGSCs, even if they are

expressed in the same neuronal cell types. Furthermore, we demonstrated in Chapter 2

that *Scn1a* is not upregulated following reduced *Scn3a* expression, further evidence that

one does not necessarily compensate for the other. Ultimately, further work is needed to

determine the extent of interaction between *Scn3a* and *Scn1a.*

In conclusion, we investigated the potential genetic interaction between *Scn3a*

and *Scn1a* and discovered that *Scn3a* deficiency increases susceptibility to flurothyl-

induced seizures in a GEFS+ *Scn1a* model. Although, additional seizure and behavioral

experiments suggest that *Scn3a* and *Scn1a* are largely independent of each other in

function, our results warrant further studies and highlight *Scn3a* as a potential, if limited,

modifier of *Scn1a* dysfunction.

Chapter 4: Conclusions and Future Directions

4.1 Overview

The experiments described in this dissertation provide greater insight into the role of *SCN3A* in epilepsy, both as a primary disease gene and as a modifier of *SCN1A*-derived epilepsy. To date, only six *SCN3A* epilepsy mutations have been reported, five of which have been shown to cause gain of function biophysical properties (Holland et al., 2008, Vanoye et al., 2014, Chen et al., 2015). Although a sixth mutation was shown to reduce channel activity, the contribution of loss of function *SCN3A* mutations to epilepsy remains unclear (Chen et al., 2015). In Chapter 2, we reported a novel, trafficking-deficient *SCN3A* mutation in a patient with partial epilepsy, providing further evidence that *SCN3A* deficiency results in increased seizure risk. We then demonstrated that partial loss of *Scn3a* expression is sufficient to increase seizure susceptibility and produce motor deficits in a hypomorphic mouse line.

In contrast to *SCN3A*, over 1200 *SCN1A* mutations have been identified in DS, most of which are loss of function (Meng et al., 2015). One hallmark of *SCN1A* disorders is the clinical heterogeneity observed. Within a single GEFS+ pedigree, for example, the phenotype may range from mild febrile seizures to DS (Scheffer and Berkovic, 1997, Singh et al., 2001, Camfield and Camfield, 2015). This variable expressivity can be partially explained by the action of genetic modifiers. Human and mouse studies have identified candidate modifiers of *SCN1A*-derived epilepsy, including the VGSCs *SCN2A* and *SCN8A* (Martin et al., 2007, Ohmori et al., 2008, Singh et al., 2009, Hawkins et al., 2011, Gaily et al., 2013, Mulley et al., 2013a, Ohmori et al., 2013). In Chapter 3, we determined that partial loss of *Scn3a* increases susceptibility to flurothyl-induced seizures but does not alter survival or the behavioral characteristics of a

GEFS+ mouse model. Furthermore, in Appendix B, we demonstrated that *Scn9a* did not modify the seizure susceptibility observed in the GEFS+ mouse model. In this chapter, I will discuss the significance of the main findings and describe future directions for this project.

4.2 The Role of *SCN3A* in Partial Epilepsy: Different Mechanisms, Common Outcome

In Chapter 2, we describe a novel *SCN3A* mutation, L247P, in a patient with partial epilepsy. Although a previous mutation was shown to slightly reduce channel activity (Chen et al., 2015), our work extends this finding by identifying the first trafficking-deficient *SCN3A* epilepsy mutation (Lamar et al., 2017). Taken together, these findings provide evidence that *SCN3A*-deficiency results in epilepsy.

These findings are intriguing since the first five identified *SCN3A* mutations were shown to have gain of function effects (Holland et al., 2008, Vanoye et al., 2014). Additionally, upregulation of *SCN3A* expression was observed in the hippocampus of human epilepsy patients and a number of rat models of epilepsy, (Aronica et al., 2001, Whitaker et al., 2001a, Guo et al., 2008, Xu et al., 2013). Although this could be a protective compensatory change in *SCN3A* expression, these results may also suggest that increased *SCN3A* expression might contribute to seizure generation. Taken together, the previous results and the results from this dissertation suggest that increased or decreased activity of *SCN3A* channels can cause epilepsy.

In a number of epilepsy genes, gain and loss of function mutations have been identified; however, each mechanism often produces different phenotypes. For example,

gain of function *KCNA2* mutations produce a more severe epileptic encephalopathy than loss of function mutations (Syrbe et al., 2015). In *SCN8A*, gain of function mutations also produce epileptic encephalopathy, while loss of function mutations appear to result in intellectual disability with or without the presence of seizures (Blanchard et al., 2015). Interestingly, in the case of *SCN3A*, the two loss of function mutations seem to produce the more severe behavioral comorbidities, including severe intellectual disability, global developmental delay, and hypotonia, suggesting that loss of function may be more deleterious than increased activity. As an explanation for the more severe phenotype observed with reduced *SCN3A* activity, I hypothesize that, similarly to *SCN1A*, *SCN3A* is expressed primarily in GABAergic interneurons, such that decreased activity of *SCN3A* results in an overall decrease in network inhibition (Ogiwara et al., 2007, Hedrich et al., 2014). There is a delicate balance of excitation and inhibition in the brain, and reduced inhibition by way of GABAergic interneuron dysfunction has been implicated in a range of neurological disorders, including epilepsy, autism, Rett syndrome, and schizophrenia (Konradi et al., 2011, Gill and Grace, 2014, Braat and Kooy, 2015, Frye et al., 2016, Jiang et al., 2016). Intellectual disability, developmental delay, motor dysfunction, and seizures are all within the range of comorbidities observed in disorders of GABAergic dysfunction, further linking reduced inhibition to the phenotype observed in *SCN3A*-deficient patients (Chao et al., 2010, Akiyama et al., 2012, Ure et al., 2016).

One caveat is that *Scn3a* expression has been demonstrated to decline in the brain during development. In fact, we were unable to detect Scn3a protein in whole brain by Western blot (Chapter 2). Although *Scn3a* is reduced in the adult brain overall, a number of studies have observed moderate to high expression in specific regions, such as the

hippocampus and the basal ganglia (Beckh et al., 1989, Furuyama et al., 1993, Lindia and Abbadie, 2003). Furthermore, previous studies in rodents have shown that *Scn3a* is expressed in both excitatory neurons, such as granule cells of the dentate gyrus and cerebellum, and inhibitory interneurons (Lindia and Abbadie, 2003, Okaty et al., 2009). However, the cell type-specific distribution of *SCN3A* in adult mice has not been fully characterized. In a future study, immunohistochemistry could be performed in brain slices from adult wild-type mice in order to determine the proportion of excitatory and inhibitory neurons that express *Scn3a*. However, expression studies alone will be insufficient to determine the mechanisms by which reduced *Scn3a* increases seizure susceptibility. To determine the contribution of specific cell-types to the epilepsy phenotype, a conditional knockout mouse could be used to selectively delete *Scn3a* in either excitatory or inhibitory neurons in the brain.

One question that may be raised is whether the disinhibition hypothesis can adequately explain the role of gain of function *SCN3A* mutations in epilepsy. Patients with gain of function *SCN3A* mutations exhibit partial seizures. However, increased GABAergic transmission has been shown to rescue the seizure and behavioral phenotypes in both patients and mouse models of epilepsy, autism, and schizophrenia (Wassef et al., 1999, Gandal et al., 2012, Han et al., 2012, Han et al., 2014, Martin et al., 2016). One possible factor in this discrepancy is the developmental expression pattern of *SCN3A*. *SCN3A* expression is highest in early development, when GABA acts as the primary excitatory neurotransmitter in the brain, rather than glutamate, and drives the maturation of excitatory neurons (Ben-Ari et al., 1989, Ganguly et al., 2001, Ben-Ari, 2002, Cancedda et al., 2007, Pfeffer et al., 2009, Kirmse et al., 2011). Increased *SCN3A*

function in GABAergic interneurons during this critical period could therefore have a long-term impact on excitability and, ultimately, seizure risk.

4.3 Potential Mechanisms of *Scn3a* Epilepsy

In Chapter 2, the in vivo consequences of *Scn3a*-deficiency were studied for the first time. We showed that mice heterozygous for a hypomorphic *Scn3a* allele, expressing approximately 60% of wild-type levels of *Scn3a*, exhibit increased susceptibility to seizures induced by the proconvulsants flurothyl and kainic acid as well as by the 6 Hz psychomotor seizure test. Each test represents a different mode of seizure induction, which permits us to speculate on potential brain regions and mechanisms that may play a role in *Scn3a*-derived epilepsy.

4.3.A. Susceptibility to Flurothyl-Induced Seizures

Both male and female $Scn3a^{+/Hyp}$ mice exhibited decreased latencies to flurothyl-induced generalized seizures. Although the mechanism of action of flurothyl is not fully understood, it is speculated to open sodium channels and is also believed to be, in part, a GABA receptor antagonist, acting at the benzodiazepine binding site (Woodbury, 1980, Krasowski, 2000, Hashimoto et al., 2006). Increased susceptibility to flurothyl is consistent with the hypothesis that reduced *Scn3a* results in reduced GABAergic inhibition. However, since flurothyl likely does not only affect GABA receptors, experiments comparing both GABAergic interneuron and excitatory neuron-specific *Scn3a* conditional knockout mice would allow us to determine whether *Scn3a* acts via inhibitory pathways in the brain.

4.3.B. Susceptibility to 6 Hz Corneal Stimulation

Scn3a$^{+/Hyp}$ mice were more susceptible to electrically induced 6 Hz seizures than WT littermates. The 6 Hz "psychomotor" seizure induction paradigm produces partial seizures and has been used as a model of refractory partial epilepsy due to its insensitivity to phenytoin and related drugs (Brown et al., 1953, Barton et al., 2001). C-fos immunohistochemistry in mice has shown that 22 mA and 32 mA stimulations, which are within the range used in this dissertation, activate limbic structures in the frontal and temporal lobe, including the piriform cortex, perirhinal cortex, and the amygdala (Barton et al., 2001).

Compared with surrounding limbic regions, the piriform cortex, the perirhinal cortex, and the amygdala are especially sensitive to kindling (McIntyre et al., 1993, McIntyre and Plant, 1993, Loscher and Ebert, 1996). Each of these regions has extensive bidirectional connections with each other and other temporal lobe structures, such as the hippocampus, placing them in prime position to contribute to the spread of temporal lobe seizures (Agster and Burwell, 2009, Vaughan and Jackson, 2014, Vismer et al., 2015, Agster et al., 2016). Furthermore, a strong inhibitory network in the perirhinal cortex has been shown to regulate the propagation of neuronal activity between the temporal cortex and hippocampus, suggesting that disinhibition in this region could result in increased excitatory input to the hippocampus (de Curtis and Pare, 2004). Consistent with the brain regions activated by 6 Hz seizure induction, the patient with the L247P trafficking-deficient mutation exhibited spontaneous seizures originating in the frontal and temporal lobe. It is possible, therefore, that reduced *SCN3A* results in increased susceptibility to seizures originating in these regions.

4.3.C. Susceptibility to Seizures Induced by Kainic Acid

$Scn3a^{+/Hyp}$ mice exhibited reduced seizure latencies and more severe kainic acid-induced seizures when compared to WT littermates. Kainic acid is an agonist of ionotropic kainate glutamate receptors. Although glutamate is an excitatory neurotransmitter, the mechanism underlying kainic acid-induced seizures has not been fully elucidated. Kainic acid has been shown to excite hippocampal pyramidal cells, particularly those in the CA3 region, which contains a high density of kainate receptors (Monaghan and Cotman, 1982, Ben-Ari and Gho, 1988, Lothman et al., 1991). However, activation of kainate receptors may also exhibit negative effects on inhibition by depressing evoked inhibitory postsynaptic currents in GABAergic interneurons of the limbic system (Rodriguez-Moreno et al., 1997, Mulle et al., 2000, Jiang et al., 2015). As further evidence of the role of kainate receptors in disinhibition, mice with a mutation in the GABA-A receptor β3 subunit gene are more susceptible to seizures induced by injection of kainic acid (Vien et al., 2015). Taking these findings into account, the increased susceptibility to systemic kainic acid provides support for increased network disinhibition in $Scn3a^{+/Hyp}$ mice compared with WT.

4.4 The role of *Scn3a* in motor behavior

$Scn3a^{+/Hyp}$ mice exhibited decreased locomotor activity when compared to WT littermates during the dark phase (more active period) of the light/dark cycle. Locomotor activity is believed to be regulated by the basal ganglia, which supports and suppresses movement via the direct and indirect pathways, respectively (Kreitzer and Malenka, 2008, Kravitz et al., 2010, Vien et al., 2015). *SCN3A* expression has been observed in all regions of the basal ganglia of adult humans and rodents, including the striatum, the

globus pallidus, and the substantia nigra (Beckh et al., 1989, Furuyama et al., 1993, Chen et al., 2000, Whitaker et al., 2001b, Lindia and Abbadie, 2003). The majority of basal ganglia neurons are GABAergic interneurons, providing further support for the possible role of *SCN3A* in neuronal inhibition (Galvan and Wichmann, 2007). Future studies could use electrophysiological techniques to determine the effect of *Scn3a* deficiency on signaling of GABAergic cells in individual regions of the basal ganglia.

Perhaps the most interesting behavioral deficit observed was the impairment in rotarod performance. $Scn3a^{+/Hyp}$ mice performed the same as WT littermates on the accelerating rotarod during early trials, but unlike WT, they failed to improve after multiple trials, suggesting a deficit in motor learning rather than coordination. Motor learning is regulated primarily by signaling from the cerebellar Purkinje cells to the deep cerebellar nuclei (Mauk, 1997). Mice with Purkinje cell-specific deletions of a number of genes exhibit impairment in motor learning tasks (Levin et al., 2006, Woodruff-Pak et al., 2006, Schonewille et al., 2010, Peter et al., 2016).

The axons of excitatory granule cells, also called parallel fibers, facilitate motor learning by innervating Purkinje cells (Hirano, 2014). A recent study demonstrated that silencing these neurons by deleting their voltage-gated calcium channels is sufficient to produce motor learning impairments in mice (Galliano et al., 2013). Although expression of Scn3a has not been observed in human or rodent Purkinje cells, Scn3a protein is present in the granule cells of adult humans and mice, suggesting that a global reduction in Scn3a may impair learning via reduced excitation of Purkinje cells (Brysch et al., 1991, Whitaker et al., 2000, Whitaker et al., 2001b, Lindia and Abbadie, 2003). Similarly, one study showed that mice with granule cell-specific deletion of the VGSC

Scn8a improved on the rotarod at a significantly slower rate than WT, providing evidence that VGSC loss in granule cells alone can result in motor learning impairment (Levin et al., 2006). In the future, it will be interesting to determine whether loss of *Scn3a* expression in the granule cells of the cerebellum is sufficient to cause motor learning deficits.

4.5 *Scn3a* as a Modifier of *Scn1a*

4.5.A. Effects on Seizure Susceptibility and Behavior

To investigate the potential role of *Scn3a* as a modifier of *Scn1*, we generated mice heterozygous for both the *Scn3a^{Hyp}* hypomorphic allele and *Scn1a^{RH}* mutation (*Scn3a$^{+/Hyp}$/Scn1a$^{+/RH}$*). The presence of the *Scn3a^{Hyp}* allele exacerbated susceptibility of *Scn1a$^{+/RH}$* mice to flurothyl-induced seizures, but not to hyperthermia- or 6 Hz-induced seizures. The phenotype of the double heterozygotes, which was mostly similar or identical to the more severe of the single mutants, suggests that while Scn3a and Scn1a are important in the regulation of neuronal excitability, these channels are functionally independent in at least some pathways. Interestingly, the increased susceptibility to flurothyl, a likely GABA receptor antagonist, provides support for the hypothesis that both channels contribute to the regulation of GABAergic interneuron excitability. A future experiment could use immunohistochemistry to determine whether *Scn3a* and *Scn1a* colocalize in various regions throughout the brain.

4.5.B. Role of *Scn3a* Dosage on Modifier Effects

In our studies of *Scn3a* as a disease gene and as a modifier, we used a gene trap mouse line, which we later determined to be hypomorphic rather than a complete null. Due to the increased lethality observed in homozygotes of this hypomorphic line, we

crossed heterozygous *Scn3a* mutants (*Scn3a$^{+/Hyp}$*) mice to *Scn1a$^{+/RH}$* mice to produce

double heterozygous progeny (*Scn3a$^{+/Hyp}$/Scn1a$^{+/RH}$*). Since *Scn3a$^{+/Hyp}$* mice express

more than 60% of WT levels of Na$_v$1.3 protein, it is possible that a larger reduction in

Scn3a expression might have a greater impact on the phenotype of the *Scn1a$^{+/RH}$* mouse.

It would therefore be interesting to study the effects of both 50% and complete loss of

Scn3a on the phenotype of the *Scn1a$^{+/RH}$* mice. In order to overcome the potential

difficulties of breeding with homozygous *Scn3a* knockout mice, double heterozygotes

(*Scn3a$^{+/-}$/Scn1a$^{+/RH}$*) can be mated to *Scn3a$^{+/-}$* to produce WT, *Scn3a$^{+/-}$*, *Scn1a$^{+/RH}$*,

Scn3a$^{-/-}$, *Scn3a$^{+/-}$/Scn1a$^{+/RH}$*, and *Scn3a$^{-/-}$/Scn1a$^{+/RH}$* littermates.

4.6 *Scn9a* as a Modifier of *Scn1a*

In Appendix B, we evaluated *Scn9a* as a modifier of GEFS+ by crossing the

Scn9a^{NY} line with the *Scn1a^{RH}* mouse. The point mutation N641Y was previously

observed in a multigenerational family in which all but one mutation-positive member

presented with a seizure phenotype ranging from simple febrile seizures to intractable

epilepsy (Singh et al., 2009). A mouse model was generated in that study by knock-in of

the mutation into the orthologous mouse gene, and homozygous *Scn9a$^{NY/NY}$* mice were

shown to be more susceptible to electrically-induced seizures (Singh et al., 2009). In our

study, neither heterozygotes nor homozygotes were more susceptible than WT to seizures

induced by flurothyl or hyperthermia. Furthermore, mice heterozygous for both the NY

and *Scn1a* RH mutations were not more seizure susceptible than *Scn1a$^{+/RH}$* mice alone,

suggesting that the N641Y allele does not alter the GEFS+ phenotype.

One caveat of our study is that, in the family carrying the *SCN9A^{NY}* allele, there

were no co-segregating *SCN1A* mutations, which suggests that the *Scn9a$^{+/NY}$/Scn1a$^{+/RH}$*

mouse might not be the ideal model in which to study interactions between these two genes. Furthermore, given the fact that the patients were heterozygous for the N641Y mutation and heterozygous mutants exhibited normal seizure thresholds in both studies, it is possible that this variant is not disease-causing. We cannot exclude the possibility, therefore, that *SCN9A* does modify *SCN1A*. A more informative future experiment would be to generate a mouse line expressing both a *SCN1A* and *SCN9A* mutation that was found in a patient.

4.7. Conclusions

To summarize our findings, we have demonstrated for the first time that 1) Loss of function *SCN3A* mutations can result in epilepsy and developmental impairment, 2) that *Scn3a*-deficiency increases seizure susceptibility and impacts motor learning, 3) *Scn1a* interacts with *Scn3a* to exacerbate response to flurothyl but the combined mutations did not alter response to other seizure induction paradigms. The findings from this study provide further support for the role of *SCN3A* as an epilepsy disease gene as well as reveal new insights into the function of VGSCs in epilepsy.

Appendix A: Additional Data and Figures from Chapter 2

A.1 Material and Methods

Histology and Immunohistochemistry

Scn3a$^{+/Hyp}$ mutants and WT littermates were deeply anesthetized and

transcardially perfused with 0.1 M phosphate buffer followed by 4% paraformaldehyde.

Brains were post-fixed overnight, cryoprotected in 30% sucrose and sectioned at 40

microns. Sections were processed for NeuN immunohistochemistry with a mouse

monoclonal anti-NeuN antibody (1:500; Chemicon MAB377, clone A60, EMD

Millipore, Billerica, MA, USA). Immunoreactivity was visualized with the streptavidin–

biotin conjugate technique using a Vectastain kit (Vector, Burlingame, CA) with $CoCl_2$

enhancement. Adjacent sections were stained with Cresyl Violet. Sections were viewed

under light microscopy on a Zeiss Axioskop upright microscope and images were

captured with a CRI Nuance multispectral camera.

Quantitative Real-time PCR (qRT-PCR) of Adult Samples

Total RNA was extracted from dissected hippocampus and cerebellum samples

from 10 week old *Scn3a*$^{+/Hyp}$ mutants and WT littermates (n =4/genotype). RNA

extraction and cDNA synthesis was performed as previously described (Makinson et al.,

2014). PCR amplification of *Scn1a*, *Scn2a*, *Scn3a* and *Scn8a* and real-time analysis was

performed as described in the main article. Data was analyzed using the two-tailed

student's t-test in Prism 6 (GraphPad Software, Inc., La Jolla, CA, USA).

Western Blot Analysis of Adult Samples

Whole brains were extracted from 10-week old WT and *Scn3a*$^{+/Hyp}$ littermates (n

= 3/genotype), and frozen at -80°C. The tissue was homogenized and Western blotting

was performed as described in the main article. Densitometry was performed using Image J software (NIH).

Behavioral Analysis

Adult male mice (4-6 months old) were used for all behavioral assays and all data was scored by an investigator blinded to genotypes. Unless otherwise specified, all results were analyzed by one-way ANOVA and *post hoc* comparisons were made using the Tukey test (SigmaPlot 10: Systat Software, Inc., San Jose, CA, USA).

Novel Cage

Scn3a$^{+/Hyp}$ mice and WT littermates (n= 10/genotype) were individually placed into a novel standard cage (30 cm × 17 cm) with corn-cob bedding and video recorded for 15 minutes. Times spent rearing, grooming, and digging were manually scored.

Open Field

Scn3a$^{+/Hyp}$ mice and WT littermates (n= 10/genotype) were individually placed in an opaque, acrylic arena (60 × 60 cm^2) and video recorded for 10 minutes. The center of the chamber was defined as a 30 × 30 cm^2 square. Time in the center, the number of entries into the center, total distance, average speed, and time spent immobile were scored using Any-Maze software (Stoelting Co, Wood Dale, Il, USA).

Marble Burying

Nineteen *Scn3a*$^{+/Hyp}$ mice and 17 WT littermates were each placed in a plastic container (62 cm × 38 cm × 16 cm) filled 13 cm deep with corn-cob bedding. Twenty black marbles were arranged on the bedding in an evenly spaced 5 x 4 grid. Mice were placed in the container for 30 minutes, and the numbers of marbles at least 2/3 buried were recorded.

Light/Dark Box

The apparatus (58 cm × 20 cm) consisted of a two acrylic compartments: one well

lit (43 cm × 20 cm) and one black (15 cm × 20 cm), separated by a partition with an 8 cm

× 5 cm opening at floor level. $Scn3a^{+/Hyp}$ mice and WT littermates (n= 10/genotype) were

individually placed in the center of the lit compartment and allowed to freely explore

both the light and dark zones. Mice were videotaped, and the time spent in the light zone,

time spent in the dark zone, and the number of entries into the dark zone were scored

using Any-Maze software.

Novel Object

Eleven $Scn3a^{+/Hyp}$ mice and 9 WT littermates were individually tested in an open

field arena (60 cm × 60 cm). The test was composed of four 5-minute trials/day for 4

days. During the first trial, mice were habituated to the empty chamber. During the

second and third trial, mice were exposed to two identical spheres. During the last trial,

mice were exposed to a familiar object (sphere) and a novel object (cube). Mice were

videotaped and the time spent exploring both the novel and familiar object were manually

scored. Exploration was defined as time spent within close proximity (< 5 mm) of the

object or with nose and whiskers in contact with the object. Object preference was

determined using the discrimination index, defined by $(T_n - T_f)/(T_n + T_f)$, where T_n is the

time (in seconds) spent with the novel object and T_f is time spent with the familiar object.

Social Interaction

Nine $Scn3a^{+/Hyp}$ mice and 10 WT littermates were individually tested in a three-

chamber acrylic glass arena (20 cm × 40 cm). The chambers were separated by two

partitions, each with a 5 cm × 5 cm opening in the bottom center. The test consisted of

three trials, each ten minutes long. A cylindrical wire cage (10 cm diameter) was used as an inanimate object or to hold the stranger mice. During the first trial (habituation phase), two empty wire cages were placed in the corners of the leftmost and rightmost sections. The experimental mouse was placed in the center chamber and allowed to freely explore the three chambers. During the second trial, which tests sociability, an age-matched and gender-matched stranger mouse was placed in one of the wire cages, and the test mouse was allowed to freely explore. During the third trial, a second stranger mouse (novel mouse) was placed in the other wire cage so that the arena now housed a novel mouse and a familiar mouse (the stranger mouse from the second trial). The test mouse was again allowed to freely explore. Each trial was videotaped, and the time spent exploring each mouse, or empty wire cage, was measured using Any-Maze software.

Porsolt Forced Swim

$Scn3a^{+/Hyp}$ mice and WT littermates (n= 10/genotype) were individually placed in a 4 L glass beaker (24 cm × 18 cm) three-quarters filled with water maintained at $25 \pm 1°C$. Behavior was videotaped for ten minutes and the time spent treading, swimming, and floating was manually scored. Treading was characterized by traveling around the beaker with minimal movement, swimming was defined as vigorous movement with forepaws breaking the water, and floating was defined as minimum activity required to remain afloat.

Visual Cliff

This task was performed in a rectangular acrylic box (62 cm × 38 cm) with a clear bottom and white paper covering the sides. The box was positioned on a table so that half of the box extended beyond the tabletop to form a "cliff". A checkered tablecloth was

placed underneath the box and draped from the tabletop to the floor to emphasize the cliff drop off. The cliff zone and "safe" zone (the half of the box on the table) were separated by a 38 cm × 10 cm opaque region designated the neutral zone. $Scn3a^{+/Hyp}$ mice and WT littermates (n= 10/genotype) were individually placed in the neutral zone and allowed to freely explore for 10 minutes. The mice were videotaped, and the latency to cliff entry, as well as the time spent in both the safe- and cliff-sides, were measured for each mouse using Any-Maze software.

Prepulse Inhibition

$Scn3a^{+/Hyp}$ mice and WT littermates (n= 10/genotype) were placed into acrylic holders in the SR-Lab Startle Response System (San Diego Instruments, San Diego, CA). The mice were acclimated to the system by exposure to background white noise (60 dB) for five minutes. After acclimation, the following randomized trials were presented: acoustic startle alone (117 dB for 40 ms), no startle, or startle preceded by one of four prepulse intensities (70, 72, 76, or 80 dB). A total of 48 trials were run (8 trials of each of the different conditions), with each trial separated by a randomized time interval. The maximum startle amplitude was measured during the first 100 ms after each trial pulse was presented. The percent prepulse inhibition was calculated using the average startle amplitude to the startle alone stimulus.

A.2 Results

A.2.A. No significant changes in Scn1a, Scn2a, and Scn8a expression were observed in Scn3a$^{+/Hyp}$ mutants

As expected, $Scn3a$ mRNA levels were significantly reduced in both the hippocampus and cerebellum of 10-week old $Scn3a^{+/Hyp}$ mice when compared with WT

littermates (Fig. A.2A). *Scn3a* protein expression was undetectable in 10-week old WT mice. To determine whether reduction of *Scn3a* expression leads to compensatory alterations in expression of the other VGSCs in the brain, we also measured *Scn1a, Scn2a,* and *Scn8a* mRNA and protein levels in the hippocampus and cerebellum (n = 4/genotype) and whole brain (n = 3/genotype) respectively (Fig. A.2B-D). We found no significant differences in either mRNA or protein expression levels for any of these sodium channels.

A.2.B. Scn3a$^{+/Hyp}$ mutants performed normally in behavioral testing

No statistically significant differences were observed between *Scn3a*$^{+/Hyp}$ mutants and WT littermates in novel cage, marble burying, light/dark box, novel object recognition, social interaction, forced swim, visual cliff, and prepulse inhibition (Supplemental Table 2). In the open field task, *Scn3a*$^{+/Hyp}$ mice entered the center of the open field significantly less than WT littermates (p < 0.05), suggesting increased anxiety. However, the time spent in the center of the open field was not significantly different between the genotypes (p > 0.05). In addition, the performance of *Scn3a*$^{+/Hyp}$ mutants and WT littermates were comparable in the marble burying and light/dark box tasks, both of which provide measures of anxiety.

Table A.1 Non-synonymous variants identified by clinical exome sequencing.

Gene	Location	rs ID	Nucleotide Change	Amino Acid Change	Inheritance	MAF % (EA/AA/Asian/Latino) (Exome Aggregation Consortium, 2016, Exome Variant Server, 2016)	Genic Intolerance Score (Exome Aggregation Consortium, 2016, Exome Variant Server, 2016) (Petrovski et al, 2013)	Provean (score) (Choi et al., 2012)	SIFT (score) (Kumar et al., 2009)	Polyphen2 (score) (Adzhubei et al., 2010)
SCN3A	2:166019293	Novel	A>G	L247P	De novo	0.0% (0.0/0.0/0.0/0.0)	-2.48 (0.97%)	Deleterious (-6.840)	Damaging (0.00)	Probably damaging (1.0)
KCNAB3	17:7832599	rs200100920	T>C	K52R	Maternal	0.3% (0.36/1.01/0.01/0.53)	-0.29 (32.94%)	Neutral (0.001)	Tolerated (0.691)	Benign (0.212)
SCN9A	2:167141109	rs41268673	G>T	P610T	Not Determined	2.4% (3.45/0.47/1.43/1.18)	0.33 (73.63%)	Neutral (-0.771)	Tolerated (0.076)	Benign (0.003)
KMT2C	7:151876973	rs140834550	C>T	R2463H	Maternal	0.074% (0.005/0.0/0.002/0.0)	-2.52 (0.91%)	Deleterious (-4.018)	Damaging (0.001)	Probably damaging (0.994)
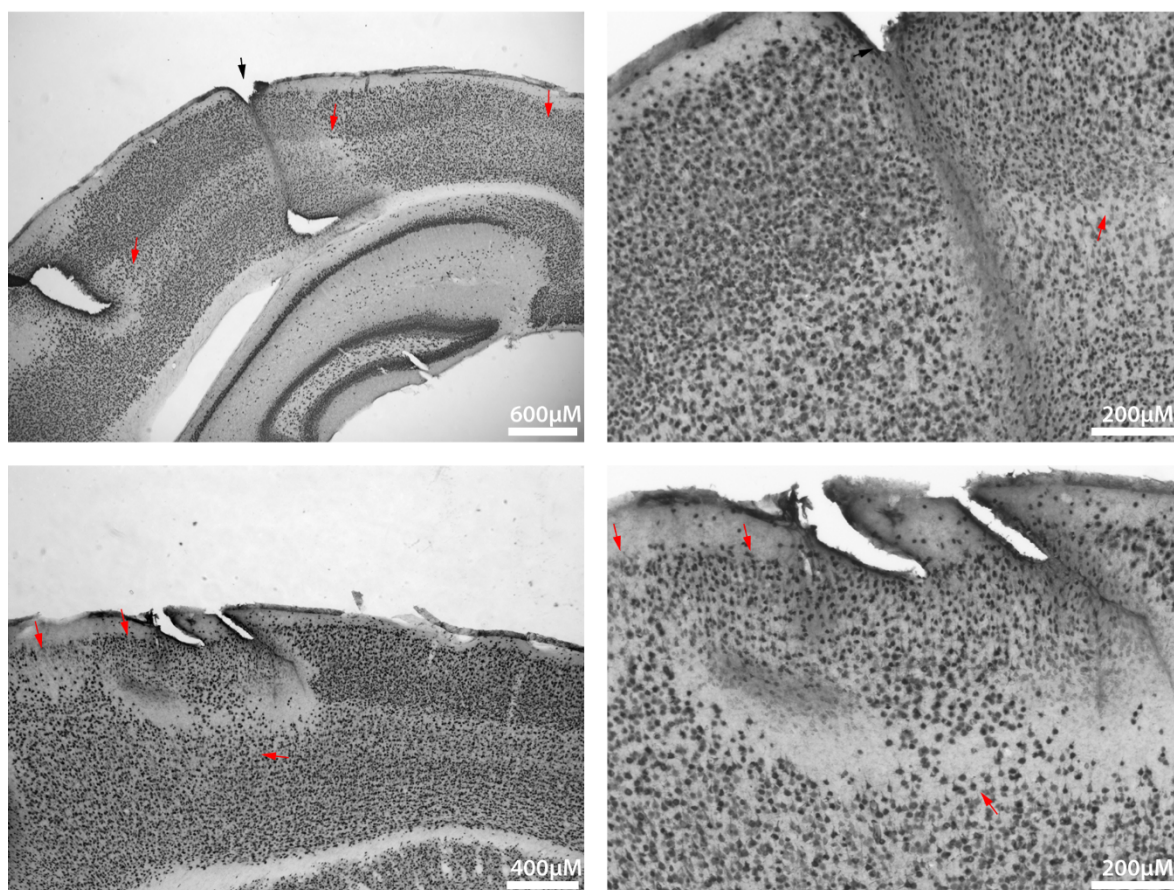
Figure A.1 Histology of *Scn3a$^{+/Hyp}$* mice.

Representative NeuN immunohistochemistry images of cortical anomalies observed in

Scn3a$^{+/Hyp}$ mice, including disrupted lamination (red arrows) and invaginations (black

arrows). Each row contains a low power (left) and high power image (right) from the

same section. Rows are independent samples. Following perfusion fixation with 4%

paraformaldehyde, brains were cryoprotected and sectioned at 40 microns. Free floating

sections were stained for NeuN immunohistochemistry using a mouse monocloncal anti-

NeuN antibody (1:500; MAB377, Clone A60, Chemicon) and detected using a vectastain

ABC kit according to the manufacturer's recommendation (Vector Labs). Slides were

viewed on a Zeiss Axioskop upright microscope and images were captured with a CRI

Nuance multispectral camera.
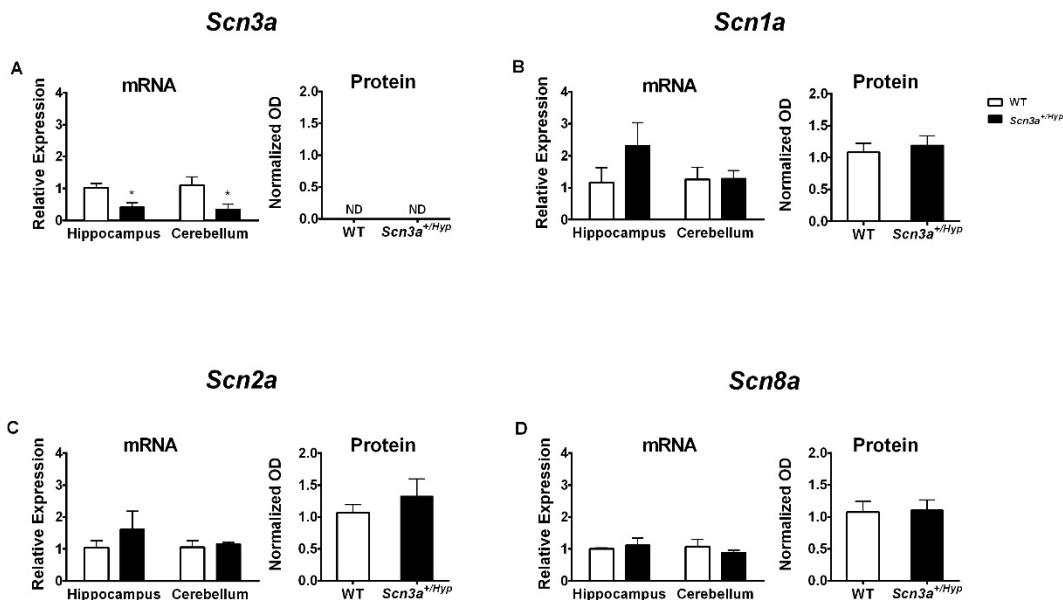
Figure A.2 Expression of VGSCs in adult *Scn3a^{+/Hyp}* mice.

(A) *Scn3a* mRNA expression is reduced by approximately 60% in both the hippocampus and cerebellum of *Scn3a^{+/Hyp}* mice relative to WT littermates. *Scn3a* protein expression was undetectable by Western blot. ND, Not detectable. No significant differences in either mRNA or protein expression were observed for (B) *Scn1a*, (C) *Scn2a*, or (D) *Scn8a*. mRNA expression values (n = 4), quantified from qRT-PCR analysis, are relative to WT and normalized to β-actin. Optical density (OD) expression values (n = 3), quantified from Western blot analysis, are relative to WT and normalized to α-tubulin. Protein results represent the mean of duplicate values for each genotype. *p < 0.05, Two-tailed Student's t-test. Error bars indicate SEM. White and black bars represent WT and *Scn3a^{+/Hyp}* mice, respectively.

Table A.2 Summary of non-motor behavioral tasks performed on *Scn3a*$^{+/Hyp}$ mice.

Values are presented as Mean ± SEM. *****p < 0.05, One-way ANOVA. Abbreviations: T,

time; s, seconds; cm, centimeters; cm/s, centimeters/second; #, number; %, percent; dB,

decibels.

Behavior	Test	N	Measurement	WT	*Scn3a*$^{+/Hyp}$
Exploration	Novel Cage	10	T digging (s)	70.9 ± 14.9	75.1 ± 15.1
			T rearing (s)	100.0 ± 9.2	79.5 ± 7.3
			T grooming (s)	33.0 ± 6.1	32.8 ± 2.7
Anxiety	Open Field	10	T in center (s)	93.4 ± 9.1	90.3 ± 19.3
			# center entries*	40.6 ± 2.9	29.4 ± 3.0
			Total Distance (cm)	4720.0 ± 240.0	4020.0 ± 370.0
			Average Speed (cm/s)	7.7 ± 0.4	6.7 ± 0.6
			Time Immobile (s)	107.1 ± 12.6	131.5 ± 19.0
	Marble Burying	19 (WT) 17 (*Scn3a*$^{+/Hyp}$)	# marbles buried	2.9 ± 0.7	4.1 ± 0.7
	Light/Dark Box	10	T in light zone (s)	153.4 ± 9.0	152.4 ± 11.4
			T in dark zone (s)	140.0 ± 9.4	142.0 ± 11.0
			# dark zone entries	18.4 ± 2.1	16.1 ± 1.6
Memory	Novel Object	9 (WT) 11 (*Scn3a*$^{+/Hyp}$)	Novel Object preference (Discrimination index)	0.4 ± 0.1	0.2 ± 0.1
Social Behavior	Social Interaction	10 (WT) 9 (*Scn3a*$^{+/Hyp}$)	%T w/ 1st stranger (Trial 1)	88.8 ± 2.0	82.6 ± 3.8
			%T w/ 2nd stranger (Trial 2)	65.9 ± 5.0	64.3 ± 8.2
Depressive-like	Forced Swim	10	T treading (s)	78.1 ± 7.0	82.1 ± 10.4
			T swimming (s)	78.8 ± 5.8	71.5 ± 6.8
			T floating (s)	288.8 ± 19.8	311.4 ± 11.6
Vision	Visual Cliff	10	Latency to cliff entry (s)	4.0 ± 1.3	6.6 ± 2.3
			T in cliff zone (s)	201.2 ± 17.3	221.5 ± 9.5
			T in safe zone (s)	300.1 ± 14.9	281.5 ± 16.2
Sensorimotor gating	Prepulse Inhibition	9 (WT) 11 (*Scn3a*$^{+/Hyp}$)	% Inhibition at:		
			70dB	3.3 ± 10.3	16.4 ± 8.3
			72dB	23.6 ± 7.2	25.0 ± 9.3
			76dB	52.4 ± 6.3	47.0 ± 5.6
			80dB	64.2 ± 6.9	64.5 ± 4.7

Appendix B: *Scn9a* does not modify the seizure phenotype of a GEFS+ mouse model.

B.1 Abstract

SCN9A mutations have been identified in patients with Dravet Syndrome who are also positive for *SCN1A* mutations, suggesting that *SCN9A* may modify *SCN1A*-derived epilepsy. There is also evidence to support *SCN9A* as a monogenic cause of epilepsy, as variants have also been found in patients with no other potential mutations. Although a number of *SCN9A* variants have been identified, the role of *SCN9A* in epilepsy is still unclear. To investigate the role of *SCN9A* as an epilepsy gene, we assessed the seizure susceptibility of knock-in mice carrying *SCN9A* mutation N641Y, identified in a family with febrile seizures and epilepsy. Both heterozygous and homozygous *Scn9a* mutants ($Scn9a^{+/NY}$ and $Scn9a^{NY/NY}$ mice respectively) exhibited comparable susceptibility to flurothyl and hyperthermia-induced seizures compared to WT mice. To test the hypothesis that *Scn9a* modifies *Scn1a*-derived epilepsy, we examined seizure susceptibility in mice heterozygous for both N641Y and the *SCN1A* GEFS+ mutation R1648H. Mice heterozygous for both mutations ($Scn9a^{+/NY}$/$Scn1a^{+/RH}$ mice) did not exhibit increased susceptibility to flurothyl or hyperthermia-induced seizures compared with *Scn1a* mutants. Taken together, these results suggest that N641Y is likely not a pathogenic mutation. Further study is therefore necessary to determine whether *SCN9A* can modify *SCN1A* dysfunction.

B.2 Introduction

As described in previous chapters, mutations in voltage-gated sodium channels (VGSCs) have been identified in a number of epilepsy disorders. The most clinically significant of these VGSCs is *SCN1A*, which is responsible for a spectrum of disorders ranging from genetic epilepsy with febrile seizures plus (GEFS+) to the severe encephalopathy Dravet syndrome (DS) (Escayg et al., 2000, Surovy et al., 2016a, Usluer et al., 2016). *SCN1A* mutations causing GEFS+ are primarily missense, whereas the majority of mutations that cause DS are frameshifting, truncations, or missense mutations in the voltage sensor/channel pore, suggesting a relationship between genotype and clinical outcome (Marini et al., 2007). However, genotype and phenotype are not perfectly correlated, as evidenced by the association of a single *SCN1A* mutation with a range of phenotypes (Hoffman-Zacharska et al., 2015, Passamonti et al., 2015). Genetic modifiers may contribute in part to this phenotypic heterogeneity; however, only a few modifier genes have been identified to date (Ohmori et al., 2008, Gaily et al., 2013, Ohmori et al., 2013).

The VGSC *SCN9A* has recently been proposed as a candidate modifier of *SCN1A*-associated disorders. Fourteen *SCN9A* mutations were identified in DS patients who were also positive for *SCN1A* mutations (Singh et al., 2009, Mulley et al., 2013a). A number of these patients expressed *SCN1A* missense mutations that would be predicted to have modest functional impact, suggesting that SCN9A dysfunction might have contributed to the severe epilepsy phenotype observed in these patients.

There is also evidence to suggest that mutations in *SCN9A* alone can result in epilepsy. In the two previous studies, ten *SCN9A* variants were found in patients with no other identified causal mutations (Singh et al., 2009, Mulley et al., 2013a). Furthermore, the *SCN9A* missense mutation N641Y was identified in a large Utah family exhibiting a range of seizure types, including febrile, partial, generalized, and absence seizures (Singh et al., 2009). Singh et al generated knock-in mice with the N641Y mutation and found that homozygotes mutants ($Scn9a^{NY/NY}$) were more susceptible to seizures induced by maximal electroshock (MES) and electrical kindling.

Although a number of *SCN9A* variants have been identified, it is still unclear whether they are pathogenic. Furthermore, when found in the presence of an *SCN1A* mutation, it is difficult to ascertain whether *SCN9A* dysfunction alters the *SCN1A* phenotype or has no effect at all. To investigate the role of *SCN9A* as a disease-causing gene, we examined the $Scn9a^{NY}$ line for susceptibility to flurothyl and hyperthermia-induced seizures. We also tested the hypothesis that *Scn9a* modifies *Scn1a*-derived epilepsy by crossing the $Scn9a^{NY}$ mouse line with the $Scn1a^{RH}$ GEFS+ mouse model and examining the susceptibility of the double heterozygous mice ($Scn9a^{+/NY}/Scn1a^{+/RH}$) to flurothyl and hyperthermia-induced seizures.

B.3 Materials and Methods

Animals

$Scn9a^{NY}$ mice were generated as previously described (Singh et al., 2009). The line was maintained by backcrossing to C57BL/6J mice (Jackson Laboratories, Bar Harbor, ME) for twelve generations. $Scn1a^{RH}$ mice were generated as previously described (Martin et al., 2010) and backcrossed to C57BL/6J mice for 12 generations.

$Scn1a^{+/RH}$ males were crossed to $Scn9a^{+/NY}$ females to obtain double heterozygotes (designated $Scn1a^{+/RH}/Scn9a^{+/NY}$). Offspring were born in expected Mendelian ratios and littermates were used in all experiments to avoid confounds due to differences in genetic background and rearing conditions. Mice were housed in an animal facility with a 12-hour light/dark cycle (lights on 7:00am – lights off 7:00pm). Food and water were available *ad libitum*. All experiments were performed in accordance with the guidelines of the Emory University Institutional Animal Care and Use Committees.

Genotyping

The $Scn1a^{RH}$ allele was detected as previously described (Martin et al., 2010). A separate PCR was performed to detect the $Scn9a^{NY}$ allele, using primers (9AF: CCCTTGGGAACAACTTCCCACC; 9AR: GTGCCTTAAAGGCTCGAATAACC) designed to flank the loxP site remaining after excision of the ACN cassette (Singh et al., 2009). The mutant *Scn9a* PCR product and the WT fragment were approximately 184 and 150 bp, respectively. $Scn1a^{+/RH}/Scn9a^{+/NY}$ mice were identified by the presence of both WT and mutant bands in both *Scn1a* and *Scn9a*.

Flurothyl Seizure Induction

Flurothyl seizure induction was performed as described in Chapter 2. To investigate *Scn9a* as a disease gene, male and female 5-9 week old WT, $Scn9a^{+/NY}$ and $Scn9a^{NY/NY}$ mice were used. To explore potential interactions between *Scn9a* and *Scn1a*, 7-11 week old $Scn1a^{+/RH}/Scn9a^{+/NY}$ mice and littermates were used.

Hyperthermia-induced Seizures

WT, $Scn9a^{+/NY}$ and $Scn9a^{NY/NY}$ mice, as well as $Scn1a^{+/RH}/Scn9a^{+/NY}$ mice and littermates, all aged P21-P22, were examined for susceptibility to hyperthermia-induced seizures as described in Chapter 2.

Statistics

All bar graphs indicate the means, and all error bars represent ± standard error of the mean (SEM). All data was analyzed using Prism 6 (GraphPad Software, Inc., La Jolla, CA, USA). Latencies to flurothyl-induced seizures were analyzed with one-way Analysis of Variance (ANOVA) followed by the Bonferroni *post hoc* comparison if a significant difference was detected. The number of animals that seized in the hyperthermia-induced seizure paradigm and the temperature at which each mouse seized per genotype were analyzed using the log-rank (Mantel-Cox) test.

B.4 Results

B.4.A. The susceptibility of $Scn9a^{NY}$ mutants to hyperthermia-induced and flurothyl-induced seizures is comparable to WT littermates.

In order to characterize the seizure susceptibility of the $Scn9a^{NY}$ line, we mated heterozygous siblings to produce WT, $Scn9a^{+/NY}$, and $Scn9a^{NY/NY}$ littermates. Since patients with the N641Y mutation often exhibit febrile seizures, we first examined mice from these litters for susceptibility to hyperthermia-induced seizures. Neither the percentage of mice seizing nor the temperature at which seizures occurred were significantly different among the genotypes (Fig. B.1A). We also examined the susceptibility of the $Scn9a$ line to flurothyl-induced seizures. No differences were observed between male and female mice, so the data from both sexes were combined.

The latencies of heterozygous and homozygous *Scn9a* mice to each seizure step (MJ, GTCS, and HLE) were not significantly different from WT (Fig. B.1B).

B.4.B. *Scn1a$^{+/RH}$/Scn9a$^{+/NY}$* mutants are not more susceptible to hyperthermia-induced or flurothyl-induced seizures than *Scn1a$^{+/RH}$* mice.

To determine whether *Scn9a* interacts with *Scn1a*, *Scn9a$^{+/NY}$* mice were crossed with *Scn1a$^{+/RH}$* mice to produce WT, *Scn9a$^{+/NY}$*, *Scn1a$^{+/RH}$*, and *Scn1a$^{+/RH}$/Scn9a$^{+/NY}$* littermates. In the hyperthermia seizure induction paradigm, both *Scn1a$^{+/RH}$* and *Scn1a$^{+/RH}$/Scn9a$^{+/NY}$* mice were significantly more susceptible than WT littermates but the two genotypes were comparable with respect to the number of mice seizing and the temperature at which the seizures occurred ($p < 0.0001$, $p = 0.67$ respectively; Fig. B.2A). We also compared latencies to flurothyl-induced seizures. No significant differences were observed between *Scn1a$^{+/RH}$* and *Scn1a$^{+/RH}$/Scn9a$^{+/NY}$* and any of the other genotypes, although there was a significant difference between *Scn9a$^{+/NY}$* and the double heterozygotes in latency to the GTCS ($p = 0.04$; respectively; Fig. B.2B).
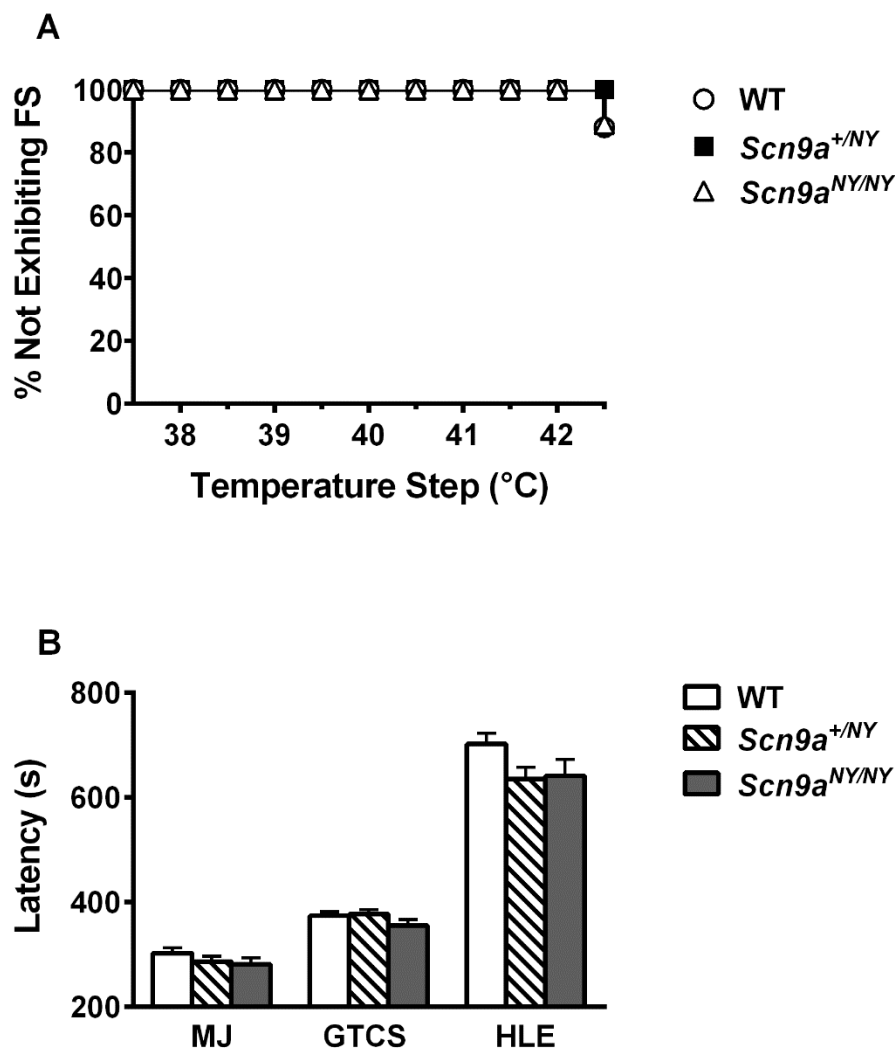
Figure B.1 Susceptibility of *Scn9a*$^{+/NY}$ and *Scn9a*$^{NY/NY}$ mice to hyperthermia and flurothyl-induced seizures

(A) Neither *Scn9a* mutant exhibited increased seizure susceptibility in response to increasing body temperature when compared with WT. n = 9-12 per group. (B) Latencies to the myoclonic jerk (MJ), first generalized seizure (GTCS), and hindlimb extension (HLE) were comparable between WT and *Scn9a* mutants. Error bars represent SEM, n = 18-21.
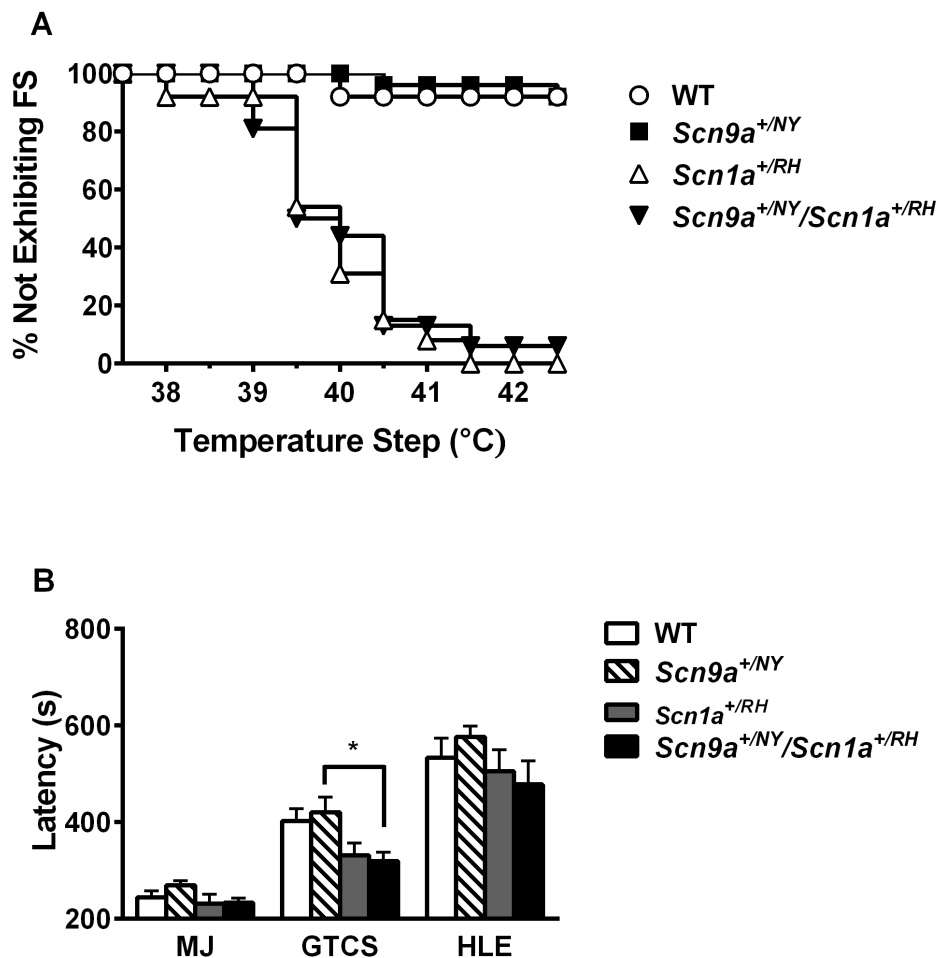
Figure B.2 Susceptibility of *Scn1a*[+/RH]/*Scn9a*[+/NY] mice to hyperthermia and flurothyl-induced seizures

(A) *Scn1a*[+/RH]/*Scn9a*[+/NY] and *Scn1a*[+/RH] mice exhibit increased but comparable susceptibility to seizures induced by increasing body temperature when compared with WT. n = 13-24 per group. (B) *Scn1a*[+/RH]/*Scn9a*[+/NY] mice exhibit significantly lower latencies to the GTCS compared with *Scn9a*[+/NY] littermates. Error bars represent SEM, p < 0.05, n = 14-16.

B.5 Discussion

Singh et al. (2009) previously reported that $Scn9a^{NY/NY}$ mice are more susceptible to MES and corneal kindling (Singh et al., 2009). We have extended their initial study by testing heterozygous and homozygous mutants for susceptibility to hyperthermia and flurothyl, tests that model febrile and generalized seizures respectively. These seizure paradigms were chosen to reflect the clinical presentation of the patients. All but one family member carrying the N641Y mutation exhibited febrile seizures, while six members also developed generalized seizures (Singh et al., 2009). Neither heterozygous nor homozygous $Scn9a^{NY}$ mutants were more susceptible to either seizure test when compared to WT. This result seemingly contradicts the published findings of increased seizure susceptibility, since Singh et al observed increased seizure susceptibility in homozygotes mutants. Taken together, our findings suggest that the N641Y mutation might not be responsible for the seizure phenotype observed in patients.

It is possible that the patients with the N641Y mutation harbor variants in additional genes that could modify the severity and types of seizures observed. It is not uncommon to observe multiple disease-causing or susceptibility genes within a single family.

Mutations in *SCN1A* have been reported to co-segregate with *SCN9A* mutations in patients with Dravet (Singh et al., 2009, Mulley et al., 2013a). To determine whether *SCN9A* can interact with *SCN1A* to exacerbate the seizure phenotype, we mated heterozygous $Scn9a^{NY}$ mutants with heterozygous $Scn1a^{RH}$ mice. Heterozygous mutants were chosen to better model the heterozygous mutations observed in human patients. We

found that the seizure responses of $Scn1a^{+/RH}/Scn9a^{+/NY}$ mutants were similar to $Scn1a^{+/RH}$ mice. It is possible, however, that the $Scn9a$ N641Y mutation is not pathogenic, since we did not observe an increase in seizure susceptibility in heterozygous or homozygous $Scn9a^{NY}$ mutants. In the future, perhaps a combination of a $SCN9A$ and $SCN1A$ mutation already identified in a Dravet patient could be tested in order to better model potential interactions between $Scn9a$ and $Scn1a$.

REFERENCES

(1989) Proposal for revised classification of epilepsies and epileptic syndromes. Commission on Classification and Terminology of the International League Against Epilepsy. Epilepsia 30:389-399.

Adzhubei IA, Schmidt S, Peshkin L, Ramensky VE, Gerasimova A, Bork P, Kondrashov AS, Sunyaev SR (2010) A method and server for predicting damaging missense mutations. Nat Methods 7:248-249.

Agster KL, Burwell RD (2009) Cortical efferents of the perirhinal, postrhinal, and entorhinal cortices of the rat. Hippocampus 19:1159-1186.

Agster KL, Tomas Pereira I, Saddoris MP, Burwell RD (2016) Subcortical connections of the perirhinal, postrhinal, and entorhinal cortices of the rat. II. efferents. Hippocampus 26:1213-1230.

Ahmad S, Dahllund L, Eriksson AB, Hellgren D, Karlsson U, Lund PE, Meijer IA, Meury L, Mills T, Moody A, Morinville A, Morten J, O'Donnell D, Raynoschek C, Salter H, Rouleau GA, Krupp JJ (2007) A stop codon mutation in SCN9A causes lack of pain sensation. Hum Mol Genet 16:2114-2121.

Akiyama M, Kobayashi K, Ohtsuka Y (2012) Dravet syndrome: a genetic epileptic disorder. Acta Med Okayama 66:369-376.

Anand G, Collett-White F, Orsini A, Thomas S, Jayapal S, Trump N, Zaiwalla Z, Jayawant S (2016) Autosomal dominant SCN8A mutation with an unusually mild phenotype. Eur J Paediatr Neurol.

Annegers JF, Hauser WA, Anderson VE, Kurland LT (1982) The risks of seizure disorders among relatives of patients with childhood onset epilepsy. Neurology 32:174-179.

Araya R, Nikolenko V, Eisenthal KB, Yuste R (2007) Sodium channels amplify spine potentials. Proc Natl Acad Sci U S A 104:12347-12352.

Aronica E, Yankaya B, Troost D, van Vliet EA, Lopes da Silva FH, Gorter JA (2001) Induction of neonatal sodium channel II and III alpha-isoform mRNAs in neurons and microglia after status epilepticus in the rat hippocampus. Eur J Neurosci 13:1261-1266.

Baasch AL, Huning I, Gilissen C, Klepper J, Veltman JA, Gillessen-Kaesbach G, Hoischen A, Lohmann K (2014) Exome sequencing identifies a de novo SCN2A mutation in a patient with intractable seizures, severe intellectual disability, optic atrophy, muscular hypotonia, and brain abnormalities. Epilepsia 55:e25-29.

Banka S, Fitzgibbon GJ, Gaunt L, Rankin WJ, Clayton-Smith J (2011) A novel 800 kb microduplication of chromosome 16q22.1 resulting in learning disability and epilepsy may explain phenotypic variability in a family with 15q13 microdeletion. Am J Med Genet A 155A:1453-1457.

Barton ME, Klein BD, Wolf HH, White HS (2001) Pharmacological characterization of the 6 Hz psychomotor seizure model of partial epilepsy. Epilepsy Res 47:217-227.

Bassuk AG, Geraghty E, Wu S, Mullen SA, Berkovic SF, Scheffer IE, Mefford HC (2013) Deletions of 16p11.2 and 19p13.2 in a family with intellectual disability and generalized epilepsy. Am J Med Genet A 161A:1722-1725.

Becanovic K, Norremolle A, Neal SJ, Kay C, Collins JA, Arenillas D, Lilja T, Gaudenzi G, Manoharan S, Doty CN, Beck J, Lahiri N, Portales-Casamar E, Warby SC, Connolly C, De Souza RA, Network RIotEHsD, Tabrizi SJ, Hermanson O, Langbehn DR, Hayden MR, Wasserman WW, Leavitt BR (2015) A SNP in the HTT promoter alters NF-kappaB binding and is a bidirectional genetic modifier of Huntington disease. Nat Neurosci 18:807-816.

Bechi G, Rusconi R, Cestele S, Striano P, Franceschetti S, Mantegazza M (2015) Rescuable folding defective NaV1.1 (SCN1A) mutants in epilepsy: Properties, occurrence, and novel rescuing strategy with peptides targeted to the endoplasmic reticulum. Neurobiology of disease 75:100-114.

Beck C, Moulard B, Steinlein O, Guipponi M, Vallee L, Montpied P, Baldy-Moulnier M, Malafosse A (1994) A nonsense mutation in the alpha4 subunit of the nicotinic acetylcholine receptor (CHRNA4) cosegregates with 20q-linked benign neonatal familial convulsions (EBNI). Neurobiol Dis 1:95-99.

Beckh S, Noda M, Lubbert H, Numa S (1989) Differential regulation of three sodium channel messenger RNAs in the rat central nervous system during development. EMBO J 8:3611-3616.

Belcher SM, Zerillo CA, Levenson R, Ritchie JM, Howe JR (1995) Cloning of a sodium channel alpha subunit from rabbit Schwann cells. Proc Natl Acad Sci U S A 92:11034-11038.

Ben-Ari Y (2002) Excitatory actions of gaba during development: the nature of the nurture. Nat Rev Neurosci 3:728-739.

Ben-Ari Y, Cherubini E, Corradetti R, Gaiarsa JL (1989) Giant synaptic potentials in immature rat CA3 hippocampal neurones. J Physiol 416:303-325.

Ben-Ari Y, Gho M (1988) Long-lasting modification of the synaptic properties of rat CA3 hippocampal neurones induced by kainic acid. J Physiol 404:365-384.

Berg AT, Berkovic SF, Brodie MJ, Buchhalter J, Cross JH, van Emde Boas W, Engel J, French J, Glauser TA, Mathern GW, Moshe SL, Nordli D, Plouin P, Scheffer IE (2010) Revised terminology and concepts for organization of seizures and epilepsies: report of the ILAE Commission on Classification and Terminology, 2005-2009. Epilepsia 51:676-685.

Berghuis B, de Kovel CG, van Iterson L, Lamberts RJ, Sander JW, Lindhout D, Koeleman BP (2015) Complex SCN8A DNA-abnormalities in an individual with therapy resistant absence epilepsy. Epilepsy Res 115:141-144.

Bergren SK, Chen S, Galecki A, Kearney JA (2005) Genetic modifiers affecting severity of epilepsy caused by mutation of sodium channel Scn2a. Mamm Genome 16:683-690.

Bergren SK, Rutter ED, Kearney JA (2009) Fine mapping of an epilepsy modifier gene on mouse Chromosome 19. Mamm Genome 20:359-366.

Berkvens JJ, Veugen I, Veendrick-Meekes MJ, Snoeijen-Schouwenaars FM, Schelhaas HJ, Willemsen MH, Tan IY, Aldenkamp AP (2015) Autism and behavior in adult patients with Dravet syndrome (DS). Epilepsy Behav 47:11-16.

Biervert C, Schroeder BC, Kubisch C, Berkovic SF, Propping P, Jentsch TJ, Steinlein OK (1998) A potassium channel mutation in neonatal human epilepsy. Science 279:403-406.

Black JA, Yokoyama S, Higashida H, Ransom BR, Waxman SG (1994) Sodium channel
mRNAs I, II and III in the CNS: cell-specific expression. Brain Res Mol Brain
Res 22:275-289.

Blanchard MG, Willemsen MH, Walker JB, Dib-Hajj SD, Waxman SG, Jongmans MC,
Kleefstra T, van de Warrenburg BP, Praamstra P, Nicolai J, Yntema HG, Bindels
RJ, Meisler MH, Kamsteeg EJ (2015) De novo gain-of-function and loss-of-
function mutations of SCN8A in patients with intellectual disabilities and
epilepsy. J Med Genet 52:330-337.

Boerma RS, Braun KP, van den Broek MP, van Berkestijn FM, Swinkels ME, Hagebeuk
EO, Lindhout D, van Kempen M, Boon M, Nicolai J, de Kovel CG, Brilstra EH,
Koeleman BP (2016) Remarkable Phenytoin Sensitivity in 4 Children with
SCN8A-related Epilepsy: A Molecular Neuropharmacological Approach.
Neurotherapeutics 13:192-197.

Boiko T, Rasband MN, Levinson SR, Caldwell JH, Mandel G, Trimmer JS, Matthews G
(2001) Compact myelin dictates the differential targeting of two sodium channel
isoforms in the same axon. Neuron 30:91-104.

Boiko T, Van Wart A, Caldwell JH, Levinson SR, Trimmer JS, Matthews G (2003)
Functional specialization of the axon initial segment by isoform-specific sodium
channel targeting. J Neurosci 23:2306-2313.

Braat S, Kooy RF (2015) The GABAA Receptor as a Therapeutic Target for
Neurodevelopmental Disorders. Neuron 86:1119-1130.

Brown WC, Schiffman DO, Swinyard EA, Goodman LS (1953) Comparative assay of an antiepileptic drugs by psychomotor seizure test and minimal electroshock threshold test. J Pharmacol Exp Ther 107:273-283.

Brysch W, Creutzfeldt OD, Luno K, Schlingensiepen R, Schlingensiepen KH (1991) Regional and temporal expression of sodium channel messenger RNAs in the rat brain during development. Exp Brain Res 86:562-567.

Buchner DA, Trudeau M, Meisler MH (2003) SCNM1, a putative RNA splicing factor that modifies disease severity in mice. Science 301:967-969.

Butler KM, da Silva C, Shafir Y, Weisfeld-Adams JD, Alexander JJ, Hegde M, Escayg A (2016) De novo and inherited SCN8A epilepsy mutations detected by gene panel analysis. Epilepsy Res 129:17-25.

Caldwell JH, Schaller KL, Lasher RS, Peles E, Levinson SR (2000) Sodium channel Na(v)1.6 is localized at nodes of ranvier, dendrites, and synapses. Proc Natl Acad Sci U S A 97:5616-5620.

Calhoun JD, Hawkins NA, Zachwieja NJ, Kearney JA (2016) Cacna1g is a genetic modifier of epilepsy caused by mutation of voltage-gated sodium channel Scn2a. Epilepsia 57:e103-107.

Camfield P, Camfield C (2015) Febrile seizures and genetic epilepsy with febrile seizures plus (GEFS+). Epileptic Disord 17:124-133.

Cancedda L, Fiumelli H, Chen K, Poo MM (2007) Excitatory GABA action is essential for morphological maturation of cortical neurons in vivo. J Neurosci 27:5224-5235.

Candenas L, Seda M, Noheda P, Buschmann H, Cintado CG, Martin JD, Pinto FM (2006) Molecular diversity of voltage-gated sodium channel alpha and beta subunit mRNAs in human tissues. Eur J Pharmacol 541:9-16.

Carranza Rojo D, Hamiwka L, McMahon JM, Dibbens LM, Arsov T, Suls A, Stodberg T, Kelley K, Wirrell E, Appleton B, Mackay M, Freeman JL, Yendle SC, Berkovic SF, Bienvenu T, De Jonghe P, Thorburn DR, Mulley JC, Mefford HC, Scheffer IE (2011) De novo SCN1A mutations in migrating partial seizures of infancy. Neurology 77:380-383.

Carvill GL, Heavin SB, Yendle SC, McMahon JM, O'Roak BJ, Cook J, Khan A, Dorschner MO, Weaver M, Calvert S, Malone S, Wallace G, Stanley T, Bye AM, Bleasel A, Howell KB, Kivity S, Mackay MT, Rodriguez-Casero V, Webster R, Korczyn A, Afawi Z, Zelnick N, Lerman-Sagie T, Lev D, Moller RS, Gill D, Andrade DM, Freeman JL, Sadleir LG, Shendure J, Berkovic SF, Scheffer IE, Mefford HC (2013) Targeted resequencing in epileptic encephalopathies identifies de novo mutations in CHD2 and SYNGAP1. Nat Genet 45:825-830.

Cestele S, Schiavon E, Rusconi R, Franceschetti S, Mantegazza M (2013) Nonfunctional NaV1.1 familial hemiplegic migraine mutant transformed into gain of function by partial rescue of folding defects. Proc Natl Acad Sci U S A 110:17546-17551.

Chanda B, Bezanilla F (2002) Tracking voltage-dependent conformational changes in skeletal muscle sodium channel during activation. The Journal of general physiology 120:629-645.

Chao HT, Chen H, Samaco RC, Xue M, Chahrour M, Yoo J, Neul JL, Gong S, Lu HC, Heintz N, Ekker M, Rubenstein JL, Noebels JL, Rosenmund C, Zoghbi HY

(2010) Dysfunction in GABA signalling mediates autism-like stereotypies and Rett syndrome phenotypes. Nature 468:263-269.

Charlier C, Singh NA, Ryan SG, Lewis TB, Reus BE, Leach RJ, Leppert M (1998) A pore mutation in a novel KQT-like potassium channel gene in an idiopathic epilepsy family. Nat Genet 18:53-55.

Cheah CS, Westenbroek RE, Roden WH, Kalume F, Oakley JC, Jansen LA, Catterall WA (2013) Correlations in timing of sodium channel expression, epilepsy, and sudden death in Dravet syndrome. Channels (Austin) 7:468-472.

Cheah CS, Yu FH, Westenbroek RE, Kalume FK, Oakley JC, Potter GB, Rubenstein JL, Catterall WA (2012) Specific deletion of NaV1.1 sodium channels in inhibitory interneurons causes seizures and premature death in a mouse model of Dravet syndrome. Proc Natl Acad Sci U S A 109:14646-14651.

Chen C, Westenbroek RE, Xu X, Edwards CA, Sorenson DR, Chen Y, McEwen DP, O'Malley HA, Bharucha V, Meadows LS, Knudsen GA, Vilaythong A, Noebels JL, Saunders TL, Scheuer T, Shrager P, Catterall WA, Isom LL (2004) Mice lacking sodium channel beta1 subunits display defects in neuronal excitability, sodium channel expression, and nodal architecture. J Neurosci 24:4030-4042.

Chen Y, Liao W, Zeng Y, Tang B, Shi Y, Meng H, Xu H, Min F, Yu L, Yi Y, Li B, Guo J, (2014a) Novel *SCN3A* mutations in epilepsy patients with febrile seizures and mental retardation

Singapore.

Chen Y, Liao W, Zeng Y, Tang B, Shi Y, Meng H, Xu H, Min F, Yu L, Yi Y, Li B, Guo J, (2014b) Novel *SCN3A* mutations in epilepsy patients with febrile seizures and mental retardation.

. In: Paper presented at the 10th Asian & Oceanian Epilepsy Congress, Singapore

Chen Y, Lu J, Pan H, Zhang Y, Wu H, Xu K, Liu X, Jiang Y, Bao X, Yao Z, Ding K, Lo WH, Qiang B, Chan P, Shen Y, Wu X (2003) Association between genetic variation of CACNA1H and childhood absence epilepsy. Ann Neurol 54:239-243.

Chen YH, Dale TJ, Romanos MA, Whitaker WR, Xie XM, Clare JJ (2000) Cloning, distribution and functional analysis of the type III sodium channel from human brain. Eur J Neurosci 12:4281-4289.

Chen YJ, Shi YW, Xu HQ, Chen ML, Gao MM, Sun WW, Tang B, Zeng Y, Liao WP (2015) Electrophysiological Differences between the Same Pore Region Mutation in SCN1A and SCN3A. Molecular neurobiology 51:1263-1270.

Choi Y, Sims GE, Murphy S, Miller JR, Chan AP (2012) Predicting the functional effect of amino acid substitutions and indels. PLoS One 7:e46688.

Claes L, Ceulemans B, Audenaert D, Smets K, Lofgren A, Del-Favero J, Ala-Mello S, Basel-Vanagaite L, Plecko B, Raskin S, Thiry P, Wolf NI, Van Broeckhoven C, De Jonghe P (2003) De novo SCN1A mutations are a major cause of severe myoclonic epilepsy of infancy. Hum Mutat 21:615-621.

Claes L, Del-Favero J, Ceulemans B, Lagae L, Van Broeckhoven C, De Jonghe P (2001) De novo mutations in the sodium-channel gene SCN1A cause severe myoclonic epilepsy of infancy. Am J Hum Genet 68:1327-1332.

Connor JX, McCormack K, Pletsch A, Gaeta S, Ganetzky B, Chiu SY, Messing A (2005) Genetic modifiers of the Kv beta2-null phenotype in mice. Genes Brain Behav 4:77-88.

Cooper DN, Krawczak M, Polychronakos C, Tyler-Smith C, Kehrer-Sawatzki H (2013) Where genotype is not predictive of phenotype: towards an understanding of the molecular basis of reduced penetrance in human inherited disease. Hum Genet 132:1077-1130.

Corvol H, Blackman SM, Boelle PY, Gallins PJ, Pace RG, Stonebraker JR, Accurso FJ, Clement A, Collaco JM, Dang H, Dang AT, Franca A, Gong J, Guillot L, Keenan K, Li W, Lin F, Patrone MV, Raraigh KS, Sun L, Zhou YH, O'Neal WK, Sontag MK, Levy H, Durie PR, Rommens JM, Drumm ML, Wright FA, Strug LJ, Cutting GR, Knowles MR (2015) Genome-wide association meta-analysis identifies five modifier loci of lung disease severity in cystic fibrosis. Nat Commun 6:8382.

Cossette P, Liu L, Brisebois K, Dong H, Lortie A, Vanasse M, Saint-Hilaire JM, Carmant L, Verner A, Lu WY, Wang YT, Rouleau GA (2002) Mutation of GABRA1 in an autosomal dominant form of juvenile myoclonic epilepsy. Nat Genet 31:184-189.

de Curtis M, Pare D (2004) The rhinal cortices: a wall of inhibition between the neocortex and the hippocampus. Prog Neurobiol 74:101-110.

de Kovel CG, Meisler MH, Brilstra EH, van Berkestijn FM, van 't Slot R, van Lieshout S, Nijman IJ, O'Brien JE, Hammer MF, Estacion M, Waxman SG, Dib-Hajj SD, Koeleman BP (2014) Characterization of a de novo SCN8A mutation in a patient with epileptic encephalopathy. Epilepsy research 108:1511-1518.

Depienne C, Trouillard O, Gourfinkel-An I, Saint-Martin C, Bouteiller D, Graber D, Barthez-Carpentier MA, Gautier A, Villeneuve N, Dravet C, Livet MO, Rivier-Ringenbach C, Adam C, Dupont S, Baulac S, Heron D, Nabbout R, Leguern E (2010) Mechanisms for variable expressivity of inherited SCN1A mutations causing Dravet syndrome. J Med Genet 47:404-410.

Dhamija R, Erickson MK, St Louis EK, Wirrell E, Kotagal S (2014) Sleep abnormalities in children with Dravet syndrome. Pediatr Neurol 50:474-478.

Dravet C (2011) The core Dravet syndrome phenotype. Epilepsia 52 Suppl 2:3-9.

Duflocq A, Le Bras B, Bullier E, Couraud F, Davenne M (2008) Nav1.1 is predominantly expressed in nodes of Ranvier and axon initial segments. Mol Cell Neurosci 39:180-192.

Dutton SB, Makinson CD, Papale LA, Shankar A, Balakrishnan B, Nakazawa K, Escayg A (2013) Preferential inactivation of Scn1a in parvalbumin interneurons increases seizure susceptibility. Neurobiol Dis 49:211-220.

Eaholtz G, Scheuer T, Catterall WA (1994) Restoration of inactivation and block of open sodium channels by an inactivation gate peptide. Neuron 12:1041-1048.

Egan ME (2016) Genetics of Cystic Fibrosis: Clinical Implications. Clin Chest Med 37:9-16.

Epi KC, Epilepsy Phenome/Genome P, Allen AS, Berkovic SF, Cossette P, Delanty N, Dlugos D, Eichler EE, Epstein MP, Glauser T, Goldstein DB, Han Y, Heinzen EL, Hitomi Y, Howell KB, Johnson MR, Kuzniecky R, Lowenstein DH, Lu YF, Madou MR, Marson AG, Mefford HC, Esmaeeli Nieh S, O'Brien TJ, Ottman R, Petrovski S, Poduri A, Ruzzo EK, Scheffer IE, Sherr EH, Yuskaitis CJ, Abou-Khalil B, Alldredge BK, Bautista JF, Berkovic SF, Boro A, Cascino GD, Consalvo D, Crumrine P, Devinsky O, Dlugos D, Epstein MP, Fiol M, Fountain NB, French J, Friedman D, Geller EB, Glauser T, Glynn S, Haut SR, Hayward J, Helmers SL, Joshi S, Kanner A, Kirsch HE, Knowlton RC, Kossoff EH, Kuperman R, Kuzniecky R, Lowenstein DH, McGuire SM, Motika PV, Novotny EJ, Ottman R, Paolicchi JM, Parent JM, Park K, Poduri A, Scheffer IE, Shellhaas RA, Sherr EH, Shih JJ, Singh R, Sirven J, Smith MC, Sullivan J, Lin Thio L, Venkat A, Vining EP, Von Allmen GK, Weisenberg JL, Widdess-Walsh P, Winawer MR (2013) De novo mutations in epileptic encephalopathies. Nature 501:217-221.

Escayg A, Goldin AL (2010) Sodium channel SCN1A and epilepsy: mutations and mechanisms. Epilepsia 51:1650-1658.

Escayg A, Heils A, MacDonald BT, Haug K, Sander T, Meisler MH (2001) A novel SCN1A mutation associated with generalized epilepsy with febrile seizures plus--and prevalence of variants in patients with epilepsy. American journal of human genetics 68:866-873.

Escayg A, MacDonald BT, Meisler MH, Baulac S, Huberfeld G, An-Gourfinkel I, Brice A, LeGuern E, Moulard B, Chaigne D, Buresi C, Malafosse A (2000) Mutations

of SCN1A, encoding a neuronal sodium channel, in two families with GEFS+2. Nat Genet 24:343-345.

Estacion M, Gasser A, Dib-Hajj SD, Waxman SG (2010) A sodium channel mutation linked to epilepsy increases ramp and persistent current of Nav1.3 and induces hyperexcitability in hippocampal neurons. Exp Neurol 224:362-368.

Estacion M, O'Brien JE, Conravey A, Hammer MF, Waxman SG, Dib-Hajj SD, Meisler MH (2014) A novel de novo mutation of SCN8A (Nav1.6) with enhanced channel activation in a child with epileptic encephalopathy. Neurobiol Dis 69:117-123.

Exome Aggregation Consortium (2016) Exome Aggregation Consortium (ExAC). Cambridge, MA.

Exome Variant Server (2016) Exome Variant Server NHLBI GO Exome Sequencing Project (ESP).   Seattle, WA.

Favre I, Moczydlowski E, Schild L (1996) On the structural basis for ionic selectivity among Na+, K+, and Ca2+ in the voltage-gated sodium channel. Biophys J 71:3110-3125.

Felts PA, Black JA, Dib-Hajj SD, Waxman SG (1997a) NaG: a sodium channel-like mRNA shared by Schwann cells and other neural crest derivatives. Glia 21:269-276.

Felts PA, Yokoyama S, Dib-Hajj S, Black JA, Waxman SG (1997b) Sodium channel alpha-subunit mRNAs I, II, III, NaG, Na6 and hNE (PN1): different expression patterns in developing rat nervous system. Brain Res Mol Brain Res 45:71-82.

Ferraro TN, Golden GT, Smith GG, Berrettini WH (1995) Differential susceptibility to seizures induced by systemic kainic acid treatment in mature DBA/2J and C57BL/6J mice. Epilepsia 36:301-307.

Fjaer R, Brodtkorb E, Oye AM, Sheng Y, Vigeland MD, Kvistad KA, Backe PH, Selmer KK (2015) Generalized epilepsy in a family with basal ganglia calcifications and mutations in SLC20A2 and CHRNB2. Eur J Med Genet 58:624-628.

Frye RE, Casanova MF, Fatemi SH, Folsom TD, Reutiman TJ, Brown GL, Edelson SM, Slattery JC, Adams JB (2016) Neuropathological Mechanisms of Seizures in Autism Spectrum Disorder. Front Neurosci 10:192.

Fujiwara T, Sugawara T, Mazaki-Miyazaki E, Takahashi Y, Fukushima K, Watanabe M, Hara K, Morikawa T, Yagi K, Yamakawa K, Inoue Y (2003) Mutations of sodium channel alpha subunit type 1 (SCN1A) in intractable childhood epilepsies with frequent generalized tonic-clonic seizures. Brain 126:531-546.

Fung LW, Kwok SL, Tsui KW (2015) SCN8A mutations in Chinese children with early onset epilepsy and intellectual disability. Epilepsia 56:1319-1320.

Furuyama T, Morita Y, Inagaki S, Takagi H (1993) Distribution of I, II and III subtypes of voltage-sensitive Na+ channel mRNA in the rat brain. Brain Res Mol Brain Res 17:169-173.

Gaily E, Anttonen AK, Valanne L, Liukkonen E, Traskelin AL, Polvi A, Lommi M, Muona M, Eriksson K, Lehesjoki AE (2013) Dravet syndrome: new potential genetic modifiers, imaging abnormalities, and ictal findings. Epilepsia 54:1577-1585.

Galliano E, Gao Z, Schonewille M, Todorov B, Simons E, Pop AS, D'Angelo E, van den Maagdenberg AM, Hoebeek FE, De Zeeuw CI (2013) Silencing the majority of cerebellar granule cells uncovers their essential role in motor learning and consolidation. Cell Rep 3:1239-1251.

Galvan A, Wichmann T (2007) GABAergic circuits in the basal ganglia and movement disorders. Prog Brain Res 160:287-312.

Gandal MJ, Anderson RL, Billingslea EN, Carlson GC, Roberts TP, Siegel SJ (2012) Mice with reduced NMDA receptor expression: more consistent with autism than schizophrenia? Genes Brain Behav 11:740-750.

Ganguly K, Schinder AF, Wong ST, Poo M (2001) GABA itself promotes the developmental switch of neuronal GABAergic responses from excitation to inhibition. Cell 105:521-532.

Gardella E, Becker F, Moller RS, Schubert J, Lemke JR, Larsen LH, Eiberg H, Nothnagel M, Thiele H, Altmuller J, Syrbe S, Merkenschlager A, Bast T, Steinhoff B, Nurnberg P, Mang Y, Bakke Moller L, Gellert P, Heron SE, Dibbens LM, Weckhuysen S, Dahl HA, Biskup S, Tommerup N, Hjalgrim H, Lerche H, Beniczky S, Weber YG (2016) Benign infantile seizures and paroxysmal dyskinesia caused by an SCN8A mutation. Ann Neurol 79:428-436.

Gazina EV, Richards KL, Mokhtar MB, Thomas EA, Reid CA, Petrou S (2010) Differential expression of exon 5 splice variants of sodium channel alpha subunit mRNAs in the developing mouse brain. Neuroscience 166:195-200.

Gellens ME, George AL, Jr., Chen LQ, Chahine M, Horn R, Barchi RL, Kallen RG (1992) Primary structure and functional expression of the human cardiac

tetrodotoxin-insensitive voltage-dependent sodium channel. Proc Natl Acad Sci U S A 89:554-558.

George AL, Jr., Ledbetter DH, Kallen RG, Barchi RL (1991) Assignment of a human skeletal muscle sodium channel alpha-subunit gene (SCN4A) to 17q23.1-25.3. Genomics 9:555-556.

Gill KM, Grace AA (2014) Corresponding decrease in neuronal markers signals progressive parvalbumin neuron loss in MAM schizophrenia model. Int J Neuropsychopharmacol 17:1609-1619.

Glasscock E, Qian J, Yoo JW, Noebels JL (2007) Masking epilepsy by combining two epilepsy genes. Nat Neurosci 10:1554-1558.

Gokben S, Berdeli A, Serdaroglu G (2009) An inherited nonsense R1645X mutation in neuronal sodium channel alpha1-subunit gene in a Turkish patient with severe myoclonic epilepsy of infancy. Neuropediatrics 40:82-84.

Goldberg-Stern H, Aharoni S, Afawi Z, Bennett O, Appenzeller S, Pendziwiat M, Kuhlenbaumer G, Basel-Vanagaite L, Shuper A, Korczyn AD, Helbig I (2014) Broad phenotypic heterogeneity due to a novel SCN1A mutation in a family with genetic epilepsy with febrile seizures plus. J Child Neurol 29:221-226.

Goldin AL (2003) Mechanisms of sodium channel inactivation. Curr Opin Neurobiol 13:284-290.

Goldin AL, Barchi RL, Caldwell JH, Hofmann F, Howe JR, Hunter JC, Kallen RG, Mandel G, Meisler MH, Netter YB, Noda M, Tamkun MM, Waxman SG, Wood JN, Catterall WA (2000) Nomenclature of voltage-gated sodium channels. Neuron 28:365-368.

Goldschen-Ohm MP, Capes DL, Oelstrom KM, Chanda B (2013) Multiple pore conformations driven by asynchronous movements of voltage sensors in a eukaryotic sodium channel. Nature communications 4:1350.

Gong B, Rhodes KJ, Bekele-Arcuri Z, Trimmer JS (1999) Type I and type II Na(+) channel alpha-subunit polypeptides exhibit distinct spatial and temporal patterning, and association with auxiliary subunits in rat brain. J Comp Neurol 412:342-352.

Gordon D, Merrick D, Auld V, Dunn R, Goldin AL, Davidson N, Catterall WA (1987) Tissue-specific expression of the RI and RII sodium channel subtypes. Proc Natl Acad Sci U S A 84:8682-8686.

Greenberg DA, Subaran R (2011) Blinders, phenotype, and fashionable genetic analysis: a critical examination of the current state of epilepsy genetic studies. Epilepsia 52:1-9.

Guo F, Yu N, Cai JQ, Quinn T, Zong ZH, Zeng YJ, Hao LY (2008) Voltage-gated sodium channel Nav1.1, Nav1.3 and beta1 subunit were up-regulated in the hippocampus of spontaneously epileptic rat. Brain Res Bull 75:179-187.

Hackenberg A, Baumer A, Sticht H, Schmitt B, Kroell-Seger J, Wille D, Joset P, Papuc S, Rauch A, Plecko B (2014) Infantile epileptic encephalopathy, transient choreoathetotic movements, and hypersomnia due to a De Novo missense mutation in the SCN2A gene. Neuropediatrics 45:261-264.

Hamill OP, Marty A, Neher E, Sakmann B, Sigworth FJ (1981) Improved patch-clamp techniques for high-resolution current recording from cells and cell-free membrane patches. Pflugers Arch 391:85-100.

Han S, Tai C, Jones CJ, Scheuer T, Catterall WA (2014) Enhancement of inhibitory neurotransmission by GABAA receptors having alpha2,3-subunits ameliorates behavioral deficits in a mouse model of autism. Neuron 81:1282-1289.

Han S, Tai C, Westenbroek RE, Yu FH, Cheah CS, Potter GB, Rubenstein JL, Scheuer T, de la Iglesia HO, Catterall WA (2012) Autistic-like behaviour in Scn1a+/- mice and rescue by enhanced GABA-mediated neurotransmission. Nature 489:385-390.

Hanlon MR, Wallace BA (2002) Structure and function of voltage-dependent ion channel regulatory beta subunits. Biochemistry 41:2886-2894.

Hartshorne RP, Catterall WA (1981) Purification of the saxitoxin receptor of the sodium channel from rat brain. Proc Natl Acad Sci U S A 78:4620-4624.

Hartshorne RP, Catterall WA (1984) The sodium channel from rat brain. Purification and subunit composition. J Biol Chem 259:1667-1675.

Hashimoto Y, Araki H, Suemaru K, Gomita Y (2006) Effects of drugs acting on the GABA-benzodiazepine receptor complex on flurothyl-induced seizures in Mongolian gerbils. Eur J Pharmacol 536:241-247.

Haug K, Hallmann K, Rebstock J, Dullinger J, Muth S, Haverkamp F, Pfeiffer H, Rau B, Elger CE, Propping P, Heils A (2001) The voltage-gated sodium channel gene SCN2A and idiopathic generalized epilepsy. Epilepsy Res 47:243-246.

Hawkins NA, Kearney JA (2012) Confirmation of an epilepsy modifier locus on mouse chromosome 11 and candidate gene analysis by RNA-Seq. Genes Brain Behav 11:452-460.

Hawkins NA, Kearney JA (2016) Hlf is a genetic modifier of epilepsy caused by voltage-gated sodium channel mutations. Epilepsy Res 119:20-23.

Hawkins NA, Martin MS, Frankel WN, Kearney JA, Escayg A (2011) Neuronal voltage-gated ion channels are genetic modifiers of generalized epilepsy with febrile seizures plus. Neurobiol Dis 41:655-660.

Hedrich UB, Liautard C, Kirschenbaum D, Pofahl M, Lavigne J, Liu Y, Theiss S, Slotta J, Escayg A, Dihne M, Beck H, Mantegazza M, Lerche H (2014) Impaired action potential initiation in GABAergic interneurons causes hyperexcitable networks in an epileptic mouse model carrying a human Na(V)1.1 mutation. J Neurosci 34:14874-14889.

Heinemann SH, Terlau H, Stuhmer W, Imoto K, Numa S (1992) Calcium channel characteristics conferred on the sodium channel by single mutations. Nature 356:441-443.

Heinzen EL, Depondt C, Cavalleri GL, Ruzzo EK, Walley NM, Need AC, Ge D, He M, Cirulli ET, Zhao Q, Cronin KD, Gumbs CE, Campbell CR, Hong LK, Maia JM, Shianna KV, McCormack M, Radtke RA, O'Conner GD, Mikati MA, Gallentine WB, Husain AM, Sinha SR, Chinthapalli K, Puranam RS, McNamara JO, Ottman R, Sisodiya SM, Delanty N, Goldstein DB (2012) Exome sequencing followed by large-scale genotyping fails to identify single rare variants of large effect in idiopathic generalized epilepsy. Am J Hum Genet 91:293-302.

Helbig I (2015) Genetic Causes of Generalized Epilepsies. Semin Neurol 35:288-292.

Hempelmann A, Taylor KP, Heils A, Lorenz S, Prud'homme JF, Nabbout R, Dulac O, Rudolf G, Zara F, Bianchi A, Robinson R, Gardiner RM, Covanis A, Lindhout D,

Stephani U, Elger CE, Weber YG, Lerche H, Nurnberg P, Kron KL, Scheffer IE,
Mulley JC, Berkovic SF, Sander T (2006) Exploration of the genetic architecture
of idiopathic generalized epilepsies. Epilepsia 47:1682-1690.

Heron SE, Crossland KM, Andermann E, Phillips HA, Hall AJ, Bleasel A, Shevell M,
Mercho S, Seni MH, Guiot MC, Mulley JC, Berkovic SF, Scheffer IE (2002)
Sodium-channel defects in benign familial neonatal-infantile seizures. Lancet
360:851-852.

Heydemann A, Doherty KR, McNally EM (2007) Genetic modifiers of muscular
dystrophy: implications for therapy. Biochim Biophys Acta 1772:216-228.

Hildebrand MS, Dahl HH, Damiano JA, Smith RJ, Scheffer IE, Berkovic SF (2013)
Recent advances in the molecular genetics of epilepsy. J Med Genet 50:271-279.

Hirano T (2014) Around LTD hypothesis in motor learning. Cerebellum 13:645-650.

Hirose S, Okada M, Kaneko S, Mitsudome A (2000) Are some idiopathic epilepsies
disorders of ion channels?: A working hypothesis. Epilepsy Res 41:191-204.

Hodgkin AL, Huxley AF (1952a) The components of membrane conductance in the giant
axon of Loligo. The Journal of physiology 116:473-496.

Hodgkin AL, Huxley AF (1952b) The dual effect of membrane potential on sodium
conductance in the giant axon of Loligo. The Journal of physiology 116:497-506.

Hodgkin AL, Huxley AF (1952c) Propagation of electrical signals along giant nerve
fibers. Proceedings of the Royal Society of London Series B, Biological sciences
140:177-183.

Hodgkin AL, Huxley AF (1952d) A quantitative description of membrane current and its application to conduction and excitation in nerve. The Journal of physiology 117:500-544.

Hoffman-Zacharska D, Szczepanik E, Terczynska I, Goszczanska-Ciuchta A, Zalewska-Miszkurka Z, Tataj R, Bal J (2015) From focal epilepsy to Dravet syndrome--Heterogeneity of the phenotype due to SCN1A mutations of the p.Arg1596 amino acid residue in the Nav1.1 subunit. Neurol Neurochir Pol 49:258-266.

Holland KD, Kearney JA, Glauser TA, Buck G, Keddache M, Blankston JR, Glaaser IW, Kass RS, Meisler MH (2008) Mutation of sodium channel SCN3A in a patient with cryptogenic pediatric partial epilepsy. Neurosci Lett 433:65-70.

Howell KB, McMahon JM, Carvill GL, Tambunan D, Mackay MT, Rodriguez-Casero V, Webster R, Clark D, Freeman JL, Calvert S, Olson HE, Mandelstam S, Poduri A, Mefford HC, Harvey AS, Scheffer IE (2015) SCN2A encephalopathy: A major cause of epilepsy of infancy with migrating focal seizures. Neurology 85:958-966.

Ito S, Ogiwara I, Yamada K, Miyamoto H, Hensch TK, Osawa M, Yamakawa K (2013) Mouse with Nav1.1 haploinsufficiency, a model for Dravet syndrome, exhibits lowered sociability and learning impairment. Neurobiol Dis 49:29-40.

Jennings MT, Bird TD (1981) Genetic influences in the epilepsies. Review of the literature with practical implications. Am J Dis Child 135:450-457.

Jiang L, Kang D, Kang J (2015) Potentiation of tonic GABAergic inhibition by activation of postsynaptic kainate receptors. Neuroscience 298:448-454.

Jiang X, Lachance M, Rossignol E (2016) Involvement of cortical fast-spiking parvalbumin-positive basket cells in epilepsy. Prog Brain Res 226:81-126.

Jorge BS, Campbell CM, Miller AR, Rutter ED, Gurnett CA, Vanoye CG, George AL, Jr., Kearney JA (2011) Voltage-gated potassium channel KCNV2 (Kv8.2) contributes to epilepsy susceptibility. Proc Natl Acad Sci U S A 108:5443-5448.

Joseph D, Petsko GA, Karplus M (1990) Anatomy of a conformational change: hinged "lid" motion of the triosephosphate isomerase loop. Science 249:1425-1428.

Kalume F (2013) Sudden unexpected death in Dravet syndrome: respiratory and other physiological dysfunctions. Respir Physiol Neurobiol 189:324-328.

Kalume F, Yu FH, Westenbroek RE, Scheuer T, Catterall WA (2007) Reduced sodium current in Purkinje neurons from Nav1.1 mutant mice: implications for ataxia in severe myoclonic epilepsy in infancy. J Neurosci 27:11065-11074.

Kamiya K, Kaneda M, Sugawara T, Mazaki E, Okamura N, Montal M, Makita N, Tanaka M, Fukushima K, Fujiwara T, Inoue Y, Yamakawa K (2004) A nonsense mutation of the sodium channel gene SCN2A in a patient with intractable epilepsy and mental decline. J Neurosci 24:2690-2698.

Kearney JA, Yang Y, Beyer B, Bergren SK, Claes L, Dejonghe P, Frankel WN (2006) Severe epilepsy resulting from genetic interaction between Scn2a and Kcnq2. Hum Mol Genet 15:1043-1048.

Kirmse K, Witte OW, Holthoff K (2011) GABAergic depolarization during early cortical development and implications for anticonvulsive therapy in neonates. Epilepsia 52:1532-1543.

Klassen T, Davis C, Goldman A, Burgess D, Chen T, Wheeler D, McPherson J, Bourquin T, Lewis L, Villasana D, Morgan M, Muzny D, Gibbs R, Noebels J (2011) Exome

sequencing of ion channel genes reveals complex profiles confounding personal risk assessment in epilepsy. Cell 145:1036-1048.

Konradi C, Yang CK, Zimmerman EI, Lohmann KM, Gresch P, Pantazopoulos H, Berretta S, Heckers S (2011) Hippocampal interneurons are abnormal in schizophrenia. Schizophr Res 131:165-173.

Kosobud AE, Crabbe JC (1990) Genetic correlations among inbred strain sensitivities to convulsions induced by 9 convulsant drugs. Brain Res 526:8-16.

Koziol LF, Barker LA (2013) Hypotonia, jaundice, and Chiari malformations: relationships to executive functions. Appl Neuropsychol Child 2:141-149.

Krasowski MD (2000) Differential modulatory actions of the volatile convulsant flurothyl and its anesthetic isomer at inhibitory ligand-gated ion channels. Neuropharmacology 39:1168-1183.

Kravitz AV, Freeze BS, Parker PR, Kay K, Thwin MT, Deisseroth K, Kreitzer AC (2010) Regulation of parkinsonian motor behaviours by optogenetic control of basal ganglia circuitry. Nature 466:622-626.

Kreitzer AC, Malenka RC (2008) Striatal plasticity and basal ganglia circuit function. Neuron 60:543-554.

Krzemien DM, Schaller KL, Levinson SR, Caldwell JH (2000) Immunolocalization of sodium channel isoform NaCh6 in the nervous system. J Comp Neurol 420:70-83.

Kumar P, Henikoff S, Ng PC (2009) Predicting the effects of coding non-synonymous variants on protein function using the SIFT algorithm. Nat Protoc 4:1073-1081.

Lai HC, Jan LY (2006) The distribution and targeting of neuronal voltage-gated ion channels. Nat Rev Neurosci 7:548-562.

Lamar T, Vanoye CG, Calhoun J, Wong JC, Dutton SB, Jorge BS, Velinov M, Escayg A, Kearney JA (2017) *SCN3A* deficiency associated with increased seizure susceptibility. Neurobiol Dis 102:38-48.

Leclercq K, Kaminski RM (2015) Genetic background of mice strongly influences treatment resistance in the 6 Hz seizure model. Epilepsia 56:310-318.

Lennox WG (1951) The heredity of epilepsy as told by relatives and twins. J Am Med Assoc 146:529-536.

Levin SI, Khaliq ZM, Aman TK, Grieco TM, Kearney JA, Raman IM, Meisler MH (2006) Impaired motor function in mice with cell-specific knockout of sodium channel Scn8a (NaV1.6) in cerebellar purkinje neurons and granule cells. J Neurophysiol 96:785-793.

Liao Y, Deprez L, Maljevic S, Pitsch J, Claes L, Hristova D, Jordanova A, Ala-Mello S, Bellan-Koch A, Blazevic D, Schubert S, Thomas EA, Petrou S, Becker AJ, De Jonghe P, Lerche H (2010) Molecular correlates of age-dependent seizures in an inherited neonatal-infantile epilepsy. Brain 133:1403-1414.

Lindia JA, Abbadie C (2003) Distribution of the voltage gated sodium channel Na(v)1.3-like immunoreactivity in the adult rat central nervous system. Brain research 960:132-141.

Lipkind GM, Fozzard HA (2008) Voltage-gated Na channel selectivity: the role of the conserved domain III lysine residue. J Gen Physiol 131:523-529.

Liu S, Zheng P (2013) Altered PKA modulation in the Na(v)1.1 epilepsy variant I1656M. J Neurophysiol 110:2090-2098.

Lorincz A, Nusser Z (2008) Cell-type-dependent molecular composition of the axon initial segment. J Neurosci 28:14329-14340.

Loscher W, Ebert U (1996) The role of the piriform cortex in kindling. Prog Neurobiol 50:427-481.

Lossin C (2009) A catalog of SCN1A variants. Brain & development 31:114-130.

Lossin C, Wang DW, Rhodes TH, Vanoye CG, George AL, Jr. (2002) Molecular basis of an inherited epilepsy. Neuron 34:877-884.

Lothman EW, Bertram EH, 3rd, Stringer JL (1991) Functional anatomy of hippocampal seizures. Prog Neurobiol 37:1-82.

Maier T, Guell M, Serrano L (2009) Correlation of mRNA and protein in complex biological samples. FEBS Lett 583:3966-3973.

Makinson CD, Tanaka BS, Lamar T, Goldin AL, Escayg A (2014) Role of the hippocampus in Nav1.6 (Scn8a) mediated seizure resistance. Neurobiology of disease 68:16-25.

Malhotra JD, Kazen-Gillespie K, Hortsch M, Isom LL (2000) Sodium channel beta subunits mediate homophilic cell adhesion and recruit ankyrin to points of cell-cell contact. J Biol Chem 275:11383-11388.

Marini C, Harkin LA, Wallace RH, Mulley JC, Scheffer IE, Berkovic SF (2003) Childhood absence epilepsy and febrile seizures: a family with a GABA(A) receptor mutation. Brain 126:230-240.

Marini C, Mei D, Temudo T, Ferrari AR, Buti D, Dravet C, Dias AI, Moreira A, Calado E, Seri S, Neville B, Narbona J, Reid E, Michelucci R, Sicca F, Cross HJ,

Guerrini R (2007) Idiopathic epilepsies with seizures precipitated by fever and SCN1A abnormalities. Epilepsia 48:1678-1685.

Martin BS, Martinez-Botella G, Loya CM, Salituro FG, Robichaud AJ, Huntsman MM, Ackley MA, Doherty JJ, Corbin JG (2016) Rescue of deficient amygdala tonic gamma-aminobutyric acidergic currents in the Fmr(-/y) mouse model of fragile X syndrome by a novel gamma-aminobutyric acid type A receptor-positive allosteric modulator. J Neurosci Res 94:568-578.

Martin MS, Dutt K, Papale LA, Dube CM, Dutton SB, de Haan G, Shankar A, Tufik S, Meisler MH, Baram TZ, Goldin AL, Escayg A (2010) Altered function of the SCN1A voltage-gated sodium channel leads to gamma-aminobutyric acid-ergic (GABAergic) interneuron abnormalities. J Biol Chem 285:9823-9834.

Martin MS, Tang B, Papale LA, Yu FH, Catterall WA, Escayg A (2007) The voltage-gated sodium channel Scn8a is a genetic modifier of severe myoclonic epilepsy of infancy. Hum Mol Genet 16:2892-2899.

Mauk MD (1997) Roles of cerebellar cortex and nuclei in motor learning: contradictions or clues? Neuron 18:343-346.

McIntyre DC, Kelly ME, Armstrong JN (1993) Kindling in the perirhinal cortex. Brain Res 615:1-6.

McIntyre DC, Plant JR (1993) Long-lasting changes in the origin of spontaneous discharges from amygdala-kindled rats: piriform vs. perirhinal cortex in vitro. Brain Res 624:268-276.

McTague A, Howell KB, Cross JH, Kurian MA, Scheffer IE (2016) The genetic landscape of the epileptic encephalopathies of infancy and childhood. Lancet Neurol 15:304-316.

Mechaly I, Scamps F, Chabbert C, Sans A, Valmier J (2005) Molecular diversity of voltage-gated sodium channel alpha subunits expressed in neuronal and non-neuronal excitable cells. Neuroscience 130:389-396.

Meng H, Xu HQ, Yu L, Lin GW, He N, Su T, Shi YW, Li B, Wang J, Liu XR, Tang B, Long YS, Yi YH, Liao WP (2015) The SCN1A mutation database: updating information and analysis of the relationships among genotype, functional alteration, and phenotype. Hum Mutat 36:573-580.

Mhanni AA, Hartley JN, Sanger WG, Chudley AE, Spriggs EL (2011) Variable expressivity of a novel mutation in the SCN1A gene leading to an autosomal dominant seizure disorder. Seizure 20:711-712.

Miller AR, Hawkins NA, McCollom CE, Kearney JA (2014) Mapping genetic modifiers of survival in a mouse model of Dravet syndrome. Genes Brain Behav 13:163-172.

Misra SN, Kahlig KM, George AL, Jr. (2008) Impaired NaV1.2 function and reduced cell surface expression in benign familial neonatal-infantile seizures. Epilepsia 49:1535-1545.

Monaghan DT, Cotman CW (1982) The distribution of [3H]kainic acid binding sites in rat CNS as determined by autoradiography. Brain Res 252:91-100.

Morgan K, Stevens EB, Shah B, Cox PJ, Dixon AK, Lee K, Pinnock RD, Hughes J, Richardson PJ, Mizuguchi K, Jackson AP (2000) beta 3: an additional auxiliary

subunit of the voltage-sensitive sodium channel that modulates channel gating with distinct kinetics. Proc Natl Acad Sci U S A 97:2308-2313.

Morinville A, Fundin B, Meury L, Jureus A, Sandberg K, Krupp J, Ahmad S, O'Donnell D (2007) Distribution of the voltage-gated sodium channel Na(v)1.7 in the rat: expression in the autonomic and endocrine systems. J Comp Neurol 504:680-689.

Mulle C, Sailer A, Swanson GT, Brana C, O'Gorman S, Bettler B, Heinemann SF (2000) Subunit composition of kainate receptors in hippocampal interneurons. Neuron 28:475-484.

Mulley JC, Hodgson B, McMahon JM, Iona X, Bellows S, Mullen SA, Farrell K, Mackay M, Sadleir L, Bleasel A, Gill D, Webster R, Wirrell EC, Harbord M, Sisodiya S, Andermann E, Kivity S, Berkovic SF, Scheffer IE, Dibbens LM (2013a) Role of the sodium channel SCN9A in genetic epilepsy with febrile seizures plus and Dravet syndrome. Epilepsia 54:e122-126.

Mulley JC, Hodgson B, McMahon JM, Iona X, Bellows S, Mullen SA, Farrell K, Mackay M, Sadleir L, Bleasel A, Gill D, Webster R, Wirrell EC, Harbord M, Sisodiya S, Andermann E, Kivity S, Berkovic SF, Scheffer IE, Dibbens LM (2013b) Role of the sodium channel SCN9A in genetic epilepsy with febrile seizures plus and Dravet syndrome. Epilepsia.

Mulley JC, Nelson P, Guerrero S, Dibbens L, Iona X, McMahon JM, Harkin L, Schouten J, Yu S, Berkovic SF, Scheffer IE (2006) A new molecular mechanism for severe myoclonic epilepsy of infancy: exonic deletions in SCN1A. Neurology 67:1094-1095.

Myers CT, Mefford HC (2015) Advancing epilepsy genetics in the genomic era. Genome Med 7:91.

Nabbout R, Baulac S, Desguerre I, Bahi-Buisson N, Chiron C, Ruberg M, Dulac O, LeGuern E (2007) New locus for febrile seizures with absence epilepsy on 3p and a possible modifier gene on 18p. Neurology 68:1374-1381.

Nie L, Wu G, Zhang W (2006) Correlation of mRNA expression and protein abundance affected by multiple sequence features related to translational efficiency in Desulfovibrio vulgaris: a quantitative analysis. Genetics 174:2229-2243.

Noebels J (2015) Pathway-driven discovery of epilepsy genes. Nat Neurosci 18:344-350.

Oakley JC, Kalume F, Yu FH, Scheuer T, Catterall WA (2009) Temperature- and age-dependent seizures in a mouse model of severe myoclonic epilepsy in infancy. Proc Natl Acad Sci U S A 106:3994-3999.

Ogiwara I, Ito K, Sawaishi Y, Osaka H, Mazaki E, Inoue I, Montal M, Hashikawa T, Shike T, Fujiwara T, Inoue Y, Kaneda M, Yamakawa K (2009) De novo mutations of voltage-gated sodium channel alphaII gene SCN2A in intractable epilepsies. Neurology 73:1046-1053.

Ogiwara I, Iwasato T, Miyamoto H, Iwata R, Yamagata T, Mazaki E, Yanagawa Y, Tamamaki N, Hensch TK, Itohara S, Yamakawa K (2013) Nav1.1 haploinsufficiency in excitatory neurons ameliorates seizure-associated sudden death in a mouse model of Dravet syndrome. Hum Mol Genet 22:4784-4804.

Ogiwara I, Miyamoto H, Morita N, Atapour N, Mazaki E, Inoue I, Takeuchi T, Itohara S, Yanagawa Y, Obata K, Furuichi T, Hensch TK, Yamakawa K (2007) Nav1.1 localizes to axons of parvalbumin-positive inhibitory interneurons: a circuit basis

for epileptic seizures in mice carrying an Scn1a gene mutation. J Neurosci 27:5903-5914.

Ohba C, Kato M, Takahashi S, Lerman-Sagie T, Lev D, Terashima H, Kubota M, Kawawaki H, Matsufuji M, Kojima Y, Tateno A, Goldberg-Stern H, Straussberg R, Marom D, Leshinsky-Silver E, Nakashima M, Nishiyama K, Tsurusaki Y, Miyake N, Tanaka F, Matsumoto N, Saitsu H (2014) Early onset epileptic encephalopathy caused by de novo SCN8A mutations. Epilepsia 55:994-1000.

Ohmori I, Ouchida M, Kobayashi K, Jitsumori Y, Mori A, Michiue H, Nishiki T, Ohtsuka Y, Matsui H (2013) CACNA1A variants may modify the epileptic phenotype of Dravet syndrome. Neurobiol Dis 50:209-217.

Ohmori I, Ouchida M, Miki T, Mimaki N, Kiyonaka S, Nishiki T, Tomizawa K, Mori Y, Matsui H (2008) A CACNB4 mutation shows that altered Ca(v)2.1 function may be a genetic modifier of severe myoclonic epilepsy in infancy. Neurobiol Dis 32:349-354.

Okaty BW, Miller MN, Sugino K, Hempel CM, Nelson SB (2009) Transcriptional and electrophysiological maturation of neocortical fast-spiking GABAergic interneurons. J Neurosci 29:7040-7052.

Oliva MK, McGarr TC, Beyer BJ, Gazina E, Kaplan DI, Cordeiro L, Thomas E, Dib-Hajj SD, Waxman SG, Frankel WN, Petrou S (2014) Physiological and genetic analysis of multiple sodium channel variants in a model of genetic absence epilepsy. Neurobiol Dis 67:180-190.

Papale LA, Beyer B, Jones JM, Sharkey LM, Tufik S, Epstein M, Letts VA, Meisler MH, Frankel WN, Escayg A (2009) Heterozygous mutations of the voltage-gated

sodium channel SCN8A are associated with spike-wave discharges and absence epilepsy in mice. Hum Mol Genet 18:1633-1641.

Papale LA, Makinson CD, Christopher Ehlen J, Tufik S, Decker MJ, Paul KN, Escayg A (2013) Altered sleep regulation in a mouse model of SCN1A-derived genetic epilepsy with febrile seizures plus (GEFS+). Epilepsia 54:625-634.

Passamonti C, Petrelli C, Mei D, Foschi N, Guerrini R, Provinciali L, Zamponi N (2015) A novel inherited SCN1A mutation associated with different neuropsychological phenotypes: is there a common core deficit? Epilepsy Behav 43:89-92.

Patino GA, Brackenbury WJ, Bao Y, Lopez-Santiago LF, O'Malley HA, Chen C, Calhoun JD, Lafreniere RG, Cossette P, Rouleau GA, Isom LL (2011) Voltage-gated Na+ channel beta1B: a secreted cell adhesion molecule involved in human epilepsy. J Neurosci 31:14577-14591.

Pelak K, Shianna KV, Ge D, Maia JM, Zhu M, Smith JP, Cirulli ET, Fellay J, Dickson SP, Gumbs CE, Heinzen EL, Need AC, Ruzzo EK, Singh A, Campbell CR, Hong LK, Lornsen KA, McKenzie AM, Sobreira NL, Hoover-Fong JE, Milner JD, Ottman R, Haynes BF, Goedert JJ, Goldstein DB (2010) The characterization of twenty sequenced human genomes. PLoS Genet 6:e1001111.

Peter S, Ten Brinke MM, Stedehouder J, Reinelt CM, Wu B, Zhou H, Zhou K, Boele HJ, Kushner SA, Lee MG, Schmeisser MJ, Boeckers TM, Schonewille M, Hoebeek FE, De Zeeuw CI (2016) Dysfunctional cerebellar Purkinje cells contribute to autism-like behaviour in Shank2-deficient mice. Nat Commun 7:12627.

Petrovski S, Wang Q, Heinzen EL, Allen AS, Goldstein DB (2013) Genic intolerance to functional variation and the interpretation of personal genomes. PLoS Genet 9:e1003709.

Pfaffl MW (2001) A new mathematical model for relative quantification in real-time RT-PCR. Nucleic acids research 29:e45.

Pfeffer CK, Stein V, Keating DJ, Maier H, Rinke I, Rudhard Y, Hentschke M, Rune GM, Jentsch TJ, Hubner CA (2009) NKCC1-dependent GABAergic excitation drives synaptic network maturation during early hippocampal development. J Neurosci 29:3419-3430.

Ptacek LJ (1997) Channelopathies: ion channel disorders of muscle as a paradigm for paroxysmal disorders of the nervous system. Neuromuscul Disord 7:250-255.

Racine RJ (1972) Modification of seizure activity by electrical stimulation. II. Motor seizure. Electroencephalography and clinical neurophysiology 32:281-294.

Raj A, Peskin CS, Tranchina D, Vargas DY, Tyagi S (2006) Stochastic mRNA synthesis in mammalian cells. PLoS Biol 4:e309.

Ramos RL, Smith PT, DeCola C, Tam D, Corzo O, Brumberg JC (2008) Cytoarchitecture and transcriptional profiles of neocortical malformations in inbred mice. Cereb Cortex 18:2614-2628.

Raymond CK, Castle J, Garrett-Engele P, Armour CD, Kan Z, Tsinoremas N, Johnson JM (2004) Expression of alternatively spliced sodium channel alpha-subunit genes. Unique splicing patterns are observed in dorsal root ganglia. J Biol Chem 279:46234-46241.

Reeber SL, Otis TS, Sillitoe RV (2013) New roles for the cerebellum in health and disease. Frontiers in systems neuroscience 7:83.

Rhodes TH, Lossin C, Vanoye CG, Wang DW, George AL, Jr. (2004) Noninactivating voltage-gated sodium channels in severe myoclonic epilepsy of infancy. Proc Natl Acad Sci U S A 101:11147-11152.

Robinson R, Taske N, Sander T, Heils A, Whitehouse W, Goutieres F, Aicardi J, Lehesjoki AE, Siren A, Laue Friis M, Kjeldsen MJ, Panayiotopoulos C, Kennedy C, Ferrie C, Rees M, Gardiner RM (2002) Linkage analysis between childhood absence epilepsy and genes encoding GABAA and GABAB receptors, voltage-dependent calcium channels, and the ECA1 region on chromosome 8q. Epilepsy Res 48:169-179.

Rodriguez-Moreno A, Herreras O, Lerma J (1997) Kainate receptors presynaptically downregulate GABAergic inhibition in the rat hippocampus. Neuron 19:893-901.

Royeck M, Horstmann MT, Remy S, Reitze M, Yaari Y, Beck H (2008) Role of axonal NaV1.6 sodium channels in action potential initiation of CA1 pyramidal neurons. J Neurophysiol 100:2361-2380.

Rusconi R, Combi R, Cestele S, Grioni D, Franceschetti S, Dalpra L, Mantegazza M (2009) A rescuable folding defective Nav1.1 (SCN1A) sodium channel mutant causes GEFS+: common mechanism in Nav1.1 related epilepsies? Hum Mutat 30:E747-760.

Rusconi R, Scalmani P, Cassulini RR, Giunti G, Gambardella A, Franceschetti S, Annesi G, Wanke E, Mantegazza M (2007) Modulatory proteins can rescue a trafficking

defective epileptogenic Nav1.1 Na+ channel mutant. The Journal of neuroscience : the official journal of the Society for Neuroscience 27:11037-11046.

Rush AM, Craner MJ, Kageyama T, Dib-Hajj SD, Waxman SG, Ranscht B (2005) Contactin regulates the current density and axonal expression of tetrodotoxin-resistant but not tetrodotoxin-sensitive sodium channels in DRG neurons. Eur J Neurosci 22:39-49.

Sabbagh A, Pasmant E, Laurendeau I, Parfait B, Barbarot S, Guillot B, Combemale P, Ferkal S, Vidaud M, Aubourg P, Vidaud D, Wolkenstein P, members of the NFFN (2009) Unravelling the genetic basis of variable clinical expression in neurofibromatosis 1. Hum Mol Genet 18:2768-2778.

Saitoh M, Ishii A, Ihara Y, Hoshino A, Terashima H, Kubota M, Kikuchi K, Yamanaka G, Amemiya K, Hirose S, Mizuguchi M (2015) Missense mutations in sodium channel SCN1A and SCN2A predispose children to encephalopathy with severe febrile seizures. Epilepsy Res 117:1-6.

Sangameswaran L, Fish LM, Koch BD, Rabert DK, Delgado SG, Ilnicka M, Jakeman LB, Novakovic S, Wong K, Sze P, Tzoumaka E, Stewart GR, Herman RC, Chan H, Eglen RM, Hunter JC (1997) A novel tetrodotoxin-sensitive, voltage-gated sodium channel expressed in rat and human dorsal root ganglia. J Biol Chem 272:14805-14809.

Sawyer NT, Helvig AW, Makinson CD, Decker MJ, Neigh GN, Escayg A (2016) Scn1a dysfunction alters behavior but not the effect of stress on seizure response. Genes Brain Behav 15:335-347.

Sawyer NT, Papale LA, Eliason J, Neigh GN, Escayg A (2014) Scn8a voltage-gated
    sodium channel mutation alters seizure and anxiety responses to acute stress.
    Psychoneuroendocrinology 39:225-236.

Schaller KL, Caldwell JH (2000) Developmental and regional expression of sodium
    channel isoform NaCh6 in the rat central nervous system. J Comp Neurol 420:84-
    97.

Scheffer IE, Berkovic SF (1997) Generalized epilepsy with febrile seizures plus. A
    genetic disorder with heterogeneous clinical phenotypes. Brain 120 (Pt 3):479-
    490.

Scheffer IE, Zhang YH, Jansen FE, Dibbens L (2009) Dravet syndrome or genetic
    (generalized) epilepsy with febrile seizures plus? Brain & development 31:394-
    400.

Schonewille M, Belmeguenai A, Koekkoek SK, Houtman SH, Boele HJ, van Beugen BJ,
    Gao Z, Badura A, Ohtsuki G, Amerika WE, Hosy E, Hoebeek FE, Elgersma Y,
    Hansel C, De Zeeuw CI (2010) Purkinje cell-specific knockout of the protein
    phosphatase PP2B impairs potentiation and cerebellar motor learning. Neuron
    67:618-628.

Schwarz N, Hahn A, Bast T, Muller S, Loffler H, Maljevic S, Gaily E, Prehl I, Biskup S,
    Joensuu T, Lehesjoki AE, Neubauer BA, Lerche H, Hedrich UB (2016) Mutations
    in the sodium channel gene SCN2A cause neonatal epilepsy with late-onset
    episodic ataxia. J Neurol 263:334-343.

Shi X, Yasumoto S, Nakagawa E, Fukasawa T, Uchiya S, Hirose S (2009) Missense

    mutation of the sodium channel gene SCN2A causes Dravet syndrome. Brain Dev

    31:758-762.

Shorvon SD (2011) The etiologic classification of epilepsy. Epilepsia 52:1052-1057.

Sievers F, Wilm A, Dineen D, Gibson TJ, Karplus K, Li W, Lopez R, McWilliam H,

    Remmert M, Soding J, Thompson JD, Higgins DG (2011) Fast, scalable

    generation of high-quality protein multiple sequence alignments using Clustal

    Omega. Molecular systems biology 7:539.

Singh NA, Charlier C, Stauffer D, DuPont BR, Leach RJ, Melis R, Ronen GM, Bjerre I,

    Quattlebaum T, Murphy JV, McHarg ML, Gagnon D, Rosales TO, Peiffer A,

    Anderson VE, Leppert M (1998) A novel potassium channel gene, KCNQ2, is

    mutated in an inherited epilepsy of newborns. Nat Genet 18:25-29.

Singh NA, Pappas C, Dahle EJ, Claes LR, Pruess TH, De Jonghe P, Thompson J, Dixon

    M, Gurnett C, Peiffer A, White HS, Filloux F, Leppert MF (2009) A role of

    SCN9A in human epilepsies, as a cause of febrile seizures and as a potential

    modifier of Dravet syndrome. PLoS Genet 5:e1000649.

Singh R, Andermann E, Whitehouse WP, Harvey AS, Keene DL, Seni MH, Crossland

    KM, Andermann F, Berkovic SF, Scheffer IE (2001) Severe myoclonic epilepsy

    of infancy: extended spectrum of GEFS+? Epilepsia 42:837-844.

Singh R, Scheffer IE, Crossland K, Berkovic SF (1999) Generalized epilepsy with febrile

    seizures plus: a common childhood-onset genetic epilepsy syndrome. Ann Neurol

    45:75-81.

Smart SL, Lopantsev V, Zhang CL, Robbins CA, Wang H, Chiu SY, Schwartzkroin PA, Messing A, Tempel BL (1998) Deletion of the K(V)1.1 potassium channel causes epilepsy in mice. Neuron 20:809-819.

Sprunger LK, Escayg A, Tallaksen-Greene S, Albin RL, Meisler MH (1999) Dystonia associated with mutation of the neuronal sodium channel Scn8a and identification of the modifier locus Scnm1 on mouse chromosome 3. Hum Mol Genet 8:471-479.

Steinberg MH, Adewoye AH (2006) Modifier genes and sickle cell anemia. Curr Opin Hematol 13:131-136.

Steinlein OK, Mulley JC, Propping P, Wallace RH, Phillips HA, Sutherland GR, Scheffer IE, Berkovic SF (1995) A missense mutation in the neuronal nicotinic acetylcholine receptor alpha 4 subunit is associated with autosomal dominant nocturnal frontal lobe epilepsy. Nature genetics 11:201-203.

Subaran RL, Greenberg DA (2014) The genetics of common epilepsy disorders: lessons learned from the channelopathy era. Curr Genet Med Rep 2:190-200.

Sugawara T, Tsurubuchi Y, Agarwala KL, Ito M, Fukuma G, Mazaki-Miyazaki E, Nagafuji H, Noda M, Imoto K, Wada K, Mitsudome A, Kaneko S, Montal M, Nagata K, Hirose S, Yamakawa K (2001) A missense mutation of the Na+ channel alpha II subunit gene Na(v)1.2 in a patient with febrile and afebrile seizures causes channel dysfunction. Proc Natl Acad Sci U S A 98:6384-6389.

Suls A, Velizarova R, Yordanova I, Deprez L, Van Dyck T, Wauters J, Guergueltcheva V, Claes LR, Kremensky I, Jordanova A, De Jonghe P (2010) Four generations of

epilepsy caused by an inherited microdeletion of the SCN1A gene. Neurology 75:72-76.

Surovy M, Soltysova A, Kolnikova M, Sykora P, Ilencikova D, Ficek A, Radvanszky J, Kadasi L (2016a) Novel SCN1A variants in Dravet syndrome and evaluating a wide approach of patient selection. Gen Physiol Biophys 35:333-342.

Surovy M, Soltysova A, Kolnikova M, Sykora P, Ilencikova D, Ficek A, Radvanszky J, Kadasi L (2016b) Novel SCN1A variants in Dravet syndrome and evaluating a wide approach of patient selection. General physiology and biophysics.

Syrbe S, Hedrich UB, Riesch E, Djemie T, Muller S, Moller RS, Maher B, Hernandez-Hernandez L, Synofzik M, Caglayan HS, Arslan M, Serratosa JM, Nothnagel M, May P, Krause R, Loffler H, Detert K, Dorn T, Vogt H, Kramer G, Schols L, Mullis PE, Linnankivi T, Lehesjoki AE, Sterbova K, Craiu DC, Hoffman-Zacharska D, Korff CM, Weber YG, Steinlin M, Gallati S, Bertsche A, Bernhard MK, Merkenschlager A, Kiess W, Euro ER, Gonzalez M, Zuchner S, Palotie A, Suls A, De Jonghe P, Helbig I, Biskup S, Wolff M, Maljevic S, Schule R, Sisodiya SM, Weckhuysen S, Lerche H, Lemke JR (2015) De novo loss- or gain-of-function mutations in KCNA2 cause epileptic encephalopathy. Nat Genet 47:393-399.

Tang B, Dutt K, Papale L, Rusconi R, Shankar A, Hunter J, Tufik S, Yu FH, Catterall WA, Mantegazza M, Goldin AL, Escayg A (2009) A BAC transgenic mouse model reveals neuron subtype-specific effects of a Generalized Epilepsy with Febrile Seizures Plus (GEFS+) mutation. Neurobiol Dis 35:91-102.

Terlau H, Heinemann SH, Stuhmer W, Pusch M, Conti F, Imoto K, Numa S (1991) Mapping the site of block by tetrodotoxin and saxitoxin of sodium channel II. FEBS Lett 293:93-96.

Thompson CH, Porter JC, Kahlig KM, Daniels MA, George AL, Jr. (2012) Nontruncating SCN1A mutations associated with severe myoclonic epilepsy of infancy impair cell surface expression. The Journal of biological chemistry 287:42001-42008.

Toledo-Aral JJ, Moss BL, He ZJ, Koszowski AG, Whisenand T, Levinson SR, Wolf JJ, Silos-Santiago I, Halegoua S, Mandel G (1997) Identification of PN1, a predominant voltage-dependent sodium channel expressed principally in peripheral neurons. Proc Natl Acad Sci U S A 94:1527-1532.

Toman JE (1951) Neuropharmacologic considerations in psychic seizures. Neurology 1:444-460.

Ure K, Lu H, Wang W, Ito-Ishida A, Wu Z, He LJ, Sztainberg Y, Chen W, Tang J, Zoghbi HY (2016) Restoration of Mecp2 expression in GABAergic neurons is sufficient to rescue multiple disease features in a mouse model of Rett syndrome. Elife 5.

Usluer S, Salar S, Arslan M, Yis U, Kara B, Tekturk P, Baykan B, Meral C, Turkdogan D, Bebek N, Yalcin Capan O, Gundogdu Eken A, Caglayan SH (2016) SCN1A gene sequencing in 46 Turkish epilepsy patients disclosed 12 novel mutations. Seizure 39:34-43.

Vadlamudi L, Andermann E, Lombroso CT, Schachter SC, Milne RL, Hopper JL, Andermann F, Berkovic SF (2004) Epilepsy in twins: insights from unique historical data of William Lennox. Neurology 62:1127-1133.

Vaher U, Noukas M, Nikopensius T, Kals M, Annilo T, Nelis M, Ounap K, Reimand T, Talvik I, Ilves P, Piirsoo A, Seppet E, Metspalu A, Talvik T (2014) De novo SCN8A mutation identified by whole-exome sequencing in a boy with neonatal epileptic encephalopathy, multiple congenital anomalies, and movement disorders. J Child Neurol 29:NP202-206.

Van Wart A, Matthews G (2006) Expression of sodium channels Nav1.2 and Nav1.6 during postnatal development of the retina. Neurosci Lett 403:315-317.

Vanoye CG, Gurnett CA, Holland KD, George AL, Jr., Kearney JA (2014) Novel SCN3A variants associated with focal epilepsy in children. Neurobiol Dis 62:313-322.

Vanoye CG, Lossin C, Rhodes TH, George AL, Jr. (2006) Single-channel properties of human NaV1.1 and mechanism of channel dysfunction in SCN1A-associated epilepsy. J Gen Physiol 127:1-14.

Vaughan DN, Jackson GD (2014) The piriform cortex and human focal epilepsy. Front Neurol 5:259.

Veeramah KR, O'Brien JE, Meisler MH, Cheng X, Dib-Hajj SD, Waxman SG, Talwar D, Girirajan S, Eichler EE, Restifo LL, Erickson RP, Hammer MF (2012) De novo pathogenic SCN8A mutation identified by whole-genome sequencing of a family quartet affected by infantile epileptic encephalopathy and SUDEP. Am J Hum Genet 90:502-510.

Vien TN, Modgil A, Abramian AM, Jurd R, Walker J, Brandon NJ, Terunuma M, Rudolph U, Maguire J, Davies PA, Moss SJ (2015) Compromising the phosphodependent regulation of the GABAAR beta3 subunit reproduces the core phenotypes of autism spectrum disorders. Proc Natl Acad Sci U S A 112:14805-14810.

Vismer MS, Forcelli PA, Skopin MD, Gale K, Koubeissi MZ (2015) The piriform, perirhinal, and entorhinal cortex in seizure generation. Front Neural Circuits 9:27.

Volkers L, Kahlig KM, Verbeek NE, Das JH, van Kempen MJ, Stroink H, Augustijn P, van Nieuwenhuizen O, Lindhout D, George AL, Jr., Koeleman BP, Rook MB (2011) Nav 1.1 dysfunction in genetic epilepsy with febrile seizures-plus or Dravet syndrome. The European journal of neuroscience 34:1268-1275.

Wallace RH, Marini C, Petrou S, Harkin LA, Bowser DN, Panchal RG, Williams DA, Sutherland GR, Mulley JC, Scheffer IE, Berkovic SF (2001) Mutant GABA(A) receptor gamma2-subunit in childhood absence epilepsy and febrile seizures. Nat Genet 28:49-52.

Wallace RH, Wang DW, Singh R, Scheffer IE, George AL, Jr., Phillips HA, Saar K, Reis A, Johnson EW, Sutherland GR, Berkovic SF, Mulley JC (1998) Febrile seizures and generalized epilepsy associated with a mutation in the Na+-channel beta1 subunit gene SCN1B. Nat Genet 19:366-370.

Wang DW, Mistry AM, Kahlig KM, Kearney JA, Xiang J, George AL, Jr. (2010) Propranolol blocks cardiac and neuronal voltage-gated sodium channels. Frontiers in pharmacology 1:144.

Wassef AA, Dott SG, Harris A, Brown A, O'Boyle M, Meyer WJ, 3rd, Rose RM (1999) Critical review of GABA-ergic drugs in the treatment of schizophrenia. J Clin Psychopharmacol 19:222-232.

Weiss J, Pyrski M, Jacobi E, Bufe B, Willnecker V, Schick B, Zizzari P, Gossage SJ, Greer CA, Leinders-Zufall T, Woods CG, Wood JN, Zufall F (2011) Loss-of-function mutations in sodium channel Nav1.7 cause anosmia. Nature 472:186-190.

Westenbroek RE, Merrick DK, Catterall WA (1989) Differential subcellular localization of the RI and RII Na+ channel subtypes in central neurons. Neuron 3:695-704.

Westenbroek RE, Noebels JL, Catterall WA (1992) Elevated expression of type II Na+ channels in hypomyelinated axons of shiverer mouse brain. J Neurosci 12:2259-2267.

Whitaker W, Faull R, Waldvogel H, Plumpton C, Burbidge S, Emson P, Clare J (1999a) Localization of the type VI voltage-gated sodium channel protein in human CNS. Neuroreport 10:3703-3709.

Whitaker WR, Clare JJ, Emson PC (1999b) Differential distribution of voltage-gated sodium channel alpha- and beta-subunits in human brain. Ann N Y Acad Sci 868:88-92.

Whitaker WR, Clare JJ, Powell AJ, Chen YH, Faull RL, Emson PC (2000) Distribution of voltage-gated sodium channel alpha-subunit and beta-subunit mRNAs in human hippocampal formation, cortex, and cerebellum. The Journal of comparative neurology 422:123-139.

Whitaker WR, Faull RL, Dragunow M, Mee EW, Emson PC, Clare JJ (2001a) Changes in the mRNAs encoding voltage-gated sodium channel types II and III in human epileptic hippocampus. Neuroscience 106:275-285.

Whitaker WR, Faull RL, Waldvogel HJ, Plumpton CJ, Emson PC, Clare JJ (2001b) Comparative distribution of voltage-gated sodium channel proteins in human brain. Brain Res Mol Brain Res 88:37-53.

Wolff M, Casse-Perrot C, Dravet C (2006) Severe myoclonic epilepsy of infants (Dravet syndrome): natural history and neuropsychological findings. Epilepsia 47 Suppl 2:45-48.

Woodbury DM (1980) Convulsant drugs: mechanisms of action. Adv Neurol 27:249-303.

Woodruff-Pak DS, Green JT, Levin SI, Meisler MH (2006) Inactivation of sodium channel Scn8A (Na-sub(v)1.6) in Purkinje neurons impairs learning in Morris water maze and delay but not trace eyeblink classical conditioning. Behav Neurosci 120:229-240.

Xu X, Guo F, Lv X, Feng R, Min D, Ma L, Liu Y, Zhao J, Wang L, Chen T, Shaw C, Hao L, Cai J (2013) Abnormal changes in voltage-gated sodium channels Na(V)1.1, Na(V)1.2, Na(V)1.3, Na(V)1.6 and in calmodulin/calmodulin-dependent protein kinase II, within the brains of spontaneously epileptic rats and tremor rats. Brain Res Bull 96:1-9.

Yang N, Horn R (1995) Evidence for voltage-dependent S4 movement in sodium channels. Neuron 15:213-218.

Yu FH, Mantegazza M, Westenbroek RE, Robbins CA, Kalume F, Burton KA, Spain WJ, McKnight GS, Scheuer T, Catterall WA (2006) Reduced sodium current in

GABAergic interneurons in a mouse model of severe myoclonic epilepsy in infancy. Nat Neurosci 9:1142-1149.

Yu FH, Westenbroek RE, Silos-Santiago I, McCormick KA, Lawson D, Ge P, Ferriera H, Lilly J, DiStefano PS, Catterall WA, Scheuer T, Curtis R (2003) Sodium channel beta4, a new disulfide-linked auxiliary subunit with similarity to beta2. J Neurosci 23:7577-7585.